Synthesis and Evaluation of Novel Carbocyclic Carbohydrate Analogues

by

Christopher William Adamson

B.Sc., University of Alberta, 2011

Thesis Submitted in Partial Fulfillment of the
Requirements for the Degree of
Master of Science

in the
Department of Chemistry
Faculty of Science

SIMON FRASER UNIVERSITY

Spring 2016

Approval

Name:	**Christopher William Adamson**
Degree:	**Master of Science**
Title:	***Synthesis and Evaluation of Novel Carbocyclic Carbohydrate Analogues***
Examining Committee:	**Chair: Dr. Roger Linington** Associate Professor

Dr. Robert A. Britton
Senior Supervisor
Professor

Dr. Andrew J. Bennet
Supervisor
Professor

Dr. Charles Walsby
Supervisor
Associate Professor

Dr. Peter D. Wilson
Supervisor
Associate Professor

Dr. David Vocadlo
Internal Examiner
Professor

Date Defended/Approved: April 15, 2016

Abstract

Carbohydrate analogues play an indispensible role in the study of glycan processing enzymes. These compounds have attracted attention as probes of enzyme mechanisms, as chemical tools for the elucidation of enzyme function and as potential pharmaceuticals.

The development of organocatalytic aldol chemistry has fundamentally altered the way chemists approach the synthesis of carbohydrate analogues. In this thesis I highlight a novel strategy toward the synthesis of carbocyclic carbohydrate analogues which utilizes a proline-catalyzed aldol reaction and a metal-catalyzed carbocyclization as key steps. This strategy was successfully implemented in the synthesis of an ensemble of galactose and *N*-acetylgalactosamine analogues. Furthermore, I present preliminary results toward the biological evaluation of these compounds.

Keywords: Carbohydrates; glycan processing enzymes; organic synthesis; proline catalysis; enzyme inhibitors

Acknowledgements

First and foremost I would like to acknowledge my supervisors Prof. Robert Britton and Prof. Andrew Bennet for their constant support during my studies. Their encouragement, optimism and knowledge helped me to overcome many challenges in the lab. Rob taught me how to approach synthetic problems, whereas from Andy I gained new appreciation for the rigorous study of mechanism in organic chemistry.

I extend my thanks to Profs. Charles Walsby and Peter Wilson for serving on my supervisory committee. Their presence has helped me to take a greater intellectual command of my projects.

I would like thank all group members, past in present, in the Britton and Bennet labs for all the good times spent in the lab or at the pub. In particular, I extend my thanks to Michael Holmes, Milan Bergeron-Brlek and Sankar Mohan for showing me the ropes of synthetic chemistry.

Finally, I would like to acknowledge my family members and friends. Their encouragement and support has made all of this possible.

Table of Contents

List of Tables

List of Figures

List of Schemes

List of Abbreviations

2,4-DNFB	2,4-dinitrofluorobenzene
4-DMAP	4-dimethylaminopyridine
ADP	adenosine diphosphate
ATP	adenosine triphosphate
Ac	acetyl
$BF_3 \cdot OEt_2$	boron trifluoride diethyletherate
°C	degrees Celsius
D	aspartic acid
DABCO	1,4-diazabicyclo[2.2.2]octane
DIBAL-H	diisobutylaluminium hydride
DMF	dimethylformamide
DMSO	dimethylsulfoxide
E	*entgegen* (German); *trans* double bond configuration
ee	enantiomeric excess
equiv.	equivalents
GalNAc	*N*-acetylgalactosamine
his	histidine
HPLC	high performance liquid chromatography
imid	imidazole
KHMDS	potassium bis(trimethylsilyl)amide
L-Selectride	lithium tri-*sec*-butylborohydride
LiHMDS	lithium bis(trimethylsilyl)amide
lys	lysine
MTPA	α-methoxy-α-trifluoromethylphenylacetic acid
NMR	nuclear magnetic resonance
nOe	nuclear Overhauser effect
NOESY	nuclear Overhauser effect spectroscopy
PBS	phosphate-buffered saline
PPTS	pyridinium *p*-toluenesulfonate
PP_i	pyrophosphate
p-TsOH	*para*-toluenesulfonic acid monohydrate

pyr	pyridine
RCM	ring-closing metathesis
RT	room temperature
TBAF	tetra-*n*-butylammonium fluoride
TBS	*tert*-butyldimethylsilyl
TES	triethylsilyl
THF	tetrahydrofuran
TIPS	triisopropylsilyl
TLC	thin layer chromatography
TMS	trimethylsilyl
*Tm*GalA	*Thermatoga maritima* α-galactosidase
UTP	uridine triphosphate

Chapter 1.

Introduction

1.1. Introduction to Glycans

Carbohydrates constitute a class of biomolecule that is ubiquitous throughout all kingdoms of Life. Carbohydrates play foundational roles in biological processes: the catabolism of glucose provides energy for cells; carbohydrates are the feedstock for biosynthesis of many secondary metabolites. The defining structural feature of carbohydrates is a polyhydroxylated scaffold of tetrahedral carbon atoms. While the word carbohydrate originates from the empirical formula $C_n(H_2O)_n$, many carbohydrates deviate from this composition, such as the iminosugars and carbasugars.

Carbohydrates in nature may exist as single monosaccharides, disaccharides, or as polymers of monosaccharides known as glycans. While mammalian glycans are formed from ten canonical monomeric units (Figure 1.1), variations such as *O*-acetylation[1] and *O*-phosphorylation[2] also occur.

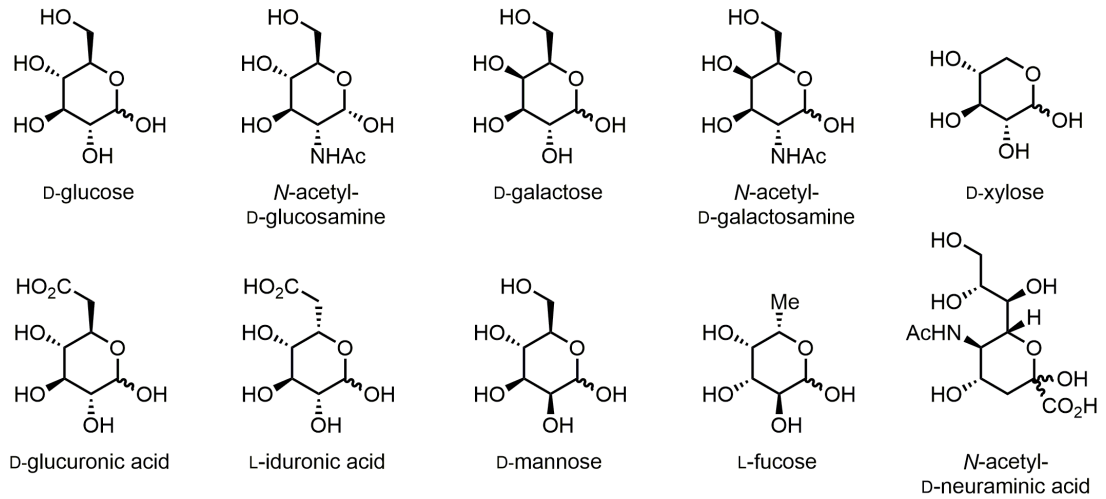

Figure 1.1. Canonical monosaccharide units of mammalian glycans.

Like peptides and nucleic acids, glycans are modular entities as they are composed of monosaccharide units joined by acetal linkages. However, glycans exhibit far greater structural diversity owing to the variable stereochemistry (α or β) and regiochemistry of these linkages. Cell surfaces are decorated with a vast array of glycans; these mediate critical physiological processes including cell adhesion,[3] signal transduction,[3] inflammation,[4] and host-pathogen interactions.[5,6] Within cells, post-translational glycosylation modulates the stability, folding, and catalytic activity of proteins.[7] Thus, the elucidation of the roles played by glycans has broad applicability within translational medicine.

1.2. Glycan Processing Enzymes

Cellular glycosylation patterns are regulated at the level of the expression and localization of glycan processing enzymes - enzymes that catalyze the assembly, degradation, and modification of glycans and glycoconjugates. These enzymes are responsible for the enormous diversity of glycan structures found in cells and typically account for 1 to 3% of the genome of most organisms.[8] The majority of glycan processing enzymes may be classified as either glycoside hydrolases or glycosyl transferases.

1.2.1. Glycoside Hydrolases

The most extensively characterized class of carbohydrate processing enzymes is the glycoside hydrolases (GHs), which hydrolytically cleave acetal linkages within a glycan or glycoconjugate. These enzymes play an important role in mammalian physiological processes, including the breakdown of ingested polysaccharides in the small intestine, the catabolism of cellular waste products, and the truncation of cell surface glycans. GHs are well-established therapeutic targets for human disease states such as diabetes[9,10] and influenza.[11] Recently, *N*-acetylglucosaminidase has attracted attention as a therapeutic target for Alzheimer's disease.[12,13]

The CAZy (**C**arbohydrate **A**ctive en**Zy**mes) database classifies carbohydrate processing enzymes into families based on amino acid sequence. To date there are

more than 130 GH families.[14] As the catalytic mechanism within a GH family is usually conserved, the CAZy system enables the prediction of the catalytic mechanism of an uncharacterized hydrolase.

Enzymatic glycosidic bond hydrolysis may occur with one of two stereochemical outcomes depending on the mechanism employed by the hydrolase. With retaining GHs, the stereochemical configuration at the anomeric centre is preserved, whereas with inverting GHs the stereochemical configuration is inverted.

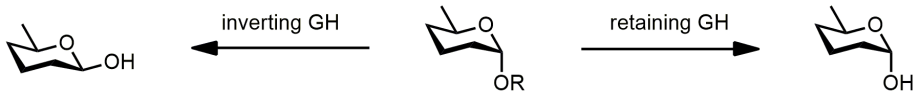

Figure 1.2. General reaction catalyzed by retaining and inverting α-GHs.

Several catalytic mechanisms have been identified for retaining GHs; of these, the double-displacement mechanism[15] is by far the most common. This mechanism features two discrete steps: glycosylation and deglycosylation. In the glycosylation step, an enzymic nucleophile (usually an aspartate or glutamate residue) displaces the leaving group (aglycone) to afford a covalent glycosyl-enzyme intermediate.[16] The departure of the aglycone is assisted by general acid catalysis. In the deglycosylation step, a water molecule displaces the enzymic residue, yielding the hydrolyzed glycoside. General base catalysis acts to increase the nucleophilicity of the water molecule. Since both steps proceed with inversion of configuration at the anomeric centre, the net reaction proceeds with retention of stereochemistry.

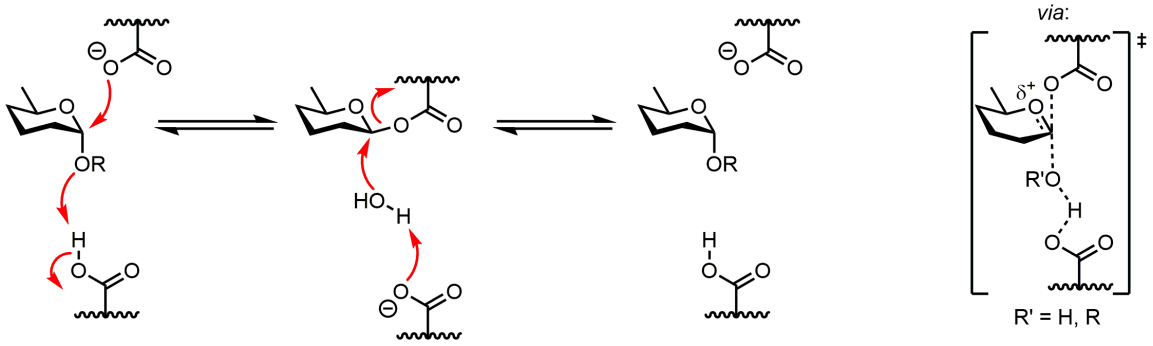

Figure 1.3. Koshland mechansm for retaining GHs.

In a manner analogous to retaining GHs, inverting GHs catalyze a S_N2-like reaction.[17] However, inverting GHs catalyze only a single displacement in which the

nucleophile is water, which leads to inversion of the anomeric configuration. General acid and general base catalysis act simultaneously to reduce the activation barrier for this reaction.

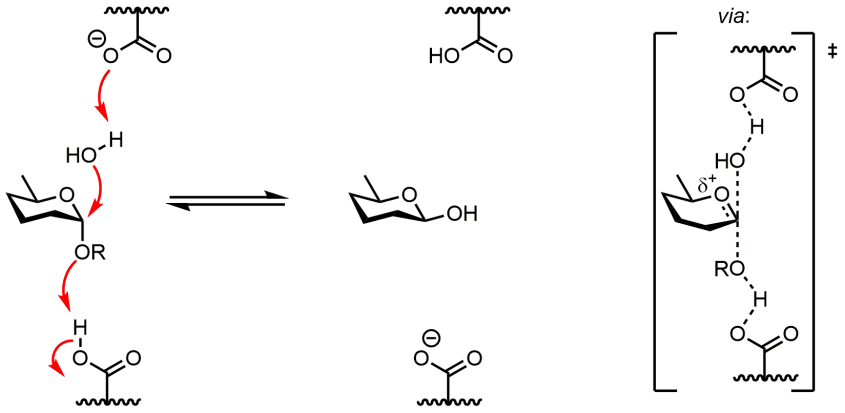

Figure 1.4 Inverting GH mechanism.

The S_N2-like mechanisms described above have transition states (TSs) in which the partially filled p-orbital of the anomeric carbon is stabilized by a π-type interaction with one of the ring oxygen atom's lone pairs, which gives the TS significant oxacarbenium ion character. This orbital interaction mandates a distorted non-chair conformation in which C(5), O, C(1), and C(2) are coplanar. Thus, four TS ring conformations are possible;[18] hydrogen bonding and hydrophobic interactions act in concert to stabilize these conformations.

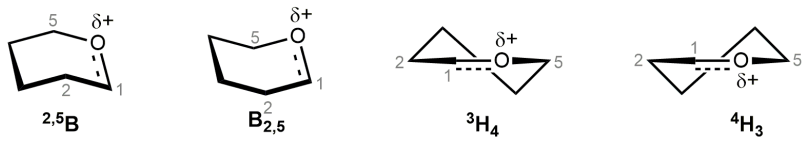

Figure 1.5 Possible TS ring conformations in S_N2-like GH mechanisms.

A highly atypical catalytic mechanism is employed by hydrolases belonging to GH families 4[19,20] and 109,[21] which use a NAD^+/NADH redox couple. In this mechanism, the C(3) hydroxyl is first oxidized to the corresponding ketone. This facilitates elimination of the aglycone across the C(1) – C(2) bond. The resulting enone is then stereoselectively hydrated, and the C(3) ketone is finally reduced back to the corresponding hydroxyl. As GHs that use this mechanism are found only in bacteria, selective inhibitors of these enzymes could potentially serve as antibacterial agents.

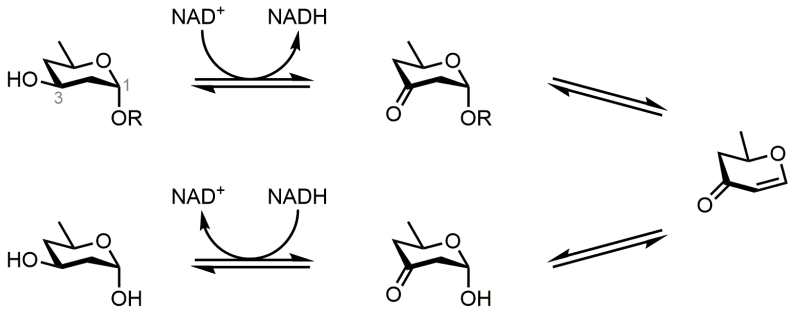

Figure 1.6 General reaction catalyzed by GH 4 and GH 109 hydrolases.

1.2.2. Glycosyltransferases

Glycosyltransferases (GTs) catalyze the formation of glycosidic bonds in the assembly of glycoproteins and glycolipids, which in mammals generally occurs in the Golgi apparatus. As GTs are frequently membrane-associated, the isolation and crystallographic characterization of these enzymes is challenging.[22] Furthermore, GTs have two substrates, which complicates activity assay development.[23] Owing to these factors GTs are poorly understood when compared with GHs.[18] Nonetheless, GTs are emerging as therapeutic targets for a number of human disease states. Bacterial enzymes known as peptidoglycan glycosyltransferases have attracted attention as potential antibacterial therapeutic targets.[24] Furthermore, human ceramide glycosyltransferase is the target of an approved drug for Gaucher's disease.[25,26,27]

GTs couple two substrates: a glycosyl donor, which is usually a monosaccharide bearing a nucleoside (di)phosphate leaving group at the anomeric position, and a glycosyl acceptor, which may be a carbohydrate, lipid, protein, or small molecule. GTs may be classified as either inverting or retaining depending on the anomeric configuration of the product glycoside relative to that of the glycosyl donor.

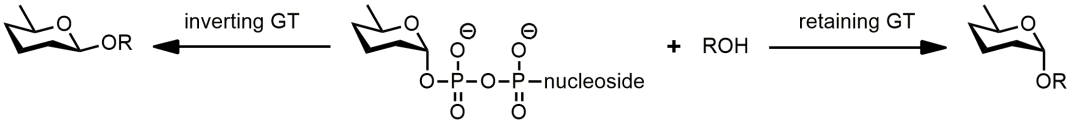

Figure 1.7 General reaction catalyzed by retaining and inverting GTs.

Inverting GTs forge glycosidic bonds using a S_N2-like mechanism in which general base catalysis increases the nucleophilicity of the glycosyl acceptor. While a Mn^{2+} or Mg^{2+} cation frequently assists the departure of the nucleoside (di)phosphate

leaving group, cationic enzyme side chains can also participate in electrophilic catalysis.[18]

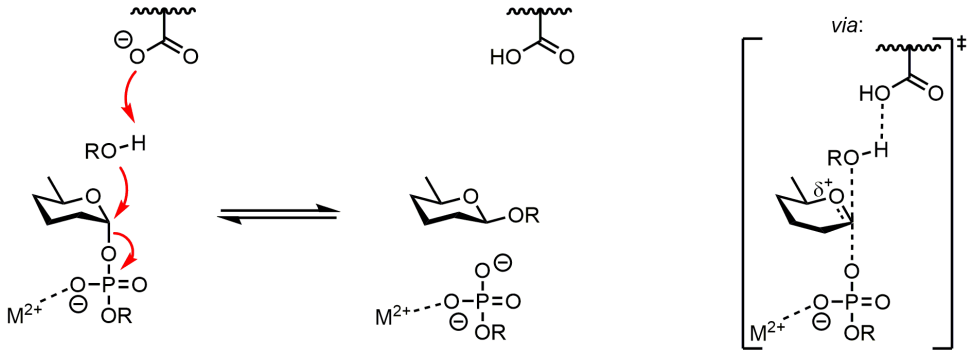

Figure 1.8 Inverting GT mechanism.

The mechanism employed by retaining GTs remains poorly understood. In contrast to retaining GHs, there is scarce evidence for formation of a covalent glycosyl-enzyme intermediate.[18] Rather, recent structural[28] and kinetic[29] evidence suggested a S_Ni mechanism which involves the formation of a short-lived oxacarbenium ion intermediate. This is followed by frontside nucleophilic attack concerted with intermolecular proton transfer from glycosyl donor to phosphate,

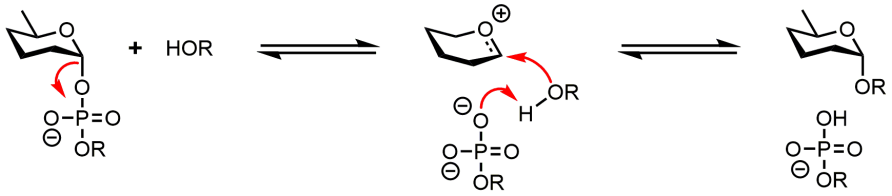

Figure 1.9 Putative retaining GT mechanism.

1.3. Glycan Processing Inhibitors

Potent, selective, and cell-permeable glycan processing inhibitors can serve as tools to elucidate the relation between glycan structure and function *in vivo*. Furthermore, inhibitors with desirable pharmacokinetic and toxicological properties can be evaluated as therapeutics in the clinic. Thus, the development of glycan processing inhibitors fuels advances in both glycobiology and translational medicine.

1.3.1. Competitive Inhibitors of Glycoside Hydrolases

Competitive inhibition occurs when a small molecule binds noncovalently within an enzyme active site to give a complex which is catalytically inactive. For enzymatic glycoside hydrolysis, the dissociation constant of the TS is often estimated to be no greater than 10^{-22} M.[30] Thus, small molecules that mimic either the cationic charge or the non-chair conformation of the glycoside hydrolysis TS are expected to bind tightly. However, it should be emphasized that some of the most potent GH inhibitors fail to qualify as true TS analogues as their resemblance to the TS is only superficial.[31]

To date, by far the most successful class of competitive GH inhibitors is the iminosugars, which are widely represented among natural products.[32] Iminosugars are GH substrate mimics which incorporate a basic nitrogen atom in place of the usual oxygen. As the nitrogen is protonated at physiological pH, iminosugars emulate the cationic charge of the TSs in enzymatic glycoside hydrolysis. Representative examples of iminosugars are shown in Figure 1.10. Swainsonine (**1**) is a naturally occurring indolizidine iminosugar that is a potent inhibitor of α-mannosidases. Isofagomine (**2**) is a potent inhibitor of β-glucosidases; notably, the nitrogen atom in iminosugar **2** is located at the pseudo-anomeric position. *N*-hydroxyethyldeoxynojirimycin (**3**) is an α-glucosidase inhibitor used clinically for the treatment of type II diabetes.[33] Lastly, deoxygalactonojirimycin (**4**) is currently under clinical evaluation for the treatment of the lysosomal storage disorder known as Fabry's disease.[34] At concentrations below K_i, iminosugar **4** paradoxically increases α-galactosidase activity by acting as a chemical chaperone for its unstable target.[35]

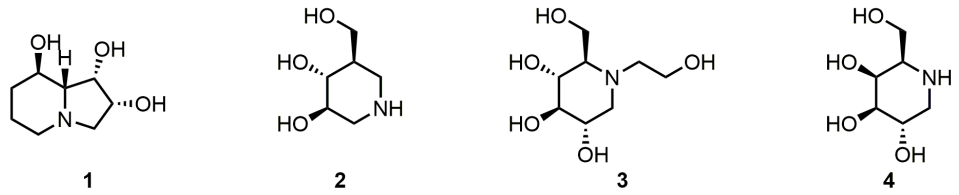

1 **2** **3** **4**

Figure 1.10 Representative examples of iminosugars.

Another tactic used in the design of competitive GH inhibitors is the incorporation of conjugated systems that mandate a boat or half-chair conformation, thus emulating the TS conformation. A seminal example of this approach was provided by Vasella and co-workers in the development of the glucotetrazole (**5**) and glucoimidazole (**6**)

scaffolds.[36,37] These compounds proved to be extremely potent inhibitors of β-glucosidases. Of note, the pyranose rings of these compounds adopt a $^4H_3$ conformation, which is the same conformation found in the TS for retaining β-glucosidases.[38]

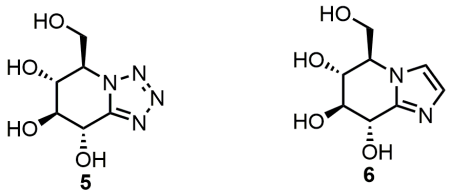

Figure 1.11 Glucotetrazole and glucoimidizole scaffolds.

1.3.2. Covalent Inhibitors of Retaining Glycoside Hydrolases

Covalent GH inhibitors are carbohydrate analogues that form stable covalent bonds with an active site residue, thus rendering the GH catalytically inactive. This can be accomplished using affinity reagents, which contain an inherently electrophilic functional group, or by mechanism-based inactivators, which undergo glycosylation in a manner similar to the native substrates of retaining GHs.[8] The following discussion will deal exclusively with mechanism-based GH inactivators.

Carbohydrate analogues bearing an epoxide functional group have proven to be useful reagents for the covalent inhibition of retaining β-GHs. General acid-assisted opening of the oxirane ring by the catalytic nucleophile results in the formation of a stable covalent adduct (Figure 1.9). The prototypical member of this inhibitor class is conduritol B epoxide (**7**). This reagent is a potent and selective covalent inhibitor of mammalian GCase, the enzyme which degrades glucocerebroside.[8,39] Inhibition of this enzyme in mice simulates the genetic disorder known as Gaucher's disease, which stems from insufficient GCase activity. This model is routinely used as a proving ground for evaluation of candidate therapeutics for Gaucher's disease.[40] The incorporation of an azide functional group in inhibitor **8** permits the attachment of a fluorescent or biotin-containing moiety by way of alkyne/azide "click" chemistry.[41] More recently, this methodology was extended to *N*-acyl aziradines such as **9**, which are potent covalent inhibitors even in the absence of general acid catalysis.[42]

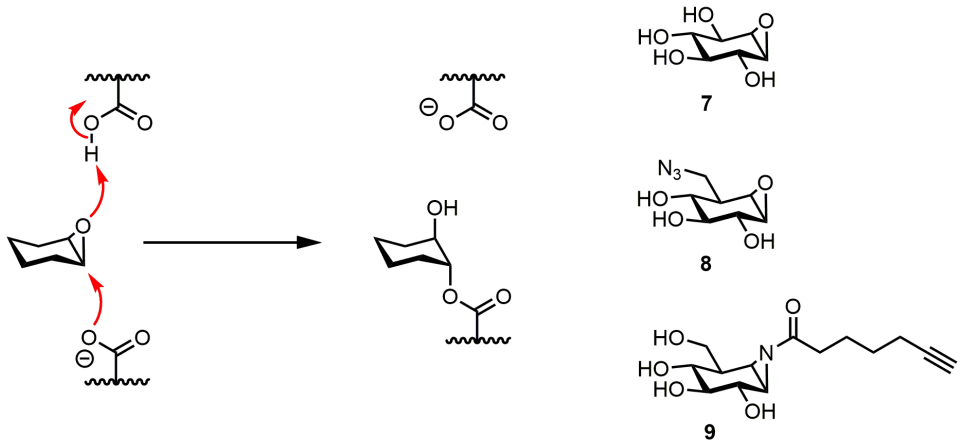

Figure 1.12 Epoxide and aziridine -containing covalent inhibitors of retaining β-GHs.

Arguably the most successful class of covalent GH inhibitors is the fluoroglycosides, which were developed by Withers and co-workers.[43,44] These carbohydrate analogues incorporate a fluorine atom at either C(2) or C(5) of the pyranoside ring. As fluorine is highly electron-withdrawing, its incorporation results in destabilization of oxacarbenium-like TSs. Furthermore, substitution of a C(2) hydroxyl with fluorine largely removes a hydrogen bonding interaction which is estimated to stabilize the TS by at least 8 kcal/mol.[45] These factors slow both the glycosylation and deglycosylation steps. However, a reactive leaving group (typically fluoride or 2,4-dinitrophenolate) is incorporated to ensure the glycosylation step proceeds at a reasonable rate. The net result is the accumulation of the glycosyl-enzyme intermediate. 2-Deoxy-2-fluoroglycosides are generally limited to the inhibition of β-GHs, whereas 5-fluoroglycosides are used to inhibit α-GHs.[8]

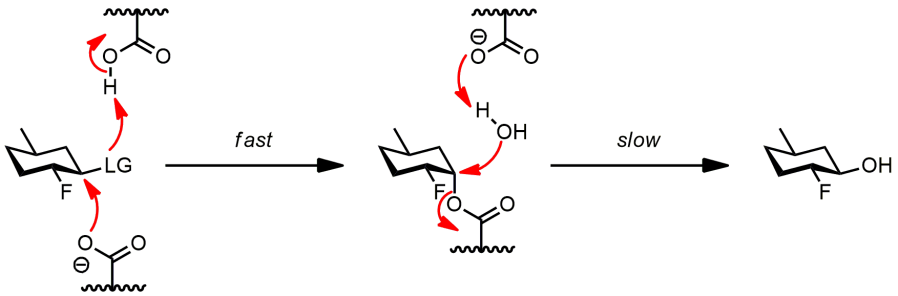

Figure 1.13 Covalent inhibition of retaining β-GHs by 2-fluoro-2-deoxyglycosides.

Fluoroglycosides may be used to identify the catalytic nucleophile of retaining GHs by tryptic MS/MS mapping of the inhibitor-enzyme adduct.[46] Once the catalytic nucleophile is known, site-directed mutagenesis can be used to determine the identity of the catalytic acid/base residue, as the mutant with little or no catalytic activity lacks this residue. Another application of fluoroglycosides is the study of the covalent glycosyl-enzyme intermediate by X-ray crystallography. The conformation of the pyranoside ring in this intermediate can lend insight into the reaction coordinate for processing of a GH's native substrate, which in turn can inform the design of inhibitors with better potency and selectivity.

The utility of fluoroglycosides was expanded to the detection of β-galactosidases in whole proteomes in an elegant example by Vocadlo and Bertozzi.[47] This approach used compound **10** to covalently label β-galactosidases; the azido group was then conjugated to a fluorophore using phosphine-azide "click"[48] chemistry. This enabled activity-based detection of β-galactosidases by gel electrophoresis. Expanding upon this work, Vocadlo and co-workers have developed compound **11** as a probe for the identification of β-D-glucosaminidases.[49]

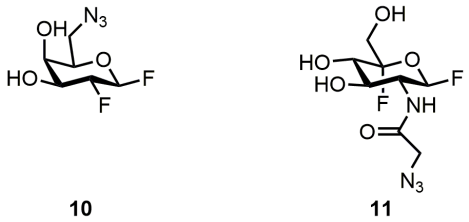

10 **11**

Figure 1.14 Azido-group containing covalent GH inhibitors.

1.3.3. Metabolic Inhibitors of Glycosyltransferases

Strategies in GT inhibitor design involve the use of donor substrate analogues, acceptor substrate analogues, and molecules which emulate both coupling partners, known as bisubstrate mimics.[50] Donor analogues hold the appeal of capitalizing on the tight hydrogen-bonding interactions between the nucleoside diphosphate moiety and the transferase. However, as the phosphate groups are negatively charged, donor analogues have virtually no membrane permeability, which makes them ineffective for use in live cells.

A solution to this problem involves the use of so-called “metabolic inhibitors”. Vocadlo proposed that carbohydrate analogues can be converted *in vivo* to the corresponding C(1) nucleoside phosphates owing to the promiscuous nature of hexosamine salvage pathway enzymes. As the resulting donor analogues are not viable GT substrates, they act as inhibitors. Additionally, the accumulation of the donor analogue down-regulates *de novo* biosynthesis of the glycosyl donor by feedback inhibition. Of note, the carbohydrate analogue must generally be peracetylated to ensure cell membrane permeability: the *O*-acetate groups which enhance lipophilicity are rapidly cleaved by esterases within the cytosol. Vocadlo first demonstrated this inhibition modality using 5-thio-*N*-acetylglucosamine (**12**).[51] Subsequently, Paulsen[52] and Nishimura[53] disclosed the use of fluoroglycosides as metabolic inhibitors of GTs.

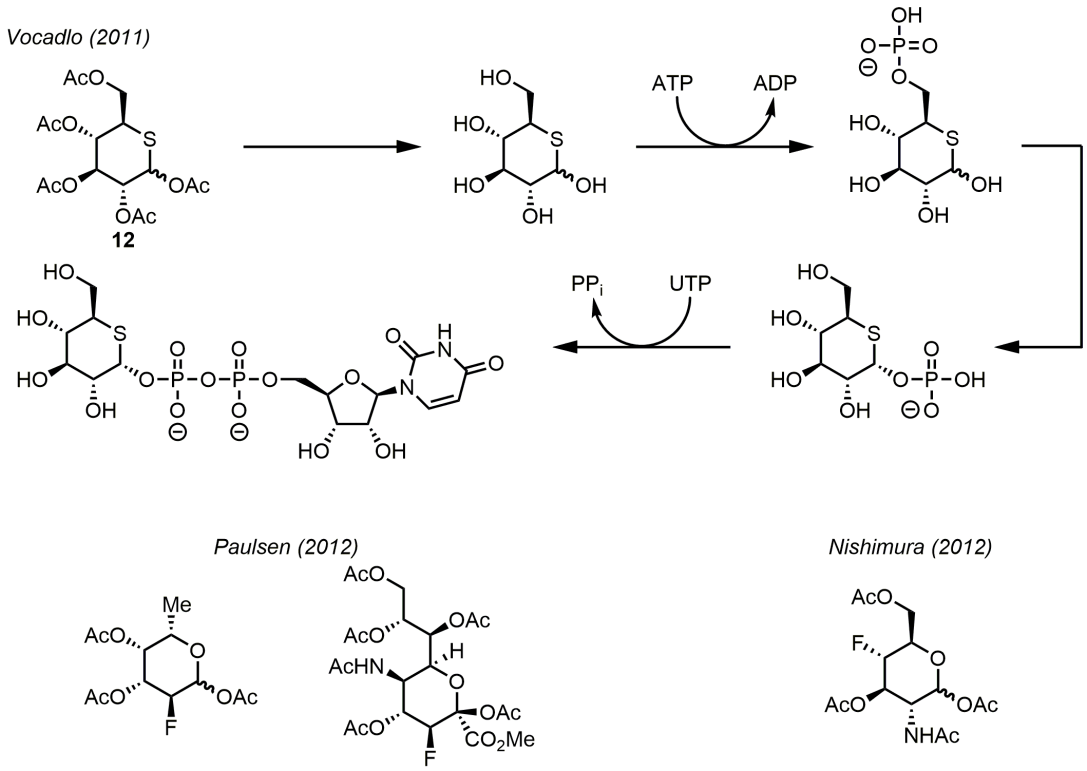

Figure 1.15 Metabolic GT inhibitor approach.

1.4. Carbohydrate Analogue Synthesis *via* Proline-Catalyzed Aldol Reactions

Carbohydrate analogues are widely used to interrogate glycan-mediated processes *in vivo*. Thus, advances in glycobiology rely on rapid access to these materials. Carbohydrate analogues have traditionally been synthesized from naturally occurring carbohydrates (chiral pool materials).[54] The advantages of this approach are the (typically) low cost of chiral pool materials and the assurance of enantiomeric purity of the final products. However, the fundamental drawback of the chiral pool approach is the difficulty of chemically distinguishing between hydroxyl groups, which frequently results in the requirement for numerous protecting group manipulation steps. Additionally, chiral pool syntheses may be unsuitable for the preparation of multiple carbohydrate analogues from a common intermediate. These drawbacks have often made the preparation of carbohydrate analogues exceedingly laborious. Thus, glycobiology stands to benefit from more concise and modular synthetic approaches for carbohydrate analogue synthesis.

1.4.1. Historical Development of Proline-Catalyzed Aldol Reactions

The key step of carbohydrate biosynthesis is the coupling of an activated α-hydroxyketone and an aldehyde (Figure 1.16). This reaction rapidly builds complexity by simultaneously forming one carbon-carbon bond and setting two stereogenic centres. Type I aldolases (found in mammals) employ an enamine as the nucleophilic coupling partner, whereas type II aldolases (found in bacteria) employ a zinc enolate.[55]

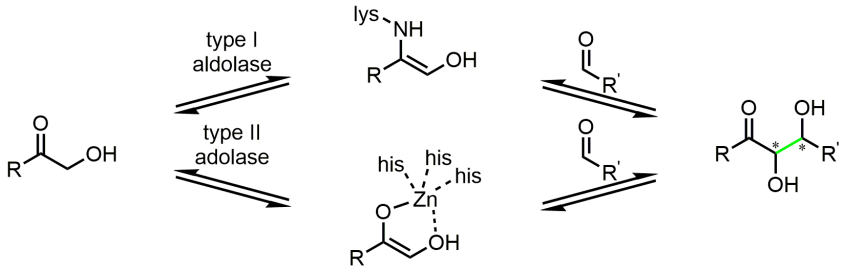

Figure 1.16 Aldol reactions in Nature.

To date, most aldol methodologies utilize the preformation of a nucleophilic metal enolate in a manner analogous to type II aldolases.[56,57,58] The following discussion will

focus exclusively on the translation of type I aldolase chemistry to the arena of *de novo* carbohydrate synthesis.

In the context of steroid synthesis, Eder, Sauer, and Wiechert reported the first proline-catalyzed intramolecular aldol condensation.[59] Independently, Hajos and Parrish discovered milder reaction conditions which permit isolation of the presumed β-hydroxy ketone intermediate.[60] Of note, these reactions convert an achiral feedstock into a highly enantioenriched product.

Scheme 1.1 First Proline-Catalyzed Aldol Reactions

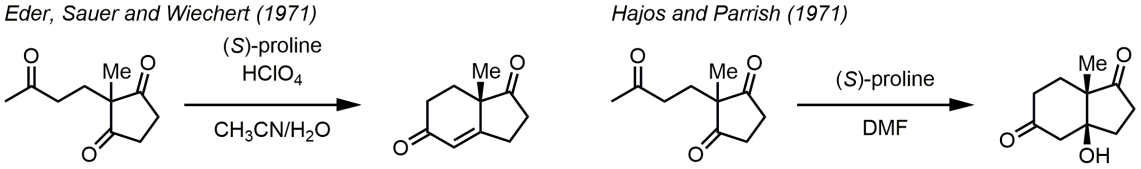

Remarkably, the proline-catalyzed *inter*molecular aldol reaction did not appear in the chemical literature for almost three decades. In 2000, List reported the reaction of acetone with various aldehydes to afford highly enantioenriched β-hydroxy ketones.[61] The aldol acceptor scope was mostly limited to benzaldehyde derivatives since α-unbranched aldehydes are prone to self-aldolization in the presence of proline.[62,63] Importantly, one α-branched aliphatic aldehyde (isobuteraldehyde) was reported to be a "well-behaved" aldol acceptor. Expanding on this work, List reported the coupling of hydroxyacetone with α-branched aliphatic aldehydes.[64] The aldol acceptor scope contained one example of an α-oxygenated aldol acceptor which was used in the assembly of a polyol framework. This reaction suggested the potential of organocatalytic aldol chemistry for *de novo* carbohydrate synthesis. A follow-up experiment employing dihydroxyacetone as the aldol donor was met with limited success as the aldol reaction proceeded with almost no stereoselectivity.[65] This limitation was resolved by Enders who reported that protection of dihydroxyacetone as the corresponding acetonide results in a highly stereoselective aldol reaction. Enders exploited this strategy to prepare the naturally occurring carbohydrate D-psicose.[66]

Scheme 1.2 Development of Proline-Catalyzed Aldol Reactions

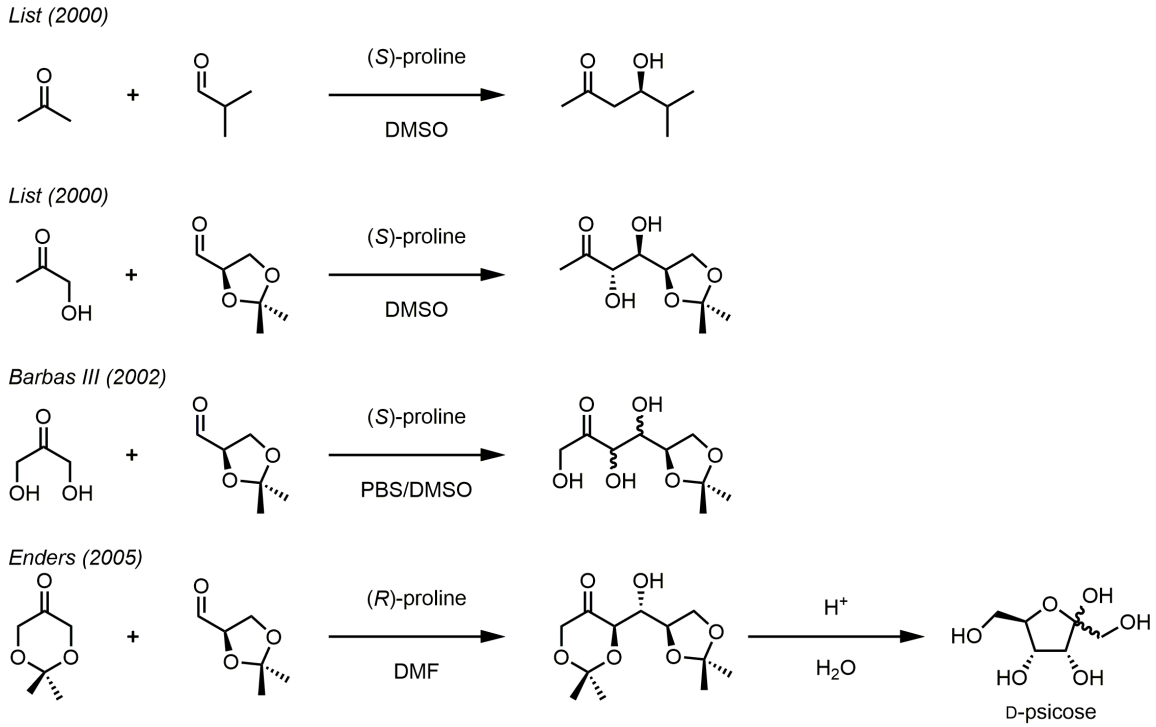

In an ingenious application of these precedents, MacMillan reported that the proline-catalyzed dimerization of α-oxy aldehydes[62] can be interfaced with Mukaiyama aldol chemistry to rapidly assemble orthogonally protected hexose monosaccharides.[67] Remarkably, the stereochemical outcome of the Mukaiyama aldol reaction was tuned by the choice of Lewis acid, solvent, and temperature. This enabled the preparation of glucose, mannose, and allose derivatives from a common intermediate.

Scheme 1.3 MacMillan's Two-Step Synthesis of Orthogonally Protected Hexoses

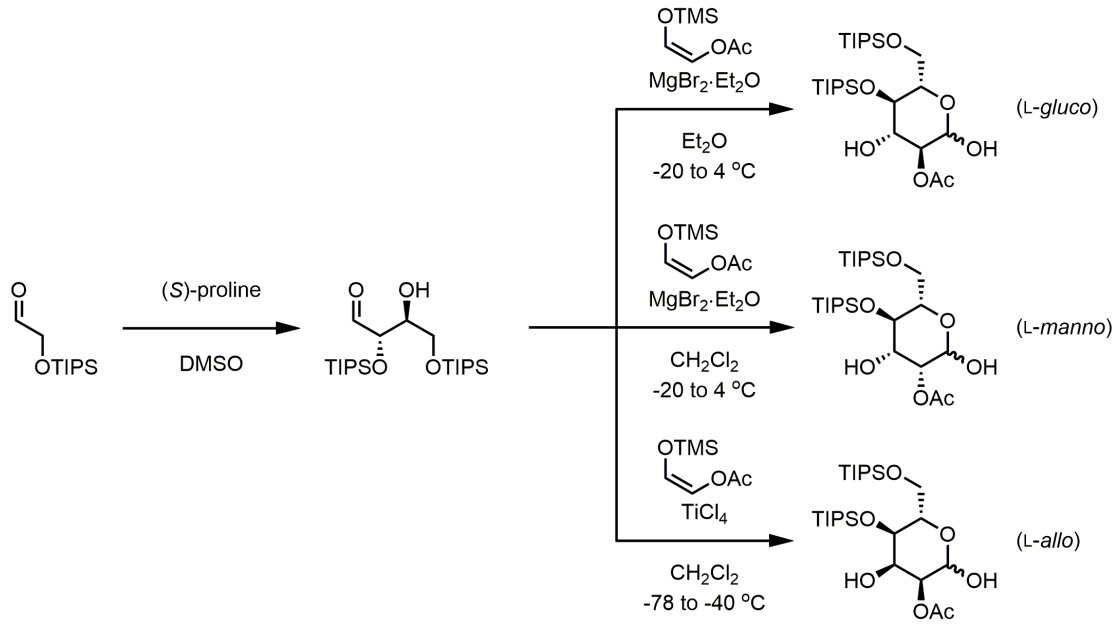

1.4.2. Mechanistic Aspects of Proline-Catalyzed Aldol Reactions

Enamines have long been thought to be the nucleophilic species involved in the product-determining step of proline-catalyzed aldol reactions.[68] To rationalize the stereochemical outcome of the coupling of hydroxyacetone with aldehydes, List invoked a Zimmerman-Traxler[69] chair TS in which the enamine hydroxyl and aldehyde R group occupy equatorial positions (Figure 1.15), which would lead to the (*R*,*S*)-configured product.[61,64] The key features of this hypothesis are: 1) proton transfer from the carboxylic acid to the forming alkoxide group, 2) *E* configuration of the enamine double bond, and 3) an s-*trans* conformation of the enamine exocyclic carbon-nitrogen bond.

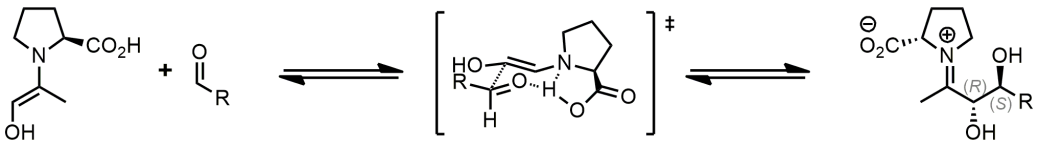

Figure 1.17 First proposed TS for proline-catalyzed intramolecular aldol reaction.

This proposal was subsequently refined by List and Houk who discarded a chair TS since the enamine nitrogen cannot hydrogen bond and assist in nucleophilic attack simultaneously. By a computational appraisal of various plausible TSs, List and Houk

noted that TSs with a s-*trans* enamine conformation are lower in energy, and that a dihedral angle of -60° for the forming carbon-carbon bond is most favourable. For the aldol addition of cyclohexane to isobuteraldehyde, List and Houk found that the lowest energy TS is the one depicted in Figure 1.18.[70]

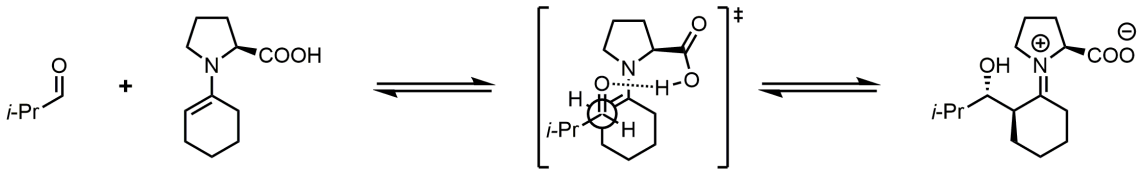

Figure 1.18 List-Houk TS.

Experimental support for this model was reported by Gschwind, who provided NMR spectroscopic characterization for the enamine arising from (*S*)-proline and propanal.[71] This species has a double bond configuration and a s-*trans* conformation about the exocyclic carbon-nitrogen bond, which is consistent with the List-Houk model.

It must be emphasized that the predominant intermediate in proline-catalyzed aldol reactions is not an enamine but rather its oxazolidinone regioisomers, which were calculated to be ~10 kcal/mol lower in energy in the gas phase.[72] Indeed, enamine intermediates have not been observed in acetonitrile or dichloromethane but only in DMSO and DMF which strongly solvate carboxylic acids.[71,72] The prevailing interpretation of these observations is that oxazolidinones are not product-determining species but rather off-cycle, "dead end" intermediates.[73] Seebach and Eschemoser challenged this viewpoint by assigning a product-determining role to oxazolidinones.[74] Their alternative model features an s-*cis* enamine carboxylate as the nucleophile since the s-*trans* conformer would give rise to the less stable *endo* oxazolidinone. The stereodefining feature of this TS is concerted antiperiplanar addition across the enamine double bond. Recent evidence suggests the Seebach-Eschemoser mechanism may operate, but only in the presence of stoichiometric base (Figure 1.17).[75,76]

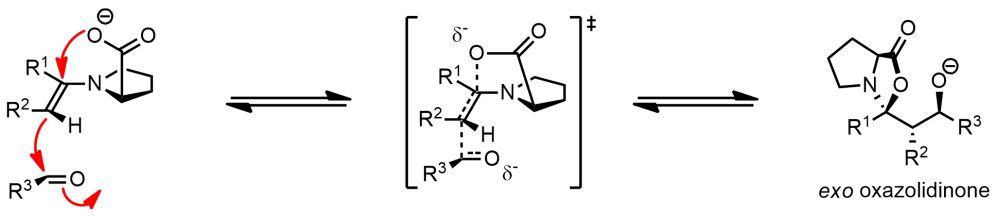

Figure 1.19 Seebach-Eschenmoser TS.

The most commonly accepted catalytic cycle for proline-catalyzed aldol reactions is depicted in Figure 1.20. Computational studies support the role of imminium carboxylates as fleeting, "central" intermediates[77] and enamine formation *via* intramolecular proton transfer of imminium carboxylates.[78]

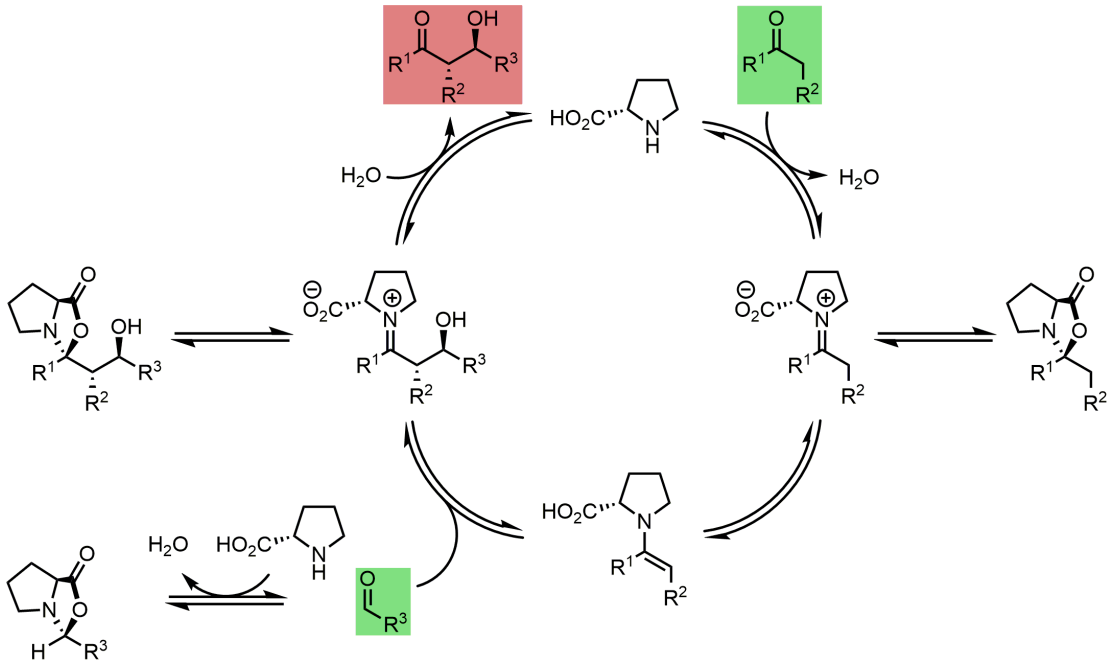

Figure 1.20 Catalytic cycle of proline-catalyzed aldol reactions.

1.4.3. Proline-Catalyzed Chlorination/Aldol Reactions

In 2013, Britton reported the proline-catalyzed coupling of the Enders dioxanone with α-chloroaldehydes.[79] In this one-pot process, proline catalyzes the chlorination of an α-unbranched aldehyde to afford a nearly racemic mixture of α-chloroaldehyde enantiomers *in situ*. This circumvents the safety and instability issues associated with the isolation of α-chloroaldehydes.[80,81] In the subsequent aldol reaction, there is a kinetic bias for consumption of one chloroaldehyde enantiomer over the other. Since the α-chloroaldehyde enantiomers rapidly equilibrate, there is a dynamic kinetic resolution of the chloroaldehyde feedstock. These factors permit the construction of the 1,2-*anti*, 2,3-*syn* framework depicted below.

Scheme 1.4 Proline-Catalyzed Chlorination/Aldol Reaction

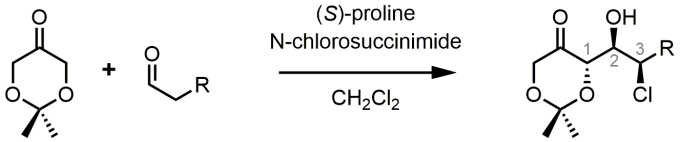

This reaction's 2,3-*syn* selectivity may be rationalized using a modified List-Houk model in which there are two possible TSs that are epimeric at the chloromethine centre. The favoured TS minimizes both steric repulsion between the aldehyde R group and the dioxanone moiety as well as dipole interactions between proximal C-Cl and C-O σ bonds.

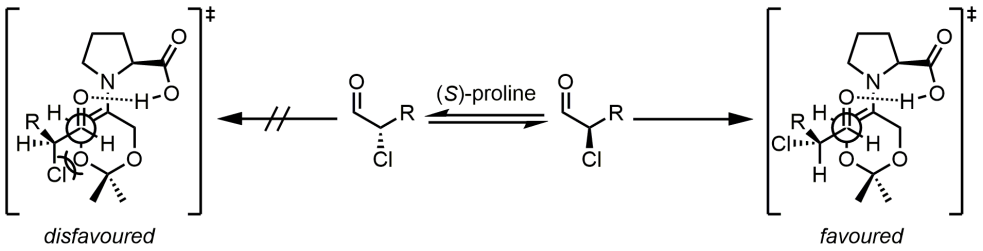

Figure 1.21 Proposed TS for chlorination/aldol reaction.

In subsequent studies, Britton and co-workers directed this methodology toward the synthesis of *ribo*-configured *C*-nucleoside analogues, which have attracted attention as inhibitors of nucleoside processing enzymes.[82] Aldol adduct **13** was subjected to 1,3-*syn* ketone reduction, intramolecular chloride displacement and acetonide deprotection to afford *C*-nucleoside analogue **14**.[79] In an similar manner, compound **13** was subjected to 1,3-*syn* reductive amination, cyclization, and deprotection to afford nucleoside hydrolase inhibitor **15**.[83]

Scheme 1.5 Britton's Synthesis of *C*-nucleoside Analogues

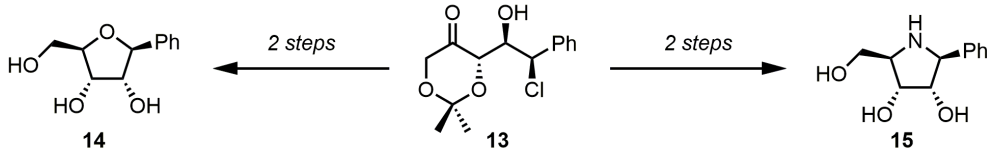

Chapter 2.

Mechanistic Probes for Covalent Inhibition of a GH 36 α-Galactosidase

Enzyme kinetic assays were performed by Saideh Shamsi in the laboratory of Andrew Bennet (Simon Fraser University). X-ray crystallographic studies were performed by Robert Pengelly in the laboratory of Tracey Gloster (St. Andrew's University).

2.1. Introduction

2.1.1. GH Inhibition by Non-Classical Carbocation Formation

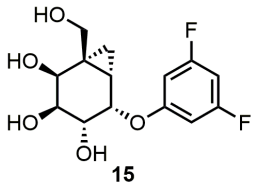

15

Figure 2.1 Covalent *Tm*GalA inhibitor (15).

In 2014, Bennet and co-workers disclosed the synthesis of carbagalactoside analogue **15** and its evaluation as a covalent inhibitor of the GH 36 enzyme *T. Maritima* α-galactosidase (*Tm*GalA).[84] This inhibitor represents a radical departure from previous designs since it features a cyclopropyl moiety in lieu of the usual pyranoside ring oxygen. Incubation of inhibitor **15** with *Tm*GalA resulted in a time-dependent loss of enzyme activity, which proceeds from the Michaelis (E:I) complex with a half-life of ca. 2.5 minutes at physiological pH and temperature. Upon dialysis of excess inhibitor **15**. *Tm*GalA regained its catalytic activity with a half-life of ca. 45 minutes. This reactivation was attributed to turnover of the covalent adduct to give hydrolyzed inhibitor. Tryptic MS/MS mapping established that inactivation occurs by the alkylation of the catalytic nucleophile residue D327, which demonstrated in conjunction with kinetic studies that

compound **15** is a *bona fide* mechanism-based inhibitor. These promising results established this compound as a starting point toward development of a new class of broadly applicable covalent GH inhibitors.

At this juncture the design of inhibitor **15** warrants explanation. The presence of a cyclopropane geminal to a leaving group dramatically accelerates S_N1 solvolysis; this stereoelectronic effect results from the formation of a non-classical bicyclobutonium cation.[85] Based on this precedent, inhibitor **15** likely forms a discrete cationic intermediate within the *Tm*GalA active site. There is a stringent geometric requirement for stabilization of a carbocation by the cyclopropyl group: the dihedral angle θ must allow for the overlap of the vacant p orbital with one of the proximal cyclopropane C-C σ bonding orbitals. With respect to compound **15**, participation of the cyclopropyl group requires that the C(1)-C(2) bond must bisect the cyclopropane ring. The two conformations that satisfy this requirement are $^3H_2$ and $^{1,4}B$.

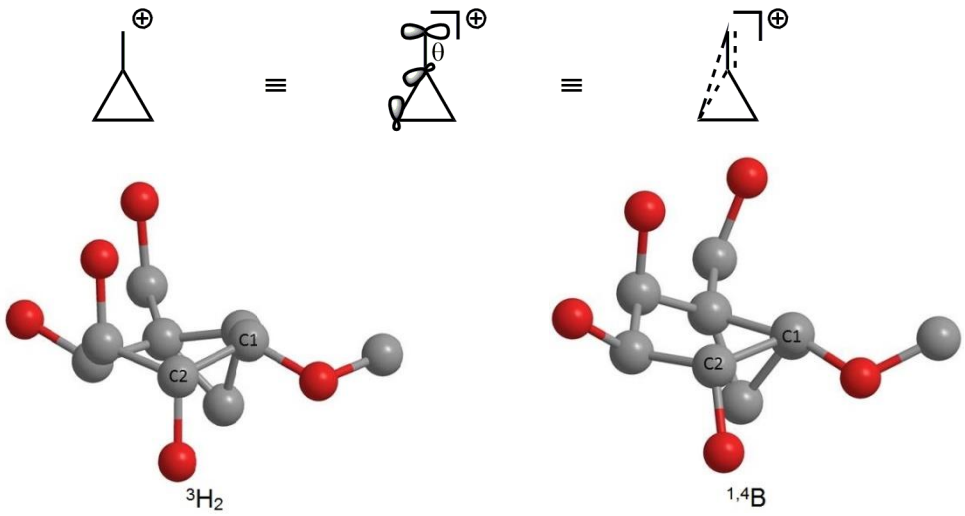

Figure 2.2 Cyclopropane participation in inhibitor (15).

To gain an intimate mechanistic understanding of this process, Bennet and co-workers used X-ray crystallography to determine the structures of the intermediates along the reaction coordinate.[86] Soaking of preformed galactosidase crystals in a solution of inhibitor **15** afforded an enzyme-substrate complex, which on standing for one week gave an enzyme-product complex.

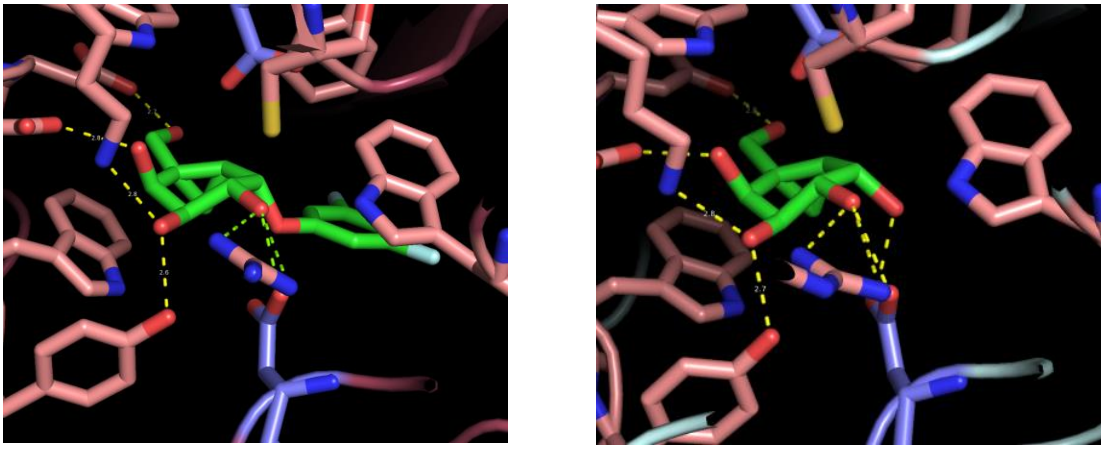

Figure 2.3 X-ray crystal structures of enzyme-substrate and enzyme-product complexes for reaction of inhibitor (15) with *Tm*GalA.

However, no crystallization protocol was successful for determining the structure of the covalent intermediate. As this intermediate hydrolyzes with a half-life of 45 minutes, it proved too reactive to be observed crystallographically. Thus, Bennet and co-workers were unable to address two critical mechanistic questions relating to the covalent inhibition of *Tm*GalA by compound **15**:

1. Given that cyclopropyl carbinyl compounds rearrange upon solvolysis[87], does covalent inhibition proceed with rearrangement of the bicyclo[4.1.0] inhibitor scaffold?
2. If rearrangement does not occur, what is the inhibitor's conformation in the covalent adduct?

A rigorous understanding of any reaction's mechanism entails structural knowledge of all species along the reaction coordinate. To this end, a new approach for determining the structure of the inhibitor-enzyme adduct was conceived.

2.1.2. Proposed Synthetic Targets

Analogues of inhibitor **15** which give rise to longer-lived covalent adducts could serve as mechanistic probes for determination of the inhibitor-enzyme adduct's crystal structure. Our design rationale was inspired by that of the 2-deoxy-2-fluoroglycosides pioneered by Withers and co-workers. In enzymatic glycoside hydrolysis, hydrogen bonding between enzymic residues and the C(2) hydroxyl plays only a minor role in substrate binding[88] but stabilizes the TS by approximately 8 kcal/mol.[45] Thus,

replacement of the C(2) hydroxyl of **15** with either a fluorine[43] or hydrogen[89] was anticipated to slow both the glycosylation and deglycosylation steps (*vide supra*). To ensure that glycosylation would still proceed at a reasonable rate, a much more reactive leaving group would be required. With these considerations in mind, we proposed the synthesis of compounds **16a** and **16b**.

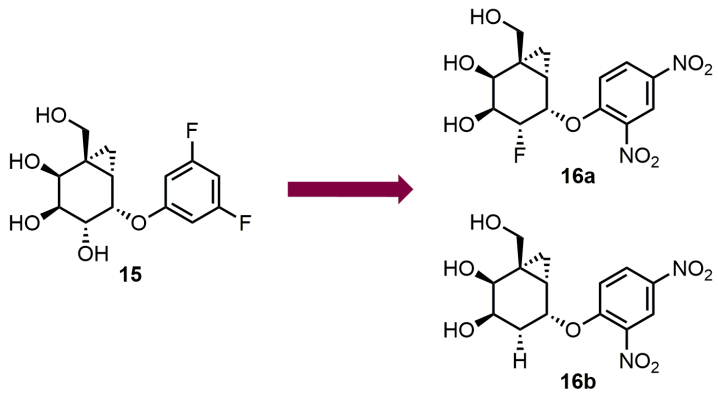

Figure 2.4 Proposed modifications to inhibitor (15).

2.2. Synthesis

2.2.1. Retrosynthetic Analysis

The carbagalactoside targets **16a** and **16b** were traced back to intermediates **17a** and **17b** *via* a series of three functional group interconversions. These two compounds could arise from opening of the epoxide function in epoxyketone **18**. Owing to the presense of the adjacent carbonyl in **18,** this reaction was expected to occur preferentially at C(2). Epoxyketone **18** could arise from an intramolecular cyclopropanation[90] of diazoketone **19**, which could in turn arise from β-ketochlorohydrin **20** *via* a series of four functional group interconversions. We anticipated that **20** could be prepared in a stereoselective manner from C_3 building blocks **21** and **22** using the chlorination/aldol methodology described by Britton and co-workers.[79]

Scheme 2.1. Retrosynthesis of Mechanistic Probes (16a) and (16b)

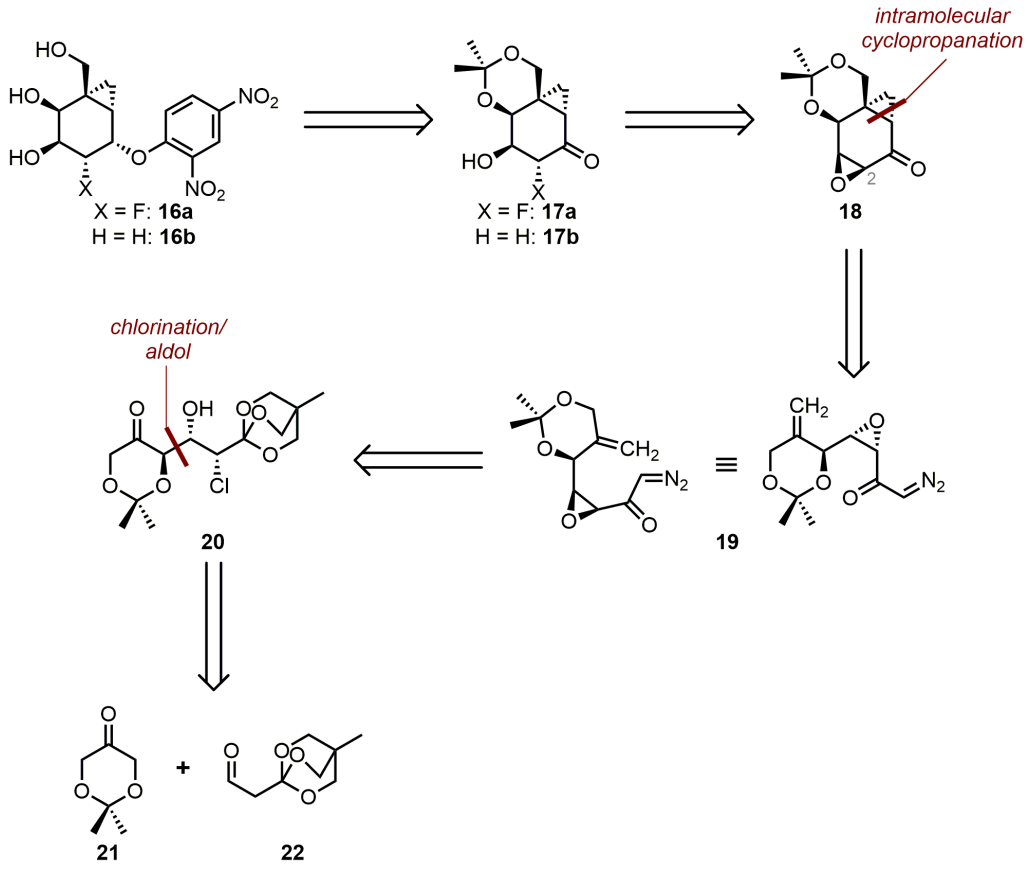

2.2.2. Synthesis of Aldehyde (22)

At the onset of these studies, a synthesis of aldehyde **22** had been developed by Taron.[91] However, the need to prepare **22** on decagram scale ruled against chromatographic separations, and so further optimization of the route was required. Heating of oxetane **23** in the presence of an excess of diethylmalonate gave a clean transesterification; diester **24** was purified simply by removal of excess diethylmalonate by short path vacuum distillation. Exposure of diester **24** to boron trifluoride etherate effected rearrangement to orthoester **25**; to avoid a difficult chromatographic separation the crude product was filtered through a pad of neutral alumina to remove polar impurities and then crystallized from hexanes/ethyl acetate. Treatment of compound **25** with 1.3 equivalents of DIBAL-H afforded aldehyde **22** with no over-reduction to the corresponding alcohol. Notably, a higher yield was obtained when dichloromethane was employed as the solvent instead of toluene. As the crude aldehyde was judged to be of

>90% purity by ^{1}H NMR, it was advanced directly to the next step without further purification. Using this optimized protocol, ca. 50 g of aldehyde **22** was prepared.

Scheme 2.2. Scalable Route to Aldehyde (22)

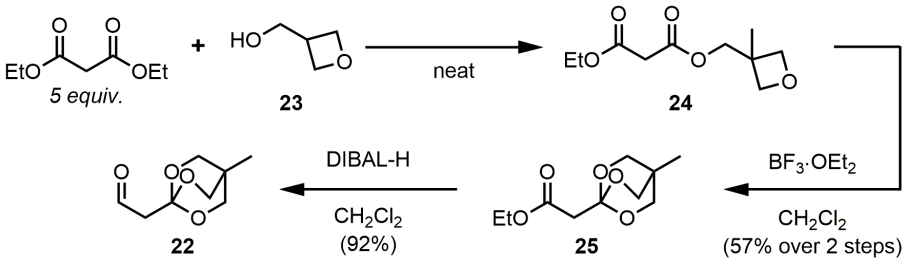

2.2.3. Preparation of β-Ketochlorohydrin (20)

The first key step in the synthesis is the assembly of β-ketochlorohydrin **20** using chlorination/aldol methodology.[79] This reaction proceeded smoothly to set three of the six contiguous stereocentres present in the target carbagalactosides. Notably, the product can be obtained in analytically pure form by precipitation from diethyl ether, thus obviating chromatographic separation.

Scheme 2.3 Proline-Catalyzed Chlorination/Aldol Reaction

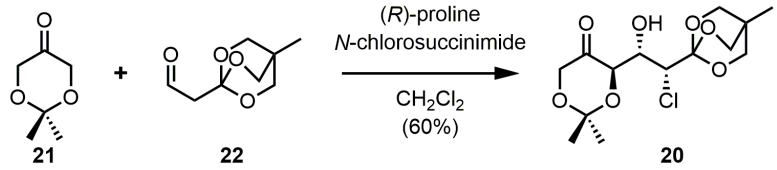

In order to determine the *ee* of this reaction product, chiral HPLC analysis was explored. Unfortunately, resolution of the enantiomeric chlorohydrins *rac*-**20** (prepared using *rac*-proline as the catalyst) was unsuccessful. Thus, the (*R*)- and (*S*)-MTPA esters[92] of β-ketochlorohydrin **20** were prepared and their crude ^{1}H NMR spectra were analyzed.

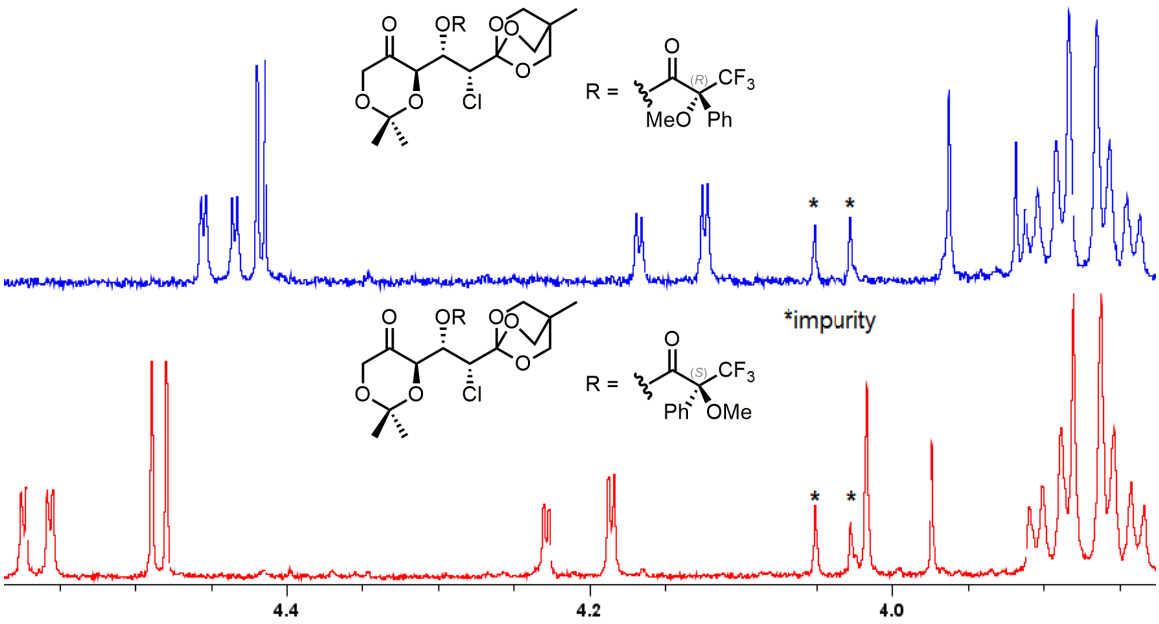

Figure 2.5 Expansion of ^{1}H NMR spectra of crude MTPA esters derived from β-ketochlorohydin (20) ($CDCl_3$, 400 MHz).

As each spectrum shows the presence of only one diastereomer, compound **20** prepared by this method can be safely estimated to possess an *ee* of 90% or higher.

2.2.4. Preparation of Diazoketone (19)

Aldol adduct **20** was next subjected to Julia-Kocienski olefination[93] to afford compound **26**. The use of tetrazole-based sulfone **27** resulted in higher yields and easier purification as compared to benzothiazole-based sulfone **28**. Base-induced epoxide formation (lithium hydroxide, 1,4-dioxane/water, 100 °C) of alkene **26** proceeded at an extremely slow rate. This may be attributed to the steric clash between the orthoester group and the dioxane moiety *en route* to the *cis*-epoxide. Thus, we decided to defer epoxide formation to a later step. Hydrolysis of the orthoester to afford triol **29** was achieved using pyridinium *p*-toluenesulfonate. The use of 1,4-dioxane as solvent in this deprotection minimized undesired hydrolysis of the acetonide protecting group. At this stage, heating triol **29** with sodium hydroxide resulted in saponification as well as chloride displacement to forge the required epoxide functional group. The $^{3}J_{HH}$ coupling constant of 4.5 Hz between geminal epoxide protons was in line with expectations for a *cis*-disubstituted epoxy acid.[94]

The instability of carboxylic acid **30** proved to be a significant challenge. Acidification of the reaction mixture to permit extraction of **30** into organic solvent resulted only in decomposition. Thus, isolation of **30** was achieved by chromatographic separation of the concentrated reaction mixture. As **30** decomposes on standing, it was immediately coupled with TMS-diazomethane to afford diazoketone **19**. This material exhibited a broad ^{1}H NMR resonance δ 5.77 ppm as well as an intense infrared absorption at 2110 cm^{-1}, which confirmed the presence of the diazoketone functional group.

Scheme 2.4 Synthetic Route to Diazoketone (19)

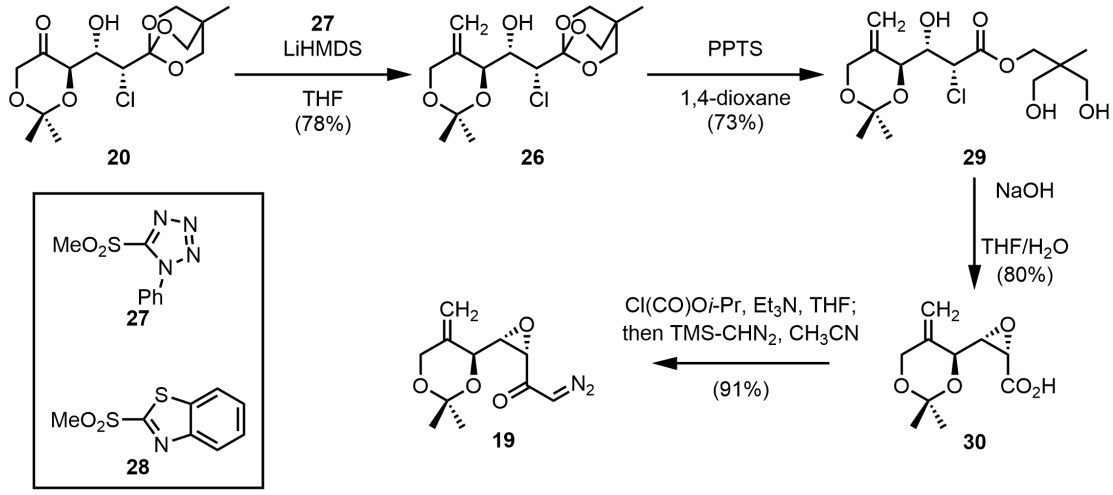

2.2.5. Intramolecular Cyclopropanation

With diazoketone **19** in hand, we next turned our attention to the second key step of the synthesis: intramolecular cyclopropanation. Initial attempts to effect this reaction were plagued with significant formation of an aldehyde by-product that was assigned as aldehyde **31** based on ^{1}H and ^{13}C NMR data of crude reaction mixtures. As this by-product proved to be unstable on silica, it was not possible to isolate it and carry out complete characterization. Considering existing precedent, aldehyde **31** likely arises from water insertion[95] into the rhodium carbenoid intermediate to afford an α-hydroxyketone that rapidly isomerizes to form enal **31** (Scheme 2.5). Armed with this knowledge, rigorous exclusion of moisture avoided formation of enal **31**.

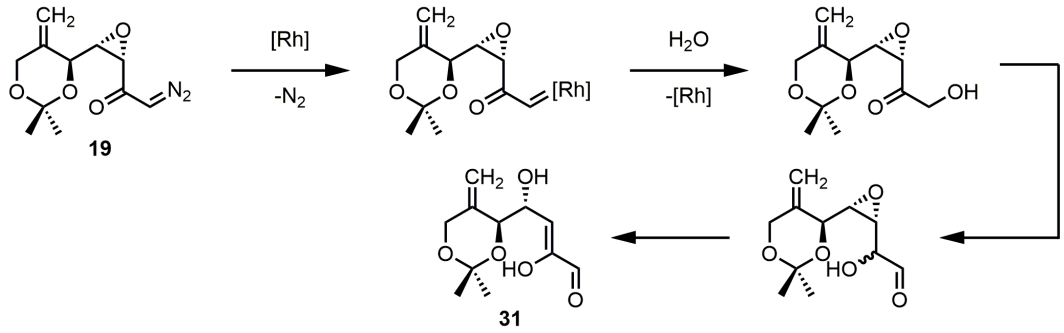

Figure 2.6 Proposed pathway for formation of aldehyde (31).

As depicted in Figure 2.6, it was expected that the C-C insertion could occur at either face of the alkene function in the diazoketone **19**, and consequently the crude reaction product was expected to contain a mixture of diastereomers **18** and **18'**. However, only one cyclopropyl diastereomer was observed by ^{1}H NMR spectroscopic analysis of crude reaction mixtures, where product detection was made simple owing to the characteristic chemical shifts of cyclopropyl protons, which resonate in a typically unoccupied region of ^{1}H NMR spectra below 0.8 ppm. While the reason for the high degree of diastereoselectivity in this reaction is not fully understood, it is worth noting that inspection of Dreiding models suggested that **18'** possesses much more ring strain than **18.** It is not unreasonable then to expect that this ring strain would affect the relative energies of the transition structures leading to either product. To determine the stereochemical configuration of the sole cyclopropane-containing product, a series of one-dimensional NOESY experiments were performed. From these experiments, a crucial nOe enhancement was observed between H_a (δ 4.46 ppm) and H_b (δ 0.69 ppm) that established spatial proximity of these two protons on the concave face of the bicyclo[4.1.0] carbon framework.

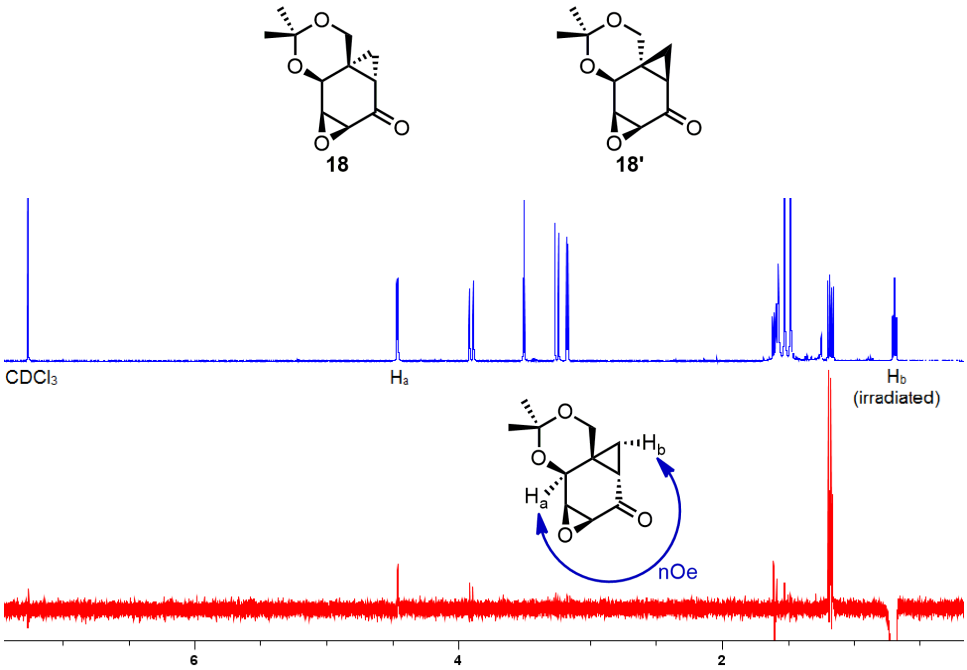

Figure 2.7 nOe analysis of epoxyketone (18).

When the cycloaddition was repeated with catalytic $Rh_2(OAc)_4$ and dichloromethane as the solvent, the reaction yielded a mixture of desired product **18** and undesired regioisomer **32** in a ca. 3:1 ratio. The spirocyclic compound **32** arises from insertion into an allylic C-H bond; this process is known to proceed with retention of stereochemistry.[96] The use of catalytic $Rh_2(octanoate)_4$ and $Rh_2(caprolactam)_4$ with dichloromethane as solvent gave comparable results; other combinations of catalysts and solvents gave inferior results as summarized in Table 2.1.

Table 2.1. Conditions for Intramolecular Cyclopropanation

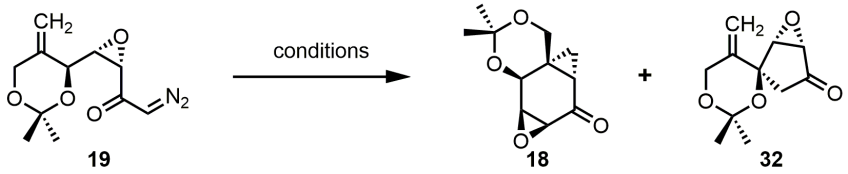

19 18 32

modification from "standard conditions": 1 mol % $Rh_2(OAc)_4$, CH_2Cl_2 ([**19**] =100 mM), RT	result (**18** : **32**)
C_6D_6 instead of CH_2Cl_2	1 : 1
$CDCl_3$ instead of CH_2Cl_2	2 : 1
THF instead of CH_2Cl_2	complex mixture
CuI instead of $Rh_2(OAc)_4$	no reaction
Rh_2(octanoate)$_4$ instead of $Rh_2(OAc)_4$	3 : 1
Rh_2(caprolactam)$_4$ instead of $Rh_2(OAc)_4$	3 : 1; other minor byproducts observed
Rh_2(heptafluorobutyrate)$_4$ instead of $Rh_2(OAc)_4$	complex mixture
$Pd(OAc)_2$ instead of $Rh_2(OAc)_4$	trace **18**, complex mixture

As epoxyketone **18** was observed to be unstable on silica, the isolated yields for the cyclopropanation ranged from 30 to 40%. Thus, crude **18** was generally used directly in the next step.

2.2.6. Elaboration of Epoxyketone (18) to the Carbagalactoside Targets

Having secured the bicyclo[4.1.0] carbon framework of the synthetic targets, our remaining tasks were epoxide opening, ketone reduction, arylation, and deprotection. Towards these goals, crude **18** was treated with TBAF to give fluorohydrin **17a**. The moderate yield of this transformation was attributed to the formation of an unidentified polar by-product. The use of (n-Bu)$_4HF_2$ or (n-Bu)$_4HF_3$ as the fluoride source gave **17a** in

approximately the same yield whereas the use of $Et_3N{\cdot}3HF$ gave only decomposition. Alternatively, epoxyketone **18** was opened in good yield using $PhSeSeCl/NaBH_4$ as a nucleophilic hydride source to afford β-hydroxyketone **17b**.

Scheme 2.5 Epoxide Opening Reactions of Epoxyketone (18)

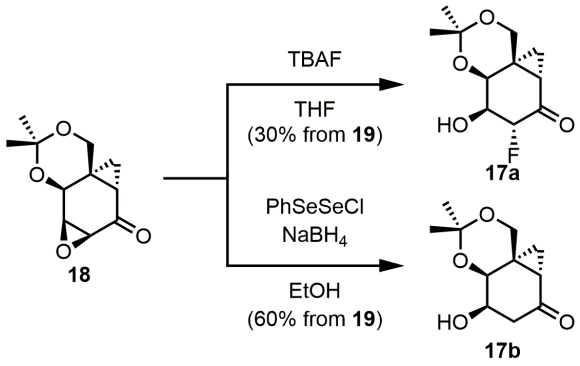

As a fluorine atom is an excellent handle for characterization by NMR spectroscopy, we judged it wise to first develop a route from **17a** to target **16a.** To identify conditions for ketone reduction, a screen of borohydride reagents was performed on fluorohydrin **17a**. Gratifyingly, L-Selectride® reduction delivered diol **33** with complete diastereoselectivity. We reasoned that the cyclopropyl methylene renders the bottom face of **17a** sterically inaccessible to reduction by the bulky tri-*sec*-butyl borohydride anion. Of note, the large difference in $^3J_{HF}$ between the C(1) proton and C(2) fluorine requires a nearly eclipsed C(1)-C(2) dihedral in both epimers.[97,98] This requirement enabled stereochemical assignment of the two epimeric alcohols.

Table 2.2. Ketone Reduction Reactions of (17a)

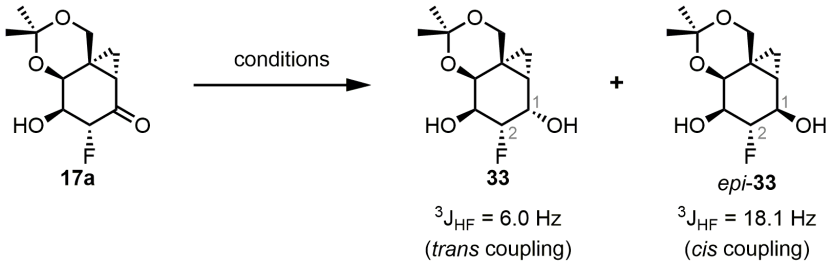

conditions	**33** : *epi*-**33**
$NaBH_4$, MeOH, RT	1 : 1.5
$NaBH_4$, $CeCl_3$, MeOH, RT	0 : 1
L-Selectride®, -78 °C	1 : 0

At this stage, it was hoped that the C(1) hydroxyl of **33** could be converted to the corresponding dinitrophenyl ether in the presence of the free C(3) hydroxyl. Attempts to arylate **33** under anionic conditions (KHMDS/LiHMDS, 2,4-DNFB, DMF) gave only decomposition or recovered starting material. When **33** was subjected to the conditions developed by Koeners and co-workers,[99] C(3) arylation predominated, giving rise to undesired regioisomer **34** as the major product.

Scheme 2.6 Attempted Arylation of Diol (33)

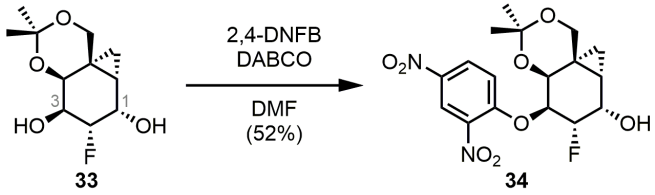

Accordingly, we reasoned that the C(3) hydroxyl should be protected prior to arylation. Thus, acetylation of **17a** followed by L-Selectride® reduction delivered **36a**. At this stage, arylation of **36a** using the Koeners protocol[99] proceeded very slowly; heating the reaction mixture resulted only in decomposition. Gratifyingly, substitution of DABCO

with quinuclidine resulted in the formation of dinitrophenyl ether **37a** in good yield. Finally, two step deprotection delivered target **16a**. β-hydroxyketone **17b** was then advanced to target **16b** in a parallel manner.

Scheme 2.7 Completion of the Carbagalactoside Syntheses

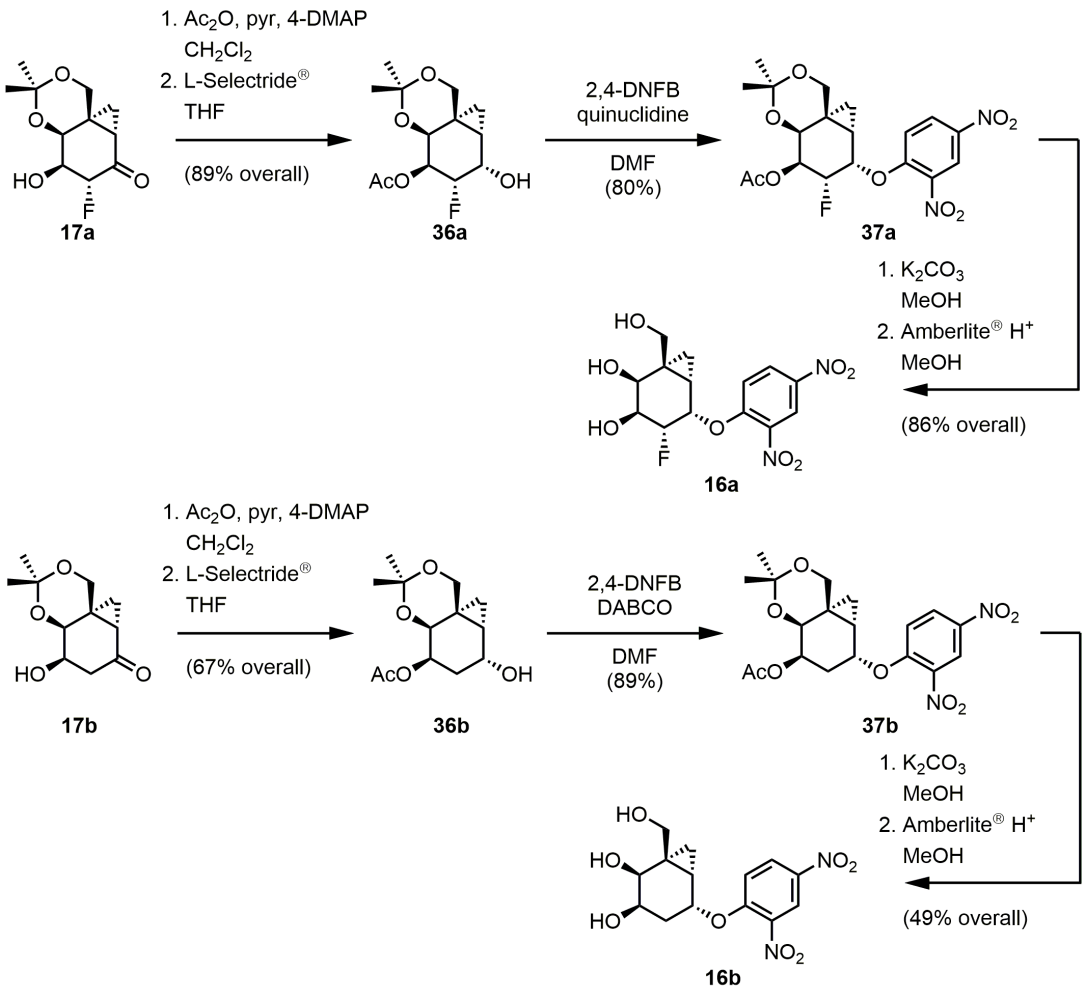

2.3. Kinetic Studies

Having prepared ample quantities of galactoside analogues **16a** and **16b**, we proceeded to identify conditions for the generation of a covalent inhibitor-enzyme adduct. Kinetic assays were used to measure the rate of formation of this covalent

adduct. In these assays, each probe was incubated with *Tm*GalA and the enzyme activity was monitored over time.

Unfortunately, **16b** displayed no measurable reactivity toward its target at room temperature: there was no time-dependent loss of enzyme activity. Heating the reaction mixture to 60 °C resulted only in non-enzymatic hydrolysis of **16b**, as indicated spectroscopically by the formation of the dinitrophenolate anion (λ = 400 nm).

Gratifyingly, probe **16a** possessed moderate activity against its target enzyme, as time-dependent loss of enzyme activity was noted (Figure 2.8a). While there was no measurable inactivation at room temperature, incubation at 60 °C resulted in the tagging of *Tm*GalA with a half-life of approximately 45 minutes. We reasoned that a 48 hour incubation period (64 half-lives) would permit essentially quantitative formation of the covalent adduct. Measurement of initial inactivation rate (V_0) at variable concentrations of **16a** (Figure 2.8b) and nonlinear fitting of the data were used to determine a binding constant (K_i) of ca. 320 μM.

a) **b)**

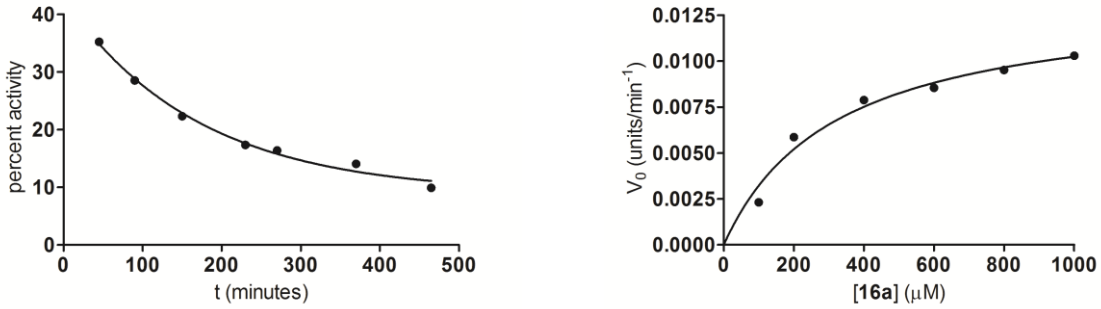

Figure 2.8 **a) Activity vs. time plot for *Tm*GalA in the presence 200 μM (16a), 60 °C; b) Michaelis-Menten plot for inactivation of *Tm*GalA by (16a).**

2.4. Crystallographic Studies

Having devised a protocol for generation of a stable inhibitor-enzyme adduct, our collaborators next used X-ray crystallography to determine the structure of this species by crystallizing the covalent adduct and then collecting and solving X-ray diffraction data. Of note, the resolution of the crystallographic data (1.45 Å) enabled us to confidently assign the structure and conformation of the covalent adduct.

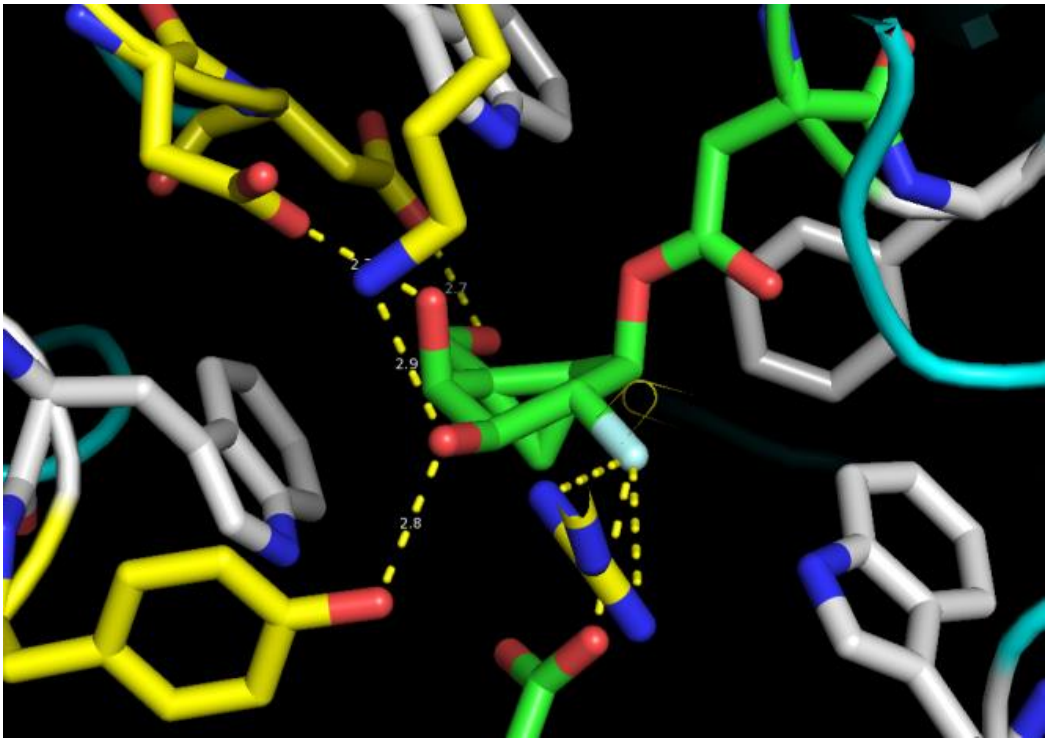

Figure 2.9 Active site structure of covalent adduct arising from (16a) and *Tm*GalA

As shown in Figure 2.9, the cyclopropane ring remains intact in the covalent adduct. Thus, covalent inactivation does not proceed with rearrangement to afford either a ring-opened homoallyl system or a change in the cyclopropyl ring stereochemistry. Additionally, we note that the pseudo-saccharide ring adopts an E_3 conformation. This is surprising since both the enzyme-substrate and enzyme-product complexes possess a $^2H_3$ conformation (*vide supra*).

2.5. Conclusion

A synthetic strategy involving a proline-catalyzed chlorination/aldol reaction and a Rh-catalyzed carbocyclization was successfully implemented in the synthesis of two mechanistic probes for the covalent inhibition of a GH 36 α-galactosidase. One of these compounds was used to determine the structure of the covalent intermediate that arises from this inhibition process. Structural knowledge of the species on both sides of the inactivation TS will allow us to interpolate the structure of this TS using computational

methods. We anticipate this intimate mechanistic understanding will facilitate the design of broadly applicable covalent GH inhibitors.

2.6. Experimental Information

2.6.1. Synthesis Procedures and Data

Preparation of diester (24):

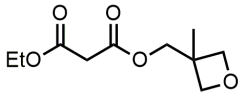

Diethyl malonate (450 mL, 2.96 mol) and 3-methyl-3-oxetanemethanol (60.0 g, 590 mmol) were stirred for 48 hours at 150 °C in a vessel equipped with a reflux condenser. The mixture was then allowed to cool to room temperature and the excess diethyl malonate was removed by short-path distillation to afford diester **24** (120 g, 555 mmol, 95%) as a colourless oil. This material (~85% pure by ^{1}H NMR) was advanced directly to the next step without further purification. To obtain an analytical sample for characterization, a small portion of the crude material was purified by column chromatography (2:1 / hexanes:EtOAc).

^{1}H NMR (400 MHz, $CDCl_3$) δ: 4.52 (d, *J* = 6.1 Hz, 2H), 4.38 (d, *J* = 6.1 Hz, 2H), 4.25 (s, 2H), 4.20 (q, *J* = 7.2 Hz, 2H), 3.42 (s, 2H), 1.34 (s, 3H), 1.28 (t, *J* = 7.2 Hz, 3H)

^{13}C NMR (101 MHz, $CDCl_3$) δ: 166.8, 166.5, 79.5, 77.4, 69.7, 61.8, 41.7, 39.2, 21.2, 14.2.

HRMS: m/z calcd. for $C_{10}H_{16}O_5Na^+$: 239.0890 (M+Na); found: 239.0892 (M+Na).

IR: 2966, 2874, 1729, 1144 cm^{-1}.

Preparation of orthoester (25):

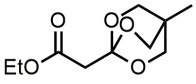

To a cooled (-15 °C) solution of diester **24** (60.0 g, 250 mmol) in CH_2Cl_2 (500 mL) was added $BF_3{\cdot}OEt_2$ (3.1 mL, 25 mmol). The mixture was stirred for 20 hours at -15 °C and then quenched by the dropwise addition of Et_3N (17.5 mL,126 mmol). After warming to room temperature, the mixture was concentrated and treated with 300 mL diethyl ether,

filtered through Celite®, and concentrated. Purification of the crude material by chromatography on a short column of neutral alumina (CH_2Cl_2) followed by recrystallization (hexanes / EtOAc) afforded orthoester **25** (36.5 g, 169 mmol, 68%) as a white powder.

^{1}H NMR (400 MHz, CD_3CN) δ: 4.06 (q, *J* = 7.1 Hz, 2H), 3.87 (s, 6H), 2.60 (s, 2H), 1.19 (t, *J* = 7.1 Hz, 3H), 0.76 (s, 3H)

^{13}C NMR (126 MHz, CD_3CN) δ: 168.2, 107.8, 73.2, 61.1, 43.6, 30.9, 14.4, 14.2.

HRMS: m/z calcd. for $C_{10}H_{17}O_5^+$: 217.1071 (M+H); found: 217.1065 (M+H).

IR: 2879, 1738, 1180, 1047 cm^{-1}.

m.p. = 53 – 56 °C.

Preparation of aldehyde (22):

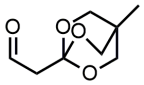

To a cooled (-78 °C) solution of orthoester **25** (8.15 g, 37.7 mmol) in CH_2Cl_2 (370 mL) was added DIBAL-H (1.0 M in hexanes, 49 mL, 49 mmol) dropwise under vigorous stirring. The reaction was then quenched by the dropwise addition of 2 mL MeOH and allowed to warm to 0 °C. After treatment with H_2O (1.5 mL), 15% aqueous NaOH (1.5 mL), and H_2O (4 mL), the cooling bath was removed and the mixture was stirred for 15 minutes. The mixture was then dried (Na_2SO_4), filtered through Celite®, and concentrated to afford aldehyde **22** (5.99 g, 35 mmol, 92%) as a colourless oil. This material (~90% pure by ^{1}H NMR) was advanced directly to the next step without further purification. To obtain an analytical sample for characterization, a small portion of the crude material was purified by column chromatography (2:1 / hexanes:EtOAc).

^{1}H NMR (400 MHz, $CDCl_3$) δ: 9.70 (t, *J* = 2.8 Hz, 1H), 3.94 (s, 1H), 2.65 (d, *J* = 2.8 Hz, 2H), 0.82 (s, 1H).

^{13}C NMR (101 MHz, $CDCl_3$) δ: 198.9, 107.0, 72.8, 49.8, 30.7, 14.6.

HRMS: m/z calcd for $C_8H_{13}O_4^+$: 173.0808 (M+H); found: 173.0829 (M+H).

IR: 2919, 1684, 1266 cm^{-1}.

Preparation of β-ketochlorohydrin (20):

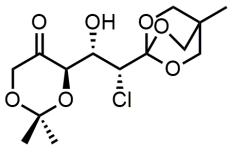

To a solution of aldehyde **22** (11.33 g, 65.8 mmol) in CH_2Cl_2 (330 mL) was added (*R*)-proline (6.06 g, 52.6 mmol), *N*-chlorosuccinimide (7.03 g, 52.6 mmol), and 2,2-dimethyl-1,3-dioxan-5-one (7.1 mL, 59 mmol). The mixture was stirred for 24 hours at ambient temperature, diluted with diethyl ether (500 mL), washed with water (3 x 150 mL) and brine (150 mL), dried (Na_2SO_4), filtered, and concentrated. Purification of the crude material by trituration with diethyl ether afforded β-ketochlorohydrin **20** (9.60g, 29 mmol, 43%) as an off-white powder.

^{1}H NMR (400 MHz, CD_3CN) δ: 4.33 (ddd, *J* = 8.5, 2.7, 1.6 Hz, 1H), 4.27 (dd, *J* = 17.6, 1.3 Hz, 1H), 4.17 (dd, *J* = 8.5, 1.3 Hz, 1H), 4.11 (d, *J* = 1.6 Hz, 1H), 4.04 (d, *J* = 17.6 Hz, 1H), 3.95 (s, 6H), 3.40 (d, *J* = 2.7 Hz, 1H), 1.44 (*J* = 0.6 Hz, 3H), 1.37 (d, *J* = 0.6 Hz, 3H), 0.80 (s, 3H).

^{13}C NMR (101 MHz, CD_3CN) δ: 208.00, 109.1, 102.4, 73.3, 68.1, 67.7, 61.3, 31.3, 24.1, 23.7, 13.9.

HRMS: m/z calcd. for $C_{14}H_{22}ClO_7^+$: 337.1049 (M+H); found: 337.1054 (M+H).

IR: 3516, 2884, 1750, 1224, 1082, 1050 cm^{-1}.

m.p. = 144 – 148 ^oC.

α_D (CH_3CN, c = 0.67): +111.

Preparation of alkene (26):

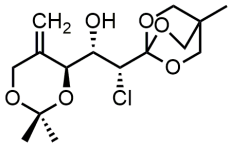

To a cooled (-78 ^oC) solution of 5-(methanesulfonyl)-1-phenyl-1*H*-tetrazole (7.42 g, 33.4 mmol) in THF (50 mL) was added dropwise a freshly prepared solution of 34.9 mmol of LiHMDS in THF (50 mL). The resulting pale yellow mixture was stirred for 30 minutes at -78 ^oC. A solution of β-ketochlorohydrin **20** (5.00 g, 14.8 mmol) in THF (50 mL) was then added dropwise and the mixture was stirred for a further 15 minutes at -78 ^oC. The

mixture was then poured into 1000 mL EtOAc and washed with H_2O (500 mL) and brine (500 mL), dried (Na_2SO_4), filtered, and concentrated. Partial purification of the crude material by column chromatography (30:70:1 to 50:50:1 / EtOAc:pentane:Et_3N) afforded a mixture of alkene **26** and 5-(methaneslfonyl)-1-phenyl-1*H*-tetrazole (7.59 g, estimated yield by ^{1}H NMR 3.92 g, 11.7 mmol, 79%), which was advanced directly to the next step without further purification. To obtain an analytical sample for characterization, a small portion of the crude material was purified by column chromatography (30:70:1 / EtOAc:pentane:Et_3N).

^{1}H NMR (400 MHz, CD_3CN) δ: 5.29 (m, 1H), 4.97 (m, 1H), 4.34 – 4.27 (m, 2H), 4.23 – 4.15 (m, 3H), 3.96 (s, 6H), 3.40 (d, *J* = 2.2 Hz, 1H), 1.43 (d, *J* = 0.6 Hz, 3H) 1.28 (d, *J* = 0.6 Hz, 3H), 0.81 (s, 3H).

^{13}C NMR (101 MHz, CD_3CN) δ: 144.0, 109.4, 109.3, 100.3, 73.6, 71.0, 70.5, 65.3, 61.2, 31.3, 28.0, 21.7, 13.9.

HRMS: m/z calcd. for $C_{15}H_{23}ClO_6Na^+$: 367.1075 (M+Na); found: 357.1079 (M+Na).

IR: 3521, 2883, 1195, 1053 cm^{-1}.

α_D (CH_3CN, c = 0.62): +25.9.

Preparation of triol (29):

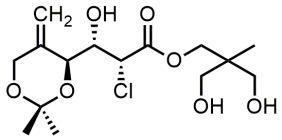

To a solution of alkene **26** (3.92 g, 11.7 mmol) in 1,4-dioxane (120 mL) was added pyridinium *p*-toluenesulfonate (150 mg, 0.60 mmol). The mixture was stirred for 24 hours at ambient temperature and then concentrated. Purification of the crude material by column chromatography (5% to 8% MeOH in CH_2Cl_2) afforded triol **29** (3.43 g, 9.71 mmol, 83%) as white crystals.

^{1}H NMR (400 MHz, CD_3CN) δ: 5.22 (m, 1H), 5.02 (m, 1H), 4.89 (d, *J* = 2.3 Hz, 1H), 4.36 – 4.22 (m, 4H), 4.14 (d, *J* = 10.8 Hz, 1H), 4.07 (d, *J* = 10.8 Hz, 1H), 3.77 (d, *J* = 6.8 Hz, 1H), 3.43 (m, 4H), 2.92 (apparent s, 2H), 1.44 (d, *J* = 0.6 Hz, 3H), 1.31 (d, *J* = 0.6 Hz, 3H), 0.85 (s, 3H).

^{13}C NMR (101 MHz, CD_3CN) δ: 169.4, 143.5, 109.9, 100.4, 73.3, 71.8, 69.0, 66.0, 65.9, 65.1, 62.0, 41.6, 28.2, 22.1, 16.9.

HRMS: m/z calcd. for $C_{15}H_{26}ClO_7^+$: 353.1362 (M+H); found: 353.1362 (M+H).

IR: 3394, 2988, 1738, 1382, 1066 cm^{-1}.

m.p. = 61 - 63 ^oC.

α_D (CH_3CN, c = 0.47): +49.7.

Preparation of carboxylic acid (30):

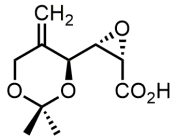

To a solution of triol **29** (2.40 g, 6.8 mmol) in THF (70 mL) was added 2.0 M aqueous NaOH (20.5 mL, 41 mmol). The mixture was heated to 50 ^oC, stirred for a further 30 minutes, allowed to cool to room temperature, and concentrated. Purification of the crude material by column chromatography (66:33:2 / EtOAc:PhMe:AcOH) afforded carboxylic acid **30** (1.05 g, 4.90 mmol, 72%) as white crystals.

^{1}H NMR (400 MHz, $CDCl_3$) δ: 7.53 (br. s, 1H), 5.16 (m, 1H), 5.04 (m, 1H), 4.43 (d, *J* = 7.4 Hz, 1H), 4.39 (d, *J* = 14.0 Hz, 1H), 4.30 (d, *J* = 14.0 Hz, 1H), 3.62 (d, *J* = 4.5 Hz, 1H), 3.43 (dd, *J* = 7.4, 4.5 Hz, 1H), 1.37 (m, 6H).

^{13}C NMR (151 MHz, $CDCl_3$) δ: 172.8, 141.9, 109.0, 99.6, 68.8, 63.8, 57.4, 50.6, 27.3, 21.2.

HRMS: m/z calcd. for $C_{10}H_{14}O_5Na^+$: 237.0733 (M+Na); found: 237.0734 (M+Na).

IR: 3650 - 2375, 2993, 1723, 1378, 1200, 1152, 1064 cm^{-1}.

m.p. = 95 - 99^oC (dec.).

α_D ($CHCl_3$, c = 1.69): +60.5.

Preparation of diazoketone (19):

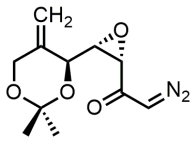

To a solution of carboxylic acid **30** (1.05 g, 4.90 mmol) in THF (50 mL) was added Et_3N (0.75 mL, 5.39 mmol). The mixture was cooled to -15 ^oC (ice / brine bath) and isopropyl chloroformate (2 M sol'n in PhMe, 2.70 mL, 5.4 mmol) was added dropwise. The resulting cloudy suspension was stirred for 1 hour while warming to 0 ^oC. The mixture was then diluted with CH_3CN (30 mL) and TMS-diazomethane (2 M sol'n in hexanes, 7.4 mL, 14.8 mmol) was added dropwise. The cooling bath was then removed, and the mixture was stirred for 24 hours at ambient temperature in the dark. The mixture was then treated with glacial acetic acid (0.6 mL 10.5 mmol), poured into 500 mL EtOAc, washed with NH_4Cl (250 mL), $NaHCO_3$ (250 mL), brine (250 mL), dried (Na_2SO_4), filtered, and concentrated. Purification of the crude material by column chromatography (30:70:1 to 50:50:1 / EtOAc:hexanes:Et_3N) afforded diazoketone **19** (0.87 g, 3.65 mmol, 74%) a yellow/green oil.

^1H NMR (400 MHz, CD_3CN) δ: 5.77 (br. s, 1H), 5.09 (apparent q, *J* = 1.4 Hz, 1H), 5.03 (apparent q, *J* = 1.6 Hz, 1H), 4.37 (apparent dq, *J* = 14.0, 1.3 Hz, 1H), 4.25 (br. m, 1H), 4.23 (app. dq, *J* = 14.0, 1.3 Hz, 1H), 3.59 (br. d, *J* = 4.5 Hz, 1H), 3.31 (dd, *J* = 7.9, 4.5 Hz, 1H), 1.31 (d, *J* = 0.6 Hz, 3H), 1.29 (d, *J* = 0.6 Hz, 3H).

^{13}C NMR (101 MHz, CD_3CN) δ: 189.3, 144.3, 108.5, 100.0, 69.4, 65.2, 58.1, 56.4, 55.9, 27.5, 21.3.

HRMS: m/z calcd. for $C_{11}H_{14}N_2O_4Na^+$: 261.0846 (M+Na); found: 261.0851 (M+Na).

IR: 3085, 2990, 2110, 1637, 1372, 1074 cm^{-1}.

α_D (CH_3CN, c = 1.07): +41.4.

Preparation of epoxyketone (18):

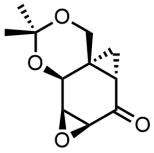

A solution of diazoketone **19** (450 mg, 1.89 mmol) in CH_2Cl_2 (20 mL) was treated with 4 Å molecular sieves (ca. 30 beads) and stirred for 30 minutes. The mixture was then treated with $Rh_2(OAc)_4$ (17 mg, 0.04 mmol) and stirred for six hours at ambient temperature. The mixture was then filtered through a pad of neutral alumina (CH_2Cl_2 rinse) and concentrated. The crude material was used directly in the next reactions. To obtain an analytical sample for characterization, a small portion of the crude material was purified by column chromatography (50:50:2 / pentane:EtOAc:Et_3N).

^{1}H NMR (400 MHz, $CDCl_3$) δ: 4.46 (dd, *J* = 3.3, 0.8 Hz, 1H), 3.90 (dd *J* = 11.6, 1.2 Hz, 1H), 3.50 (apparent t, *J* = 3.5 Hz, 1H), 3.25 (d, *J* = 11.6 Hz, 1H), 3.17 (dd, *J* = 3.6, 1.2 Hz, 1H), 1.60 (apparent ddt, *J* = 10.4, 5.4, 1.1 Hz, 1H), 1.53 (s, 3H), 1.48 (s, 3H), 1.18 (dd, *J* = 10.4, 5.7 Hz, 1H), 0.69 (apparent td, *J* = 5.5, 1.2 Hz, 1H).

^{13}C NMR (101 MHz, $CDCl_3$) δ: 199.1, 101.3, 64.6, 64.0, 53.3, 51.3, 25.9, 23.4, 23.0, 22.9, 16.8.

HRMS: m/z calcd. for $C_{11}H_{15}O_4^+$: 211.0965 (M+H); found: 211.0970 (M+H).

IR: 2993, 1703, 1383, 1223, 1088 cm^{-1}.

α_D ($CHCl_3$, c = 0.54): -57.9.

Preparation of fluorohydrin (17a):

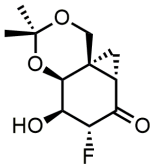

A cooled (0 °C) solution of crude epoxyketone **18** (360 mg) in THF (1 mL) was treated with TBAF (1 M sol'n in THF, 8.0 mL, 8.0 mmol) and stirred for 8 hours at 0 °C. Purification of the crude material by adsorption onto silica gel followed by column chromatography (3:1 / EtOAc:pentane) afforded fluorohydrin **17a** (129 mg, 0.56 mmol, 30% over 2 steps based on 1.89 mmol diazoketone **19**) as a yellow oil.

^{1}H NMR (400 MHz, $CDCl_3$) δ: 4.89 (dd, *J* = 48.4, 10.6 Hz, 1H), 4.77 (m, 1H), 4.33 (d, *J* = 12.4 Hz, 1H), 3.88 (m, 1H), 3.03 (d, *J* = 12.4 Hz, 1H), 2.65 (br. d, *J* = 9.4 Hz, 1H), 1.89 (m, 1H), 1.59 (s, 3H), 1.47 (s, 3H), 1.14 (dd, *J* = 6.4, 5.0 Hz, 1H) 1.07 (dd, *J* = 10.5, 6.4 Hz, 1H).

^{13}C NMR (101 MHz, $CDCl_3$) δ: 199.6 (d, *J* = 14.4 Hz), 100.4, 92.1 (d, *J* = 189.5 Hz), 69.4 (d, *J* = 9.1 Hz), 66.9 (d, *J* = 18.6 Hz), 65.4, 29.7 (d, *J* = 0.8 Hz), 29.5, 24.9 (d, *J* = 0.8 Hz), 19.0, 12.3.

HRMS: m/z calcd. for $C_{11}H_{16}O_4F^+$: 231.1027 (M+H); found: 231.1038 (M+H).

IR: 3442, 2925, 1714, 1382, 1228, 1198, 1098, 1075 cm^{-1}.

α_D ($CHCl_3$, c = 0.89) +34.0.

Preparation of acetate (35a):

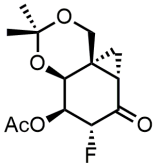

A solution of fluorohydrin **17a** (114 mg, 0.49 mmol) in CH_2Cl_2 (5 mL) was treated with pyridine (0.4 mL, 5.0 mmol), 4-dimethylaminopyridine (one crystal), and Ac_2O (0.19 mL, 2.0 mmol). The mixture was stirred for 4 hours at ambient temperature and was then diluted with CH_2Cl_2 (25 mL), washed with NH_4Cl (10 mL), $NaHCO_3$ (10 mL), brine (10 mL), dried (Na_2SO_4), filtered, and concentrated. Purification of the crude material by column chromatography (1:1 / pentane:EtOAc) afforded acetate **35a** (134 mg, 0.49 mmol, 99%) as a colourless oil.

^{1}H NMR (400 MHz, $CDCl_3$) δ: 5.11 (d, *J* = 1.4 Hz, 1H), 5.03 (apparent dd, *J* = 37.7, 11.0 Hz, 1H), 4.86 (m, 1H), 4.33 (d, *J* = 12.3 Hz, 1H), 2.99 (d, *J* = 12.3 Hz, 1H), 2.16 (s, 3H), 1.94 (m, 1H), 1.52 (d, *J* = 0.5 Hz, 1H), 1.45 (d, *J* = 0.5 Hz, 1H), 1.40 (dd, *J* = 6.6, 4.8 Hz, 1H), 1.13 (dd, *J* = 10.4, 6.6 Hz, 1H).

^{13}C NMR (151 MHz, $CDCl_3$) δ: 198.9 (d, *J* = 14.0 Hz), 170.4, 100.2, 88.3 (d, *J* = 190.7 Hz), 67.9 (d, *J* = 18.2 Hz), 67.7 (d, *J* = 8.8 Hz), 65.7, 29.9, 29.6, 26.2 (d, *J* = 0.8 Hz), 21.0 (d, *J* = 0.8 Hz), 18.9, 13.4.

HRMS: m/z calcd. for $C_{13}H_{17}O_5FNa^+$: 295.0952 (M+Na); found: 295.0955.

IR: 2923, 1740, 1721, 1376, 1233, 1089, 1071 cm^{-1}.

α_D ($CHCl_3$, c = 1.54): +100.

Preparation of alcohol (36a):

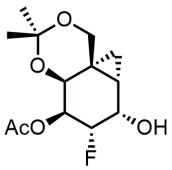

A cooled (-78 ^oC) solution of acetate **35a** (134 mg, 0.49 mmol) in THF (5 mL) was treated with L-selectride (1 M sol'n in THF, 0.49 mL, 0.49 mmol). The mixture was stirred at -78 ^oC for 15 minutes. Purification of the crude material by adsorption onto silica gel followed by column chromatography (3:2 / EtOAc:pentane) afforded alcohol **36a** (113 mg, 0.41 mmol, 84%) as a white solid.

^1H NMR (400 MHz, $CDCl_3$) δ: 5.07 – 4.90 (m, 2H), 4.69 (m, 2H), 4.17 (d, *J* = 12.3 Hz), 2.90 (d, *J* = 12.3 Hz), 2.20 (br. d, *J* = 3.8 Hz), 2.12 (s, 3H), 1.48 (s, 3H), 1.47 – 1.40 (m, 1H), 1.44 (s, 3H), 1.11 (dd, *J* = 6.2, 5.2 Hz), 0.48 (ddd, *J* = 9.4, 6.2, 1.3 Hz, 1H).

^{13}C NMR (151 MHz, $CDCl_3$) δ: 170.7, 99.2, 88.0 (d, *J* = 180.2 Hz), 69.0 (d, *J* = 7.0 Hz), 66.8, 66.4 (d, *J* = 17.1 Hz), 64.3 (d, *J* = 17.2 Hz), 29.6, 23.3, 22.6 (d, *J* = 5.8 Hz), 21.2, 19.1, 7.8.

HRMS: m/z calcd. for $C_{13}H_{20}O_5F^+$: 275.1289 (M+H); found: 273.1311 (M+H).

IR: 3475, 2996, 1740, 1376, 1240, 1107 cm^{-1}.

m.p. = 162 – 166 ^oC.

α_D ($CHCl_3$, c = 1.00): +115.

Preparation of dinitrophenyl ether (37a):

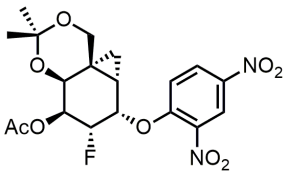

A solution of alcohol **36a** (110 mg, 0.40 mmol) and quinuclidine (445 mg, 4.0 mmol) in DMF (1 mL) was treated with 4 Å molecular sieves (ca. 10 beads) and stirred for 30 minutes. The mixture was then treated with a solution of 2,4-dinitrofluorobenzene (298

mg, 1.6 mmol) in DMF (0.5 mL). The resulting dark-green solution was stirred for 24 hours at ambient temperature and then diluted with EtOAc (20 mL), washed with NH_4Cl (10 mL), $NaHCO_3$ (10 mL), brine (10 mL), dried (Na_2SO_4), filtered, and concentrated. Purification of the crude material by adsorption onto silica gel followed by column chromatography (3:2 to 1:1 / pentane:EtOAc) afforded dinitrophenyl ether **37a** (143 mg, 0.33 mmol, 81%) as a white solid.

^{1}H NMR (400 MHz, $CDCl_3$) δ: 8.77 (d, *J* = 2.8 Hz, 1H), 8.41 (dd, *J* = 9.4, 2.8 Hz, 1H), 7.27 (d, *J* = 9.4 Hz, 1H), 5.48 (ddd, *J* = 7.7, 4.8, 2.8 Hz, 1H), 5.29 (ddd, *J* = 47.5, 11.0, 4.8, 4.8 Hz, 1H), 5.16 (ddd, *J* = 11.0, 5.0, 3.2 Hz, 1H), 4.85 (apparent t, *J* = 3.1 Hz, 1H), 4.22 (d, *J* = 12.5 Hz, 1H), 2.88 (d, *J* = 12.5 Hz, 1H), 2.12 (s, 3H), 1.59 (m, 1H), 1.50 (s, 3H), 1.46 (s, 3H), 1.21 (dd, *J* = 6.5, 5.0 Hz, 1H), 0.55 (ddd, *J* = 9.3, 6.5, 1.1 Hz, 1H).

^{13}C NMR (151 MHz, $CDCl_3$) δ: 170.2, 155.9, 140.6, 139.5, 129.0, 122.3, 116.1 (d, *J* = 2.3 Hz), 99.4, 85.7 (d, *J* = 191.8 Hz), 73.9 (d, *J* = 15.6 Hz), 68.2 (d, *J* = 6.8 Hz), 66.4, 65.9 (d, *J* = 16.8 Hz), 29.5, 24.4, 21.5 (d, *J* = 5.6 Hz), 21.0, 18.9, 9.0.

HRMS: m/z calcd. for $C_{19}H_{22}O_9N_2F^+$: 441.1304 (M+H); found: 441.1291 (M+H).

IR: 2923, 1744, 1607, 1534, 1345, 1275, 1239 cm^{-1}.

m.p. = 149 - 153 °C.

α_D ($CHCl_3$, c = 2.15): +204.

Preparation of alcohol (38a):

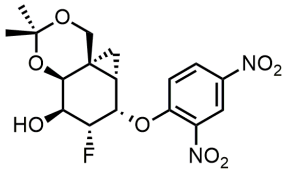

A cooled (0 °C) solution of dinitrophenyl ether **37a** (136 mg, 0.31 mmol) in MeOH (6.2 mL) was treated with K_2CO_3 (64 mg, 0.46 mmol) and stirred at 0 °C for 30 minutes. The resulting orange solution was diluted with CH_2Cl_2 (20 mL), washed with NH_4Cl (10 mL), $NaHCO_3$ (10 mL), brine (10 mL), dried (Na_2SO_4), filtered, and concentrated. Purification of the crude material by column chromatography (1:1 / pentane:EtOAc) afforded alcohol **38a** (113 mg, 0.28 mmol, 92%) as a white solid.

^{1}H NMR (600 MHz, $CDCl_3$) δ: 8.76 (d, *J* = 2.7 Hz, 1H), 8.42 (dd, *J* = 9.2, 2.7 Hz, 1H), 7.27 (d, *J* = 9.2 Hz, 1H), 5.43 (m, 1H), 5.01 (ddd, *J* = 48.0, 10.5, 4.6 Hz, 1H), 4.71 (apparent t, *J* = 3.3 Hz, 1H), 4.21 (d, *J* = 12.5 Hz, 1H), 4.02 (m, 1H), 2.94 (d, *J* = 12.5 Hz, 1H), 2.52 (br. d, *J* = 9.1 Hz, 1H), 1.59 – 1.54 (m, 1H), 1.57 (s, 3H), 1.48 (s, 3H), 1.06 (dd, *J* = 6.3, 5.3 Hz, 1H), 0.52 (ddd, J = 9.4, 6.3, 0.9 Hz, 1H).

^{13}C NMR (151 MHz, $CDCl_3$) δ: 155.8, 140.5, 139.5, 129.0, 122.3, 115.8 (d, *J* = 1.7 Hz), 99.7, 88.6 (d, *J* = 188.2 Hz), 73.9 (d, *J* = 16.0 Hz), 69.9 (d, *J* = 7.1 Hz), 66.2, 64.2 (d, *J* = 18.3 Hz), 29.4, 23.9, 22.1 (d, *J* = 5.9 Hz), 19.1, 8.8.

HRMS: m/z calcd. for $C_{17}H_{19}N_2O_8FNa^+$: 421.1018 (M+Na); found: 421.1018.

IR: 3545, 2995, 1607, 1531, 1345, 1280, 1098 cm^{-1}.

m.p. = 176 - 180 ^{o}C.

α_D ($CHCl_3$, c = 0.63): +179.

Preparation of carbagalactoside (16a):

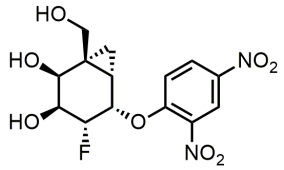

A solution of alcohol **38a** (110 mg, 0.28 mmol) in methanol (6 mL) was treated with Amberlite® IR 120 H^+ resin (ca. 100 beads) and stirred at ambient temperature for 24 hours. The mixture was then filtered and concentrated. Purification of the crude material by adsorption onto Celite® followed by reversed phase column chromatography (0 to 100% CH_3CN in H_2O) afforded carbagalactoside **16a** (80.2 mg, 0.22 mmol, 81%) as a white solid.

^{1}H NMR (400 MHz, CD_3CN) δ: 8.67 (d, *J* = 2.8 Hz, 1H), 8.43 (dd, *J* = 9.4, 2.8 Hz, 1H), 7.49 (d, *J* = 9.4 Hz, 1H), 5.51 (m, 1H), 4.80 (ddd, *J* = 47.7, 10.5, 4.8 Hz, 1H), 4.40 (m, 1H), 3.82 (m, 1H), 3.79 (d, *J* = 3.1 Hz, 1H), 3.51 (dd, *J* = 11.4, 7.4 Hz, 1H), 3.50 (d, *J* = 6.3 Hz, 1H), 3.43 (dd, *J* = 11.4, 4.5 Hz, 1H), 3.02 (dd, *J* = 7.4, 4.5 Hz, 1H), 1.62 (m, 1H), 0.71 (apparent td, J = 5.4, 0.7 Hz, 1H), 0.61 (ddd, *J* = 9.4, 5.5, 1.4 Hz, 1H).

^{13}C NMR (151 MHz, CD_3CN) δ: 156.3, 141.3, 140.4, 129.9, 122.4, 117.6, 89.4 (d, *J* = 186.0 Hz), 74.9 (d, *J* = 15.5 Hz), 71.9 (d, *J* = 7.2 Hz), 66.9, 65.7 (d, *J* = 17.2 Hz), 30.4 (d, *J* = 1.1 Hz), 19.4 (d, *J* = 5.6 Hz), 11.0.

HRMS: m/z calcd. for $C_{14}H_{15}N_2O_8FNa^+$: 381.0705 (M+Na); found: 381.0702.

IR: 3391, 2928, 1607, 1530, 1347, 1284, 1082 cm^{-1}.

m.p. = 186 - 190 °C.

α_D ($CHCl_3$, c = 1.54): +211.

Preparation of β-hydroxyketone (17b):

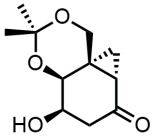

A cooled (0 °C) solution of diphenyl diselenide (936 mg, 3.0 mmol) in EtOH (10 mL) was cautiously treated with $NaBH_4$ (227 mg, 6.0 mmol) and stirred for 30 minutes at 0 °C. The resulting solution was added dropwise to a cooled (0 °C) solution of crude epoxyketone **18** (417 mg) in EtOH (5 mL), and the mixture was stirred for 30 minutes at 0 °C. The mixture was then diluted with CH_2Cl_2 (100 mL) and washed with NH_4Cl (20 mL) and $NaHCO_3$ (20 mL). The combined aqueous material was extracted with CH_2Cl_2 (3 x 20 mL). The combined organic material was washed with brine (20 mL), dried (Na_2SO_4), filtered and concentrated. Purification of the crude material by column chromatography (1:1 / pentane:EtOAc then 3% MeOH in EtOAc) afforded β-hydroxyketone **17b** (261 mg, 1.23 mmol, 60% over 2 steps based on 2.06 mmol diazoketone **19**) as a white solid.

^{1}H NMR (400 MHz, $CDCl_3$) δ: 4.51 (dd, *J* = 3.8, 0.8 Hz, 1H), 4.16 (d, *J* = 12.0 Hz, 1H), 3.94 (m, 1H), 3.19 (d, *J* = 12.0 Hz, 1H), 2.52 (dd, *J* = 17.4, 5.5 Hz, 1H), 2.44 (dd, *J* = 17.4, 10.2 Hz, 1H), 2.39 (br. d, *J* = 9.4 Hz, 1H), 1.81 (dd, *J* = 10.1, 5.1 Hz, 1H), 1.58 (d, *J* = 0.5 Hz, 3H), 1.45 (d, *J* = 0.5 Hz, 3H), 1.11 (dd, *J* = 6.2, 5.1 Hz, 1H), 1.05 (dd, *J* = 10.1, 6.2 Hz, 1H).

^{13}C NMR (151 MHz, $CDCl_3$) δ: 205.6, 100.3, 67.8, 65.9, 65.2, 41.9, 30.0, 29.0, 27.0, 20.2, 13.7.

HRMS: m/z calcd. for $C_{11}H_{17}O_4^+$: 213.1121 (M+H); found: 213.1133 (M+H).

IR: 3440, 2914, 1688, 1378, 1270, 1225, 1198, 1071 cm^{-1}.

m.p. = 93 - 96 ^{o}C.

α_D ($CHCl_3$, c = 0.35): -2.0.

Preparation of acetate (35b):

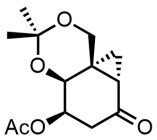

A solution of β-hydroxyketone **17b** (261 mg, 1.23 mmol) in CH_2Cl_2 (15 mL) was treated with pyridine (1.0 mL, 12.3 mmol), 4-dimethylaminopyridine (one crystal), and Ac_2O (0.47 mL, 4.9 mmol). The mixture was stirred for 16 hours at ambient temperature and was then diluted with CH_2Cl_2 (100 mL), washed with NH_4Cl (40 mL), $NaHCO_3$ (40 mL), brine (40 mL), dried (Na_2SO_4), filtered, and concentrated. Purification of the crude material by column chromatography (1:1 / hexanes:EtOAc) afforded acetate **35b** (202 mg, 0.79 mmol, 65%) as white crystals.

^{1}H NMR (400 MHz, $CDCl_3$) δ: 5.03 (ddd, *J* =11.7, 5.9, 3.0 Hz, 1H), 4.68 (d, *J* = 3.0 Hz, 1H), 4.32 (d, *J* = 12.1 Hz, 1H), 3.04 (d, *J* = 12.1 Hz, 1H), 2.64 (dd, *J* = 17.7, 11.7 Hz, 1H), 2.47 (dd, *J* = 17.7, 5.9 Hz, 1H), 2.09 (s, 3H), 1.86 (dd, *J* = 10.1, 4.9 Hz, 1H), 1.54 (s, 3H), 1.44 (s, 3H), 1.34 (dd, *J* = 6.5, 4.9 Hz, 1H), 1.06 (dd, *J* = 10.1, 6.5 Hz, 1H).

^{13}C NMR (151 MHz, $CDCl_3$) δ: 204.6, 170.6, 100.0, 66.24, 66.23, 65.9, 37.9, 30.9, 29.5, 27.4, 21.2, 19.5, 13.6.

HRMS: m/z calcd. for $C_{13}H_{18}O_5Na^{+}$: 277.1046 (M+Na); found: 277.1036.

IR: 2993, 1732, 1692, 1374, 1238, 1037 cm^{-1}.

m.p. 142 - 145 ^{o}C.

α_D ($CHCl_3$, c = 3.23): +38.5.

Preparation of alcohol (36b):

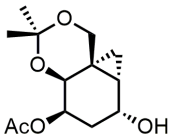

A cooled (-78 ^{o}C) solution of acetate **35b** (198 mg, 0.78 mmol) in THF (8 mL) was treated with L-selectride (1 M sol'n in THF, 0.78 mL, 0.78 mmol). The mixture was stirred at -78 ^{o}C for 15 minutes. Purification of the crude material by adsorption onto silica gel followed by column chromatography (3:2 to 3:1 / EtOAc:pentane) afforded alcohol **36b** (137 mg, 0.53 mmol, 68%) as a colourless oil.

^{1}H NMR (600 MHz, $CDCl_3$) δ: 4.68 (ddd, *J* = 9.8, 4.7, 3.7 Hz, 1H), 4.46 (d, *J* = 3.7 Hz, 1H), 4.09 – 4.04 (m, 1H), 4.08 (d, *J* = 11.9 Hz, 1H) 3.06 (d, *J* = 11.9 Hz, 1H), 2.71 (br. d, J = 8.7 Hz, 1H), 2.07 (s, 3H), 1.96 (ddd, *J* = 13.2, 9.8, 7.2 Hz, 1H), 1.85 (ddd, *J* = 13.2, 5.6, 5.0 Hz, 1H), 1.49 (s, 3H), 1.46 (s, 3H), 1.15 (dd, *J* = 9.5, 5.6 Hz, 1H), 0.56 (dd, *J* = 9.5, 6.3 Hz, 1H), 0.41 (apparent t, *J* = 5.9 Hz, 1H).

^{13}C NMR (151 MHz, $CDCl_3$) δ: 170.6, 99.7, 67.4, 67.3, 67.2, 66.7, 32.1, 29.4, 25.4, 22.7, 21.3, 20.0, 11.3.

HRMS: m/z calcd. for $C_{13}H_{24}NO_5^+$: 274.1649 ($M+NH_4$); found: 274.1656.

IR: 3445, 2993, 1731, 1374, 1246, 1029 cm^{-1}.

α_D ($CHCl_3$, c = 2.31): +68.7.

Preparation of dinitrophenyl ether (37b):

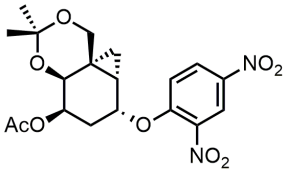

A solution of alcohol **36b** (130 mg, 0.51 mmol) and DABCO (455 mg, 4.1 mmol) in \ DMF (1.7 mL) was treated with 4 Å molecular sieves (ca. 10 beads) and stirred for 30 minutes. The mixture was then treated with 2,4-dinitrofluorobenzene (255 µL, 2.0 mmol). The resulting brown solution was stirred for 16 hours at ambient temperature and then diluted with EtOAc (30 mL), washed with NH_4Cl (15 mL), $NaHCO_3$ (15 mL), brine (15 mL), dried (Na_2SO_4), filtered, and concentrated. Purification of the crude material by

adsorption onto silica gel followed by column chromatography (1:1 / pentane:EtOAc) afforded dinitrophenyl ether **37b** (189 mg, 0.45 mmol, 88%) as an off-white foam.

^{1}H NMR (600 MHz, $CDCl_3$) δ: 8.74 (d, *J* = 2.8 Hz, 1H), 8.42 (dd, *J* = 9.3, 2.8 Hz, 1H), 7.35 (d, *J* = 9.3 Hz, 1H), 4.73 (dd, *J* = 10.1, 6.6 Hz, 1H), 4.63 (apparent dt, *J* = 12.7, 2.9 Hz, 1H), 4.52 (d, *J* = 2.8 Hz, 1H), 4.20 (d, *J* = 12.2 Hz, 1H), 2.96 (d, *J* = 12.2 Hz, 1H), 2.52 (apparent td, *J* = 12.2, 10.1 Hz, 1H), 2.10 (s, 3H), 1.98 (ddd, *J* = 11.9, 6.6, 2.9 Hz, 1H), 1.53 (s, 3H), 1.51 (s, 3H), 1.20 (dd, *J* = 9.6, 5.6 Hz, 1H), 0.70 (dd, *J* = 9.6, 6.2 Hz, 1H), 0.58 (apparent t, *J* = 5.9 Hz, 1H).

^{13}C NMR (151 MHz, $CDCl_3$) δ: 170.8, 155.3, 140.3, 139.8, 128.9, 122.2, 115.8, 99.3, 76.6, 66.9, 66.8, 65.7, 29.4, 28.1, 24.3, 22.6, 21.3, 19.6, 10.8.

HRMS: m/z calcd. for $C_{19}H_{23}N_2O_9^+$: 423.1398 (M+H); found: 423.1396.

IR: 2993, 1730, 1605, 1537, 1345, 1244 cm^{-1}.

α_D ($CHCl_3$, c = 0.77): -0.9.

Preparation of alcohol (38b):

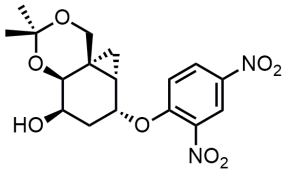

A cooled (0 °C) solution of dinitrophenyl ether **37b** (184 mg, 0.44 mmol) in MeOH (5 mL) was treated with K_2CO_3 (90 mg, 0.65 mmol) and stirred at 0 °C for 30 minutes. The resulting orange solution was diluted with CH_2Cl_2 (20 mL), washed with NH_4Cl (10 mL), $NaHCO_3$ (10 mL), brine (10 mL), dried (Na_2SO_4), filtered, and concentrated. Purification of the crude material by column chromatography (50:1 / diethyl ether:MeOH) afforded alcohol **38b** (165 mg, 0.43 mmol, 99%) as a white foam.

^{1}H NMR (400 MHz, $CDCl_3$) δ: 8.75 (d, *J* = 2.7 Hz, 1H), 8.42 (dd, *J* = 9.3, 2.7 Hz, 1H), 7.33 (d, *J* = 9.3 Hz, 1H) 4.58 (dd, *J* = 10.4, 6.2 Hz, 1H), 4.43 (d, *J* = 3.3 Hz, 1H), 4.23 (d, *J* = 12.2 Hz, 1H), 3.50 (m, 1H), 2.96 (d, *J* = 12.2 Hz, 1H), 2.51 (d, *J* = 10.9 Hz, 1H), 2.25 (apparent td, *J* = 12.1, 10.7 Hz, 1H), 2.05 (ddd, *J* = 11.8, 6.1, 3.1 Hz, 1H), 1.57 (s, 3H), 1.50 (s, 3H), 1.18 (dd, *J* = 9.5, 5.6 Hz, 1H), 0.70 (dd, *J* = 9.5, 6.0 Hz, 1H), 0.40 (apparent t, *J* = 5.9 Hz, 1H).

^{13}C NMR (151 MHz, $CDCl_3$) δ: 155.5, 140.3, 139.7, 128.9, 122.2, 115.7, 99.5, 77.2, 67.1, 66.5, 65.0, 32.0, 29.4, 24.0, 23.3, 19.6, 10.2.

HRMS: m/z calcd. for $C_{17}H_{21}N_2O_8^+$: 381.1292 (M+H); found: 381.1278.

IR: 3550, 2997, 1604, 1536, 1346, 1284 cm^{-1}.

α_D ($CHCl_3$, c = 0.77): -17.9.

Preparation of carbagalactoside (16b):

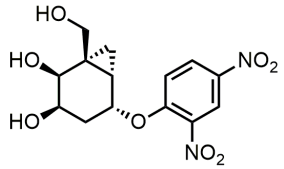

A solution of alcohol **38b** (159 mg, 0.42 mmol) in methanol (7 mL) was treated with Amberlite® IR 120 H^+ resin (ca. 100 beads) and stirred at ambient temperature for 24 hours. The mixture was then filtered and concentrated. Purification of the crude material by adsorption onto Celite® followed by reversed phase column chromatography (0 to 100% CH_3CN in H_2O) afforded carbagalactoside **16b** (70.0 mg, 0.21 mmol, 50%) as a slightly yellow solid.

^{1}H NMR (400 MHz, CD_3CN) δ: 8.66 (d, *J* = 2.8 Hz, 1H), 8.43 (dd, *J* = 2.8, 9.4 Hz, 1H), 7.45 (d, *J* = 9.4 Hz, 1H), 4.89 (apparent t, *J* = 7.8 Hz, 1H), 4.14 (apparent t, *J* = 3.4 Hz, 1H) 3.56, (dd, *J* = 11.3, 6.4 Hz, 1H), 3.52 (d, *J* = 4.0 Hz, 1H), 3.49 (m, 1H), 3.42 (dd, J = 11.3, 3.2 Hz, 1H), 3.06 (d, *J* = 7.2 Hz, 1H), 3.01 (apparent t, *J* = 5.2 Hz, 1H), 1.97-1.84 (m, 2H, obscured by CHD_2CN peak) 1.13 (dd, *J* = 5.6, 9.8 Hz, 1H), 0.77 (dd, *J* = 5.6, 9.8 Hz, 1H), 0.42 (apparent t, *J* = 5.6 Hz, 1H).

^{13}C NMR (151 MHz, CD_3CN) δ: 156.3, 141.0, 140.4, 130.0, 122.5, 117.2, 77.6, 69.4, 67.5, 65.7, 31.9, 30.1, 20.6, 11.6.

HRMS: m/z calcd. for $C_{14}H_{16}N_2O_8Na^+$: 363.0799 (M+Na); found: 363.0799.

IR: 3378, 3284, 3079, 2890, 1601, 1521, 1350, 1290 cm^{-1}.

m.p. = 113 – 115 ^{o}C.

α_D (CH_3CN, c = 0.80): -33.6.

2.6.2. Kinetic Procedures

In a 500 µL cuvette, variable concentrations of probe **16a** were incubated in the presence of *T. Maritima* α-galactosidase (0.89 µM) in 50 mM HEPES buffer (pH = 7.45) at 60 °C. Reaction temperatures were maintained using a calibrated heating block. At fixed time intervals, 20 µL reaction aliquots were transferred to a 1 mL cuvette and incubated at 25 °C for 3 minutes. A solution containing the chromogenic substrate 4-nitrophenyl-α-D-galactopyranoside (0.1 mM) in 50 mM HEPES buffer (pH = 7.45) also kept at 25 °C was then added to the cuvette. The absorbance (λ = 400 nm) was monitored over time using a Cary 4000 UV-Vis-NIR spectrophotometer.

2.6.3. X-ray Crystallographic Experimental Parameters

Table 2.3 Crystallographic data for covalent adduct of inhibitor (16a) and *T. Maritima* α-galactosidase

beamline	i02
wavelength	0.98
high resolution limit (Å)	1.45
low resolution limit (Å)	54.93
completeness (outer Shell)	100 (99.6)
multiplicity	6.4 (5.3)
I/σ	9.6 (1.2)
R_{merge}	0.076 (1.379)
R_{meas}	0.089 (1.644)
R_{pim}	0.035 (0.699)
Wilson B factor	16.836
total observations	716882

total unique	112088
space group	$P2_12_12_1$
unit cell a, b, c	66.90, 96.24, 97.59
unit cell α, β, γ	90.0, 90.0, 90.0
R (%)	18.06
R_{free} (%)	20.70
rmsd (bonds) (Å)	0.021
rmsd (angles) (°)	2.077

Chapter 3.

Candidate Galactosaminidase Inhibitors Based on a Cyclohexene Scaffold

Jason Draper conceived the synthetic route and performed extensive optimization studies on the preparation of intermediates **48** and **56**.

3.1. Introduction

Several potent and selective GH inhibitors are based on a cyclohexene scaffold. Representative examples include the glucosidase inhibitor valienamine (**39**) and the neuraminidase inhibitor oseltamivir (**40**). These molecules owe their potency in part to their olefinic bonds, which mandate non-chair conformations that emulate aspects of enzymatic glycoside hydrolysis TSs (see section 1.3.1. for a more full discussion).

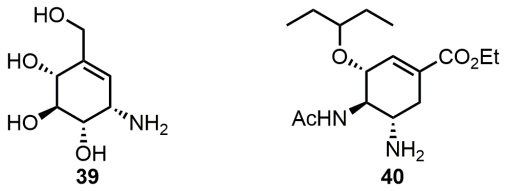

Figure 3.1 Examples of GH inhibitors based on a cyclohexene scaffold.

The substitution of a monosaccharide's pyranoside ring oxygen with an alkene imparts differences not only in conformation but also in reactivity. These differences can be exploited for the development of conceptually novel inhibitors. We anticipated that the chlorination/aldol protocol developed by Britton and co-workers and exploited previously in the preparation of galactoside analogues **16a** and **16b** (chapter 2) could give rapid access to a panel of carbocyclic *N*-acetylgalactosamine (GalNAc) analogues for evaluation as inhibitors of GalNAc processing enzymes.

3.1.1. Mechanism-Based Inhibitors of GH 4 and 109 Hydrolases

Hydrolases belonging to GH families 4 and 109 use a redox-elimination mechanism which involves formation of an enone intermediate (*vide supra*). We hypothesized that a construct that substitutes the pyranoside ring oxygen with an alkene function will be processed in a similar manner to the natural substrate. That is, oxidation of C(3) and proton abstraction followed by rapid and irreversible leaving group departure would afford a dienone intermediate. This intermediate could rapidly tautomerize to the corresponding phenol, which would leave the hydrolase in its catalytically incompetent NADH oxidation state.

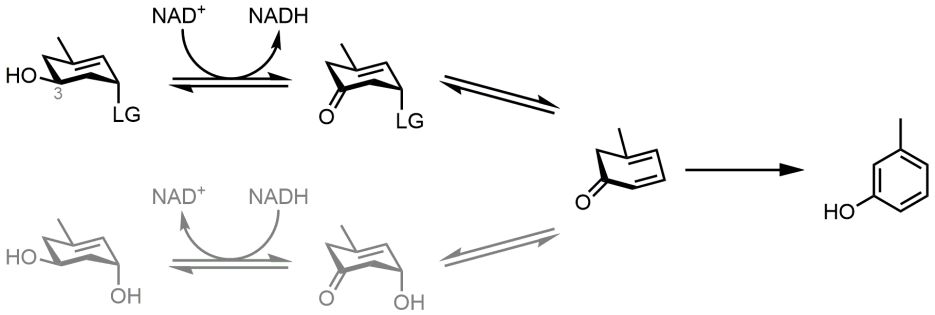

Figure 3.2 Proposed inhibition modality for GH 4 and 109 hydrolases.

Thus, we set out to develop mechanism-based inhibitors of GH 4 and 109 hydrolases. As these are found exclusively in bacteria, inhibitors specific to these hydrolases could find use as antibacterial agents. Of note, the most extensively characterized GH 109 hydolase is found in a bacterium which causes meningitis in human infants.[100] We targeted carbagalactosides **41** and **42** for synthesis, which employ 2,4-dinitrophenolate and carbon dioxide respectively as reactive leaving groups.

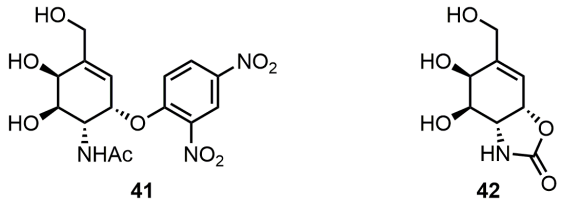

Figure 3.3 Proposed mechanism-based inhibitors of GH 4 and 109 hydrolases.

3.1.2. Metabolic Inhibitors of Galactosaminyltransferases

Recent studies have described the use of 5-thioglycosides and deoxyfluoroglycosides as “metabolic inhibitors” of GTs (*vide supra*). We proposed that carbocycle **43** may possess inhibitory activity against GTs *via* the formation of the transferase donor substrate analog **45**. As **43** may possess insufficient membrane permeability, we also proposed to synthesize its peracetylated congener **44**.

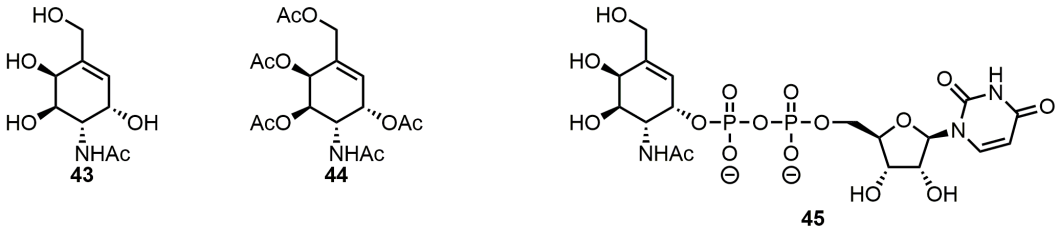

Figure 3.4 Proposed metabolic GT inhibitors.

Transfer of a GalNAc residue to a protein is the committed step in the biosynthesis of mucin glycoproteins. Novel reagents which can disrupt this process *in vivo* may allow for a better understanding of the roles played by mucin glycoproteins in the immune response and cancer pathogenesis.[101]

3.2. Synthesis

3.2.1. Retrosynthetic Analysis

The four carbagalactoside targets were traced back to common intermediate **46**. We anticipated that the free hydroxyl group in **46** could serve as a tether to enforce regioselective epoxide opening at C(2) using known isocyanate chemistry.[102] Epoxyalcohol **46** could be arise from diene **47** through a ring-closing metathesis (RCM) reaction; we were encouraged by the ample precedents for ring-closure of carbohydrate diene substrates.[103,104,105] Diene **47** could be prepared from silyl protected β-ketochlorohydrin **48** in a three step sequence. We expected that **48** could be prepared in a stereoselective manner from readly available materials **21** and **49** using Britton’s chlorination/aldol protocol.[79]

Scheme 3.1 Retrosynthetic Analysis of GalNAc Analogue Targets

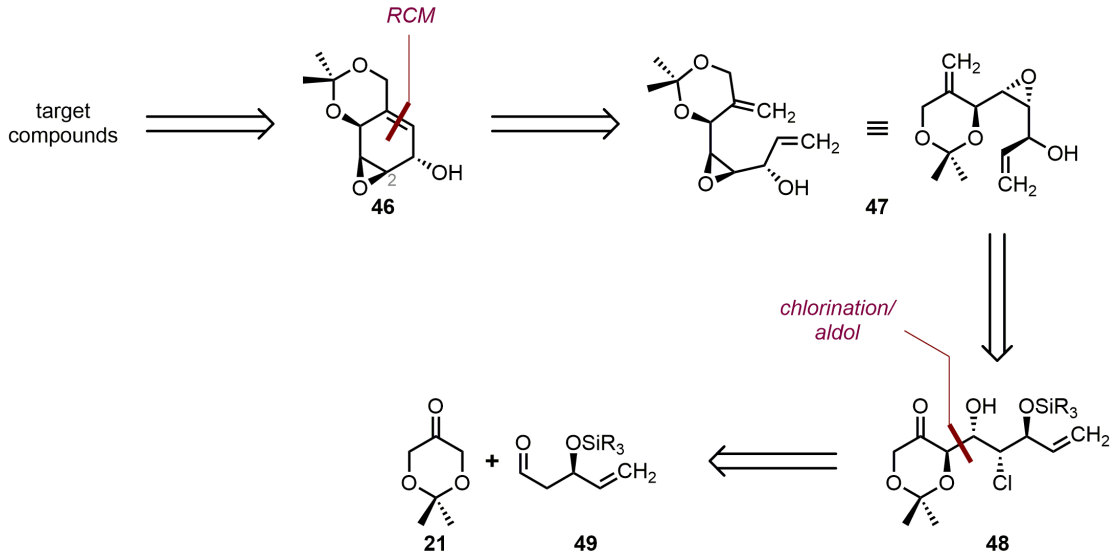

3.2.2. Synthesis of Aldehyde (49)

The first task of the synthesis was to develop a scalable route to aldehyde **49**. Evans reported a scalable synthesis of aldehyde **51** from known D-ribose derivative **50**.[106] We reasoned that aldehyde **49** could be prepared in an analogous manner from commercially available 2-deoxy-L-ribose (**52**). Thus, **52** was subjected to the known sequence of glycosylation and iodination[107] to afford iodoacetal **53**. Unfortunately, this latter operation required laborious chromatographic purification. Acetal **53** was then protected as the corresponding TIPS ether. It was crucial to allow this silylation reaction to proceed for no more than 24 hours as the slow formation of an inseparable impurity was noted after this period of time. Finally, a reductive fragmentation[108] delivered aldehyde **49**. Approximately 25 g this material was prepared using this route.

Scheme 3.2 Scalable Route to Aldehyde (49)

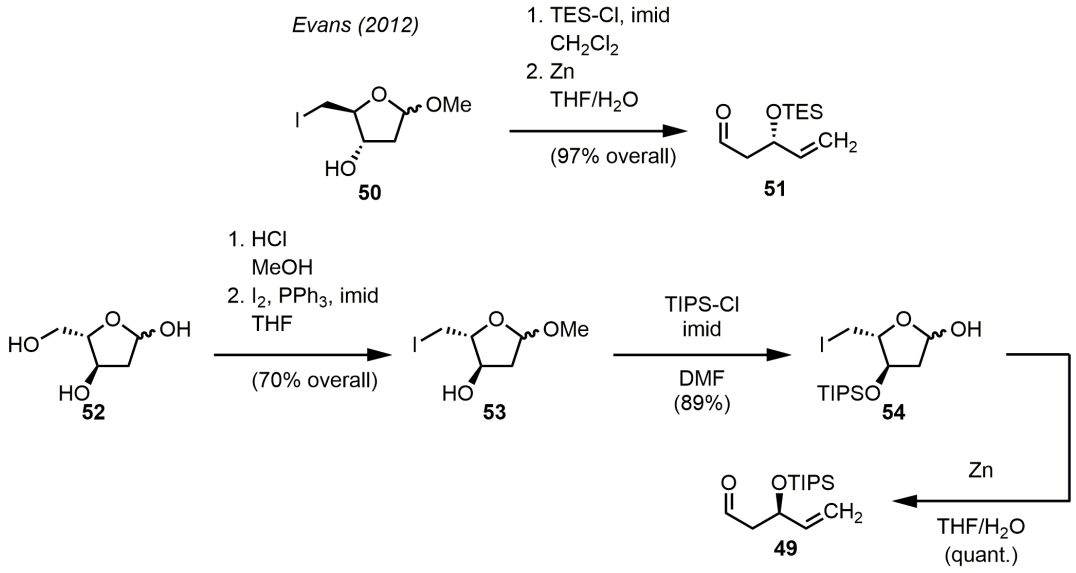

3.2.3. Preparation of β-Ketochlorohydrin (48)

The first key step of the synthesis of the GalNAc analogues was the proline-catalyzed aldol reaction. The aldehyde substrate of this process is highly prone to proline-catalyzed β-elimination. Optimization studies performed by Draper[109] revealed that use of the TIPS protecting group was critical to avoid this undesired process. Aldehyde **49** was readily converted to β-ketochlorohydrin **48** on scales greater than 10 g. Inspection of crude ^{1}H NMR spectra showed a clean reaction with **48** present as a single diastereomer. Since the product possesses one predefined stereogenic centre, there was no need to determine the *ee* of the reaction product.

Scheme 3.3 Proline-Catalyzed Chlorination/Aldol Reaction

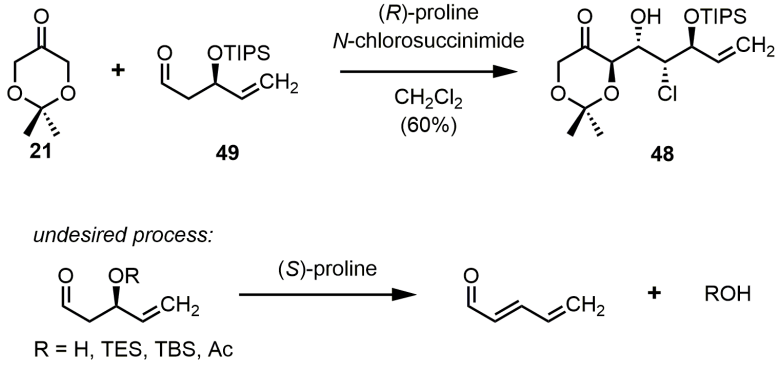

3.2.4. Preparation of Diene (47)

The next task of the synthesis was to advance aldol adduct **48** to RCM precursor **47**. Towards this goal, **48** was subjected to Julia-Kocienski olefination[93] to provide alkene **55**. In prior optimization studies,[109] Draper evaluated a wide variety of bases for the epoxide formation step and found that cesium hydroxide provides epoxide **56** in the highest yield. Of note, the epoxide formation affords a side product (ca. 30% yield) which was assigned as diol **57** on the basis of ^{1}H and ^{13}C NMR data; this material arises from disilylation, *trans*-epoxide formation, and epoxide opening at the allylic position. Desilylation of **56** proceeded uneventfully to provide diene **47** in quantitative yield.

Scheme 3.4 Synthetic Route to Diene (47)

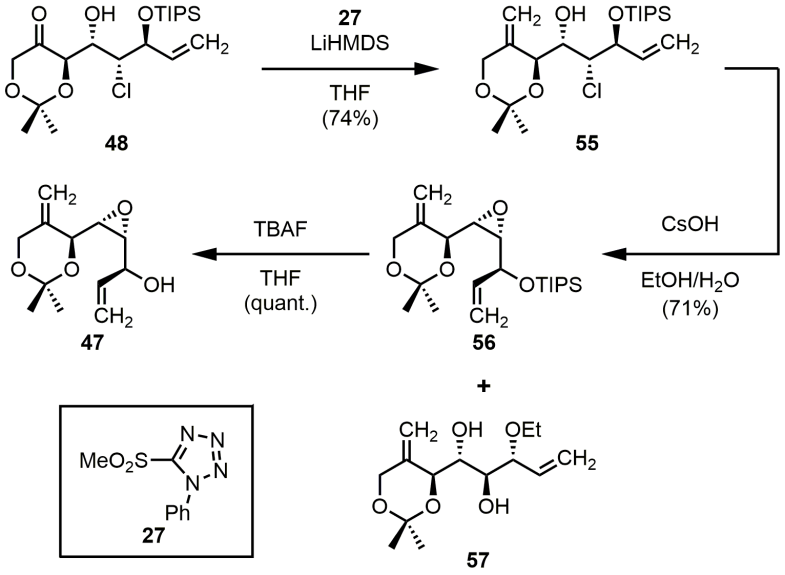

3.2.5. Ru-catalyzed Carbocyclization

The second key step of this synthesis involved the formation of carbocycle **46** *via* RCM. In preliminary studies, Draper had utilized the 2nd Generation Grubbs' Catalyst (**59**) for this transformation; however on scales greater than 100 mg the use of **59** resulted in extensive degradation. A subsequent screen of ruthenium catalysts identified the Stewart-Grubbs' Catalyst (**60**) as optimal. Use of this catalyst permitted the preparation of carbocycle **46** on scales of up to 1 g. Of note, ^{1}H NMR analysis of reaction aliquots revealed that the formation of **46** proceeded *via* the C_2-symmetric dimer **58**.

Scheme 3.5 Ring-Closing Metathesis of Diene (47)

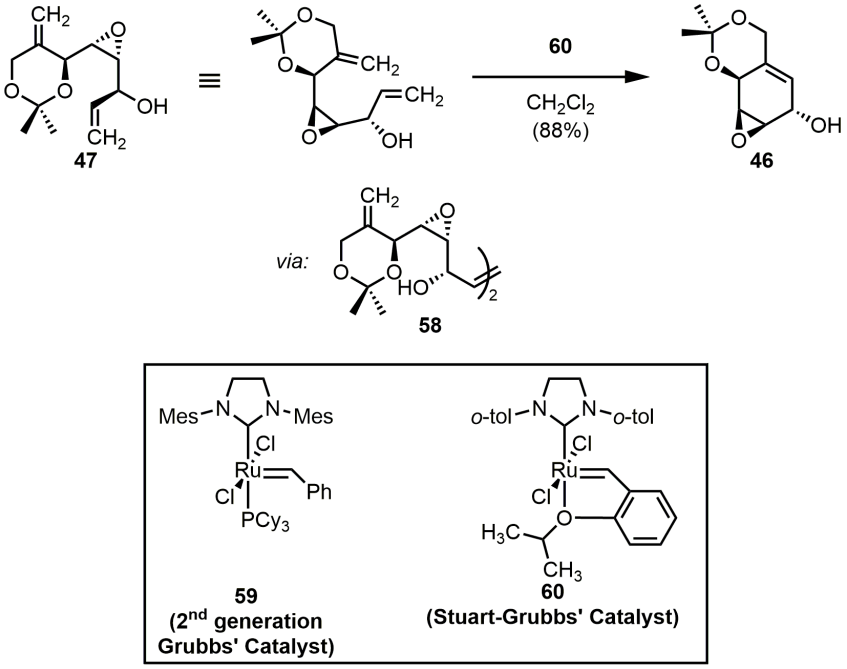

3.2.6. Elaboration of Epoxy-Alcohol (46) to the Carbagalactoside Targets

The synthesis of the carbagalactoside targets utilized the strategy conceived by Draper in which the free hydroxyl in carbocycle **46** serves as a tether to direct regioselective epoxide opening. Indeed, on treatment with freshly prepared acetyl isocyanate, aqueous workup, and treatment with cesium carbonate, **46** was converted to oxazolidinone **61**. As the crude ^{1}H NMR spectrum of this reaction included only resonances attributed to the product, the instability of **61** on silica was the suspected cause of the observed poor yield. Alternatively, **61** can be treated *in situ* with potassium hydroxide to afford aminodiol **62** in a three-step one-pot protocol. Having prepared ample quantities of the key intermediates **61** and **62**, we advanced to the preparation of the carbagalactoside targets.

Deprotection of oxazolidinone **61** proceeded smoothly to give target **42** in good yield. Alternatively, aminodiol **62** was deprotected under acidic conditions; prolonged heating at 100 ^{o}C was required to effect this transformation as the added acid protonates the substrate's amino group. The resulting crude aminotetrol was directly peracetylated

to afford target **44**. This two-step process gave a minor impurity which could be removed only by preparative TLC. Alternatively, aminodiol **62** was monoacetylated at the amino group with complete regioselectivity by employing 2,6-lutidine as a sacrificial base. *N*-acetate **63** was then deprotected to yield target **43**. At this juncture an attempt to prepare dinitrophenyl ether **41** failed, and bis-arylated material was isolated as the major product. While the crude reaction mixture appeared to contain **41**, selectivity for arylation of the C(1) hydroxyl is lacking.

Scheme 3.6 Completion of the Carbagalactoside Syntheses

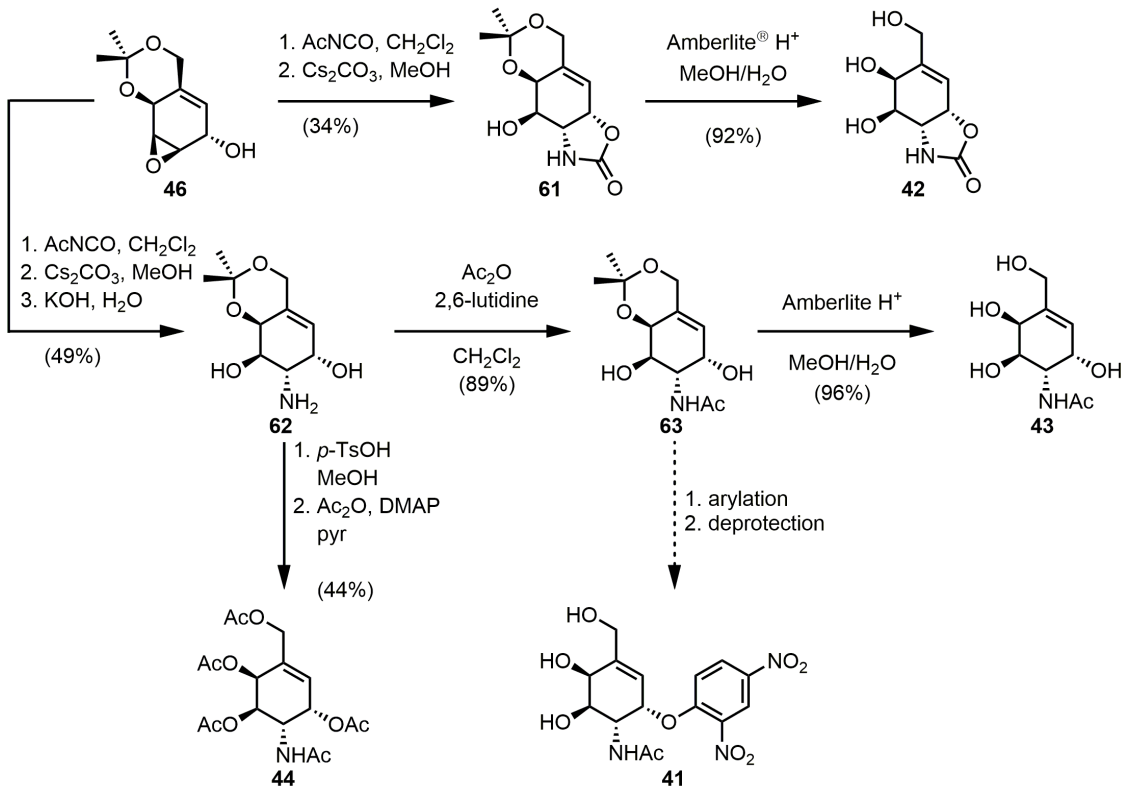

3.3. Conclusion

A synthetic strategy involving a proline-catalyzed chlorination/aldol reaction and a Ru-catalyzed carbocyclization was successfully implemented in the synthesis of three candidate inhibitors of GalNAc processing enzymes. Future work will include the testing of compounds **42**, **43**, and **44** on a panel of bacterial and mammalian enzymes in order to determine these compounds' potency and specificity. Furthermore, as even minor

structural variations can alter inhibitor specificity, we aim to evaluate the cyclopropane-containing congeners of these compounds. Simmons-Smith cyclopropanation of allylic alcohol **46** would provide compound **64**, a logical entry point to the cyclopropyl series.

Scheme 3.7 Proposed Entry to Cyclopropyl Series

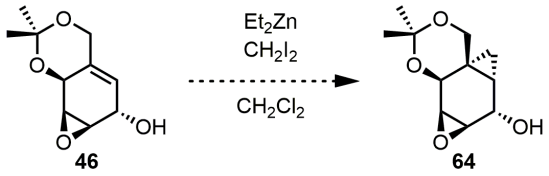

46 **64**

3.4. Experimental Information

3.4.1. Synthesis Procedures and Data

Preparation of acetal (54):

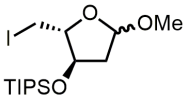

To a solution of (*2R*, *3R*)-2-iodomethyl-5-methoxytetrahydrofuran-3-ol[107] (5.00 g, 19.4 mmol) in DMF (32 mL) was added imidazole (2.90 g, 42.6 mmol), 4-dimethylaminopyridine (ca. 5 grains), and TIPS-Cl (4.56 mL, 21.3 mmol). The mixture was stirred for 16 h and then diluted with EtOAc (500 mL), washed with water (100 mL), washed with brine (4 x 100 mL), dried ($MgSO_4$), filtered, and concentrated. Purification of the crude material by column chromatography (60:40 / CH_2Cl_2:pentane) afforded acetal **54** (6.42 g, 15.5 mmol, 80%) as a colourless oil.

^{1}H NMR (400 MHz, $CDCl_3$) δ: 5.15 – 4.99 (m, 1H), 4.51 – 4.06 (m, 1H), 4.05 – 3.59 (m, 1H), 3.53, 3.36 – 3.21 (m, 2H), 3.40 – 3.38 (m, 3H), 2.56 – 2.20 (m, 1H), 2.17 – 1.87 (m, 1H), 1.08 – 1.03 (m, 21H).

^{13}C NMR (151 MHz, $CDCl_3$) δ: 104.9, 103.7, 86.0, 80.9, 75.3, 74.8, 55.0, 42.3, 42.0, 17.6 – 17.4 (several peaks), 11.7, 11.6, 7.8, 7.5.

HRMS: m/z calcd. for $C_{15}H_{32}O_3ISi^+$: 415.1160 (M+H); found: 415.1150 (M+H).

IR: 2944, 2866, 1464, 1369, 1108, 1033 cm^{-1}.

α_D ($CHCl_3$, c = 0.75): -5.3.

Preparation of aldehyde (49):

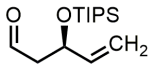

To a solution of acetal **54** (7.55 g, 18.2 mmol) in 4:1 / THF:H_2O (75 mL) was added Zn dust (11.9 g, 182 mmol). The resulting cloudy suspension was refluxed for 2 h, cooled to room temperature, and filtered through a Celite® pad (diethyl ether rinse). The solution was further diluted with diethyl ether to a volume of ca. 500 mL, was washed with H_2O (250 mL), washed with brine (250 mL), dried ($MgSO_4$), filtered, and concentrated. The crude colourless oil (4.66 g, 18.2 mmol, 100%) was advanced to the next step without further purification.

^{1}H NMR (400 MHz, $CDCl_3$) δ: 9.81 (t, *J* = 2.5 Hz, 1H), 5.92 (ddd, J = 17.0, 10.4, 6.1 Hz, 1H), 5.28 (apparent dt, J = 17.1, 1.2 Hz, 1H), 5.14 (apparent dt, J = 10.4, 1.2 Hz, 1H), 4.76 (apparent qt, J = 5.7, 1.2 Hz, 1H), 2.62 (dd, J = 5.6, 2.5 Hz, 1H), 1.06 (m, 21H).

^{13}C NMR (151 MHz, $CDCl_3$) δ: 201.9, 140.3, 115.2, 70.0, 51.6, 18.17, 18.15, 12.4.

HRMS: m/z calcd. for $C_{14}H_{29}O_2Si^+$: 257.1931 (M+H); found: 257.1928 (M+H).

IR: 2945, 2868, 1727, 1466, 1099 cm^{-1}.

α_D ($CHCl_3$, c = 0.22): -13.9.

Preparation of β-ketochlorohydrin (48):

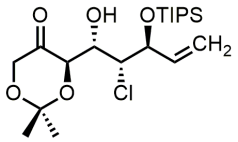

To a solution of aldehyde **49** (4.66 g, 18.2 mmol) in CH_2Cl_2 (90 mL) was added (*R*)-proline (1.62 g, 14.0 mmol), *N*-chlorosuccinimide (2.12 g, 15.9 mmol), and 2,2-dimethyl-1,3,-dioxan-5-one (2.20 mL, 18.7 mmol). The mixture was stirred for 24 h at room temperature, diluted with diethyl ether (500 mL), washed with H_2O (2 x 500 mL), washed with brine (500 mL), dried ($MgSO_4$), filtered, and concentrated. Purification of the crude material by column chromatography (10 to 30% diethyl ether in pentane) afforded β-ketochlorohydrin **48** (4.44 g, 10.5 mmol, 58%) as a colourless oil.

^{1}H NMR (400 MHz, $CDCl_3$) δ: 5.87 (ddd, *J* = 18.0, 10.3, 7.8 Hz, 1H), 5.34 (apparent dt, *J* = 17.2, 1.0 Hz, 1H), 5.28 (apparent dt, *J* = 10.3, 0.9 Hz, 1H), 4.57 (apparent t, *J* = 7.6 Hz, 1H), 4.46 (ddd, *J* = 8.9, 2.5, 1.5 Hz, 1H), 4.37 (dd, *J* = 8.9, 1.3 Hz, 1H), 4.29 (dd *J* =

17.6, 1.4 Hz, 1H), 4.08 (d, *J* = 17.6 Hz, 1H), 3.99 (dd, *J* = 7.5, 1.0 Hz, 1H), 3.49 (dd, *J* = 2.5, 0.9 Hz, 1H), 1.50 (s, 3H), 1.42 (s, 3H), 1.06 (m, 21H).

^{13}C NMR (151 MHz, $CDCl_3$) δ: 211.4, 138.4, 118.6, 101.7, 75.6, 72.8, 67.9, 66.7, 63.5, 24.0, 23.5, 18.21, 18.20, 12.6.

HRMS: m/z calcd. for $C_{20}H_{38}ClO_5Si^+$: 421.2172 (M+H); found: 421.2188 (M+H).

IR: 3538, 2944, 2868, 1738, 1223, 1086 cm^{-1}.

α_D ($CHCl_3$, c = 0.89): +88.5.

Preparation of alkene (55):

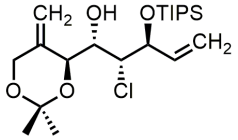

To a freshly-prepared, cooled (-78 °C) solution of LiHMDS (21.4 mmol) in THF (50 mL) was added dropwise *via* cannula a solution of 5-(methanesulfonyl)-1-phenyl-1*H*-tetrazole (4.64 g, 20.9 mmol) in 25 mL THF. The resulting yellow solution was stirred for 30 minutes at -78 °C. A solution of β-ketochlorohydrin **48** (4.40 g, 10.4 mmol) in 20 mL THF was then added *via* cannula followed by a THF rinse (5 mL). The resulting mixture was stirred for 15 minutes at -78 °C, diluted with diethyl ether (1000 mL), washed with water (500 mL), washed with brine (500 mL), dried ($MgSO_4$), filtered, and concentrated. Purification of the crude material by column chromatography (8 to 12% diethyl ether in pentane) afforded alkene **55** (3.24 g, 7.70 mmol, 74%) as a colourless oil.

^{1}H NMR (400 MHz, $CDCl_3$) δ: 5.96 (ddd, *J* = 17.3, 10.4, 7.1 Hz, 1H), 5.36 (m, 1H), 5.35 (dt, *J* = 17.3, 1.1 Hz, 1H), 5.30 (dt, *J* = 10.4, 1.0 Hz, 1H), 5.02 (m, 1H), 4.71 (ddt, 7.1, 4.1, 1.0 Hz, 1H), 4.38-4.23 (m, 5H), 3.58 (d, 2.7 Hz, 1H), 1.49 (s, 3H), 1.34 (s, 3H), 1.10 (m, 21H).

^{13}C NMR (151 MHz, $CDCl_3$) δ: 142.0, 138.1, 118.3, 109.9, 99.7, 79.1, 71.3, 70.8, 65.1, 64.1, 28.3, 21.8, 18.20, 18.18, 12.6.

HRMS: m/z calcd. for $C_{21}H_{40}ClO_4Si^+$: 419.2367 (M+H); found: 419.2379 (M+H).

IR: 3485, 2968, 1380, 1228, 1067 cm^{-1}.

α_D ($CHCl_3$, c = 0.45): +22.2.

Preparation of epoxide (56):

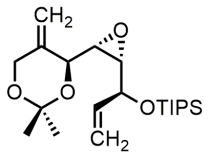

To a solution of alkene **55** (9.11 g, 21.7 mmol) in 5:1 / EtOH:H_2O (150 mL) was added CsOH (50% w/w in H_2O, 21.0 mL, 109 mmol). The resulting orange/brown mixture was stirred at 80 ^oC for 3 h, cooled to room temperature, diluted with CH_2Cl_2 (600 mL), washed with NH_4Cl (300 mL), washed with $NaHCO_3$ (300 mL), washed with brine (300 mL), dried ($MgSO_4$), filtered, and concentrated. Purification of the crude material by column chromatography (10% diethyl ether in pentane) afforded epoxide **56** (5.91 g, 15.4 mmol, 71%) as a colourless oil.

^1H NMR (400 MHz, $CDCl_3$) δ: 6.00 (ddd, *J* = 17.2, 10.6, 3.9 Hz, 1H), 5.51 (dt, *J* = 17.2, 1.8 Hz, 1H), 5.23 (m, 1H), 5.22 (dt, *J* = 10.6, 1.8 Hz, 1H), 5.01 (m, 1H), 4.38 (d, *J* = 13.8 Hz, 1H), 4.30 (d, *J* = 13.8 Hz, 1H), 4.21 (m, 1H), 4.17 (d, *J* = 7.7 Hz, 1H), 3.17 (dd, *J* = 7.7, 4.2 Hz, 1H), 2.93 (dd, *J* = 8.0, 4.2 Hz, 1H), 1.44 (s, 3H), 1.40 (s, 3H), 1.10 (m, 21H).

^{13}C NMR (151 MHz, $CDCl_3$) δ: 142.7, 136.8, 115.9, 109.1, 99.4, 72.6, 69.9, 64.0, 59.9, 56.4, 27.5, 21.5, 18.2, 18.1, 12.6.

HRMS: m/z calcd. for $C_{21}H_{39}O_4Si^+$: 383.2612 (M+H); found: 383.2600 (M+H).

IR: 2927, 2867, 1464, 1381, 1222, 1133, 1087 cm^{-1}.

α_D ($CHCl_3$, c = 0.31): -16.6.

Preparation of diene (47):

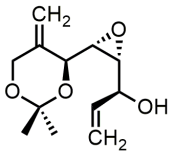

To a solution of epoxide **56** (1.05 g, 2.74 mmol) in THF (5.5 mL) was added dropwise TBAF (1 M in THF, 3.4 mL, 3.4 mmol). The resulting mixture was stirred at room temperature for 1 h and then adsorbed onto ca. 3 g silica. Purification of the crude material by column chromatography (2:1 / pentane:EtOAc) afforded diene **47** (609 mg, 2.69 mmol, 98%) as a white solid.

^{1}H NMR (400 MHz, $CDCl_3$) δ: 6.00 (ddd, *J* = 17.4, 10.7, 4.5 Hz, 1H), 5.48 (dt, *J* = 17.4, 1.5 Hz, 1H), 5.28 (dt, *J* = 10.7, 1.5 Hz, 1H), 5.20 (m, 1H), 5.03 (m, 1H), 4.39 (d, *J* = 14.0 Hz, 1H), 4.29 (d, *J* = 14.0 Hz, 1H), 4.26 (d, *J* = 7.8 Hz, 1H), 4.17 (m, 1H), 3.26 (dd, *J* = 7.8, 4.2 Hz, 1H), 3.03 (dd, *J* = 7.8, 4.2 Hz, 1H), 1.44 (s, 3H), 1.40 (s, 3H).

^{13}C NMR (151 MHz, $CDCl_3$) δ: 142.4, 135.9, 116.7, 109.1, 99.4, 70.9, 69.8, 64.0, 58.8, 57.3,

HRMS: m/z calcd. for $C_{12}H_{18}O_4Na^+$: 249.1097 (M+Na); found: 249.1111 (M+Na).

IR: 3445, 2991, 1372, 1222, 1199, 1158, 1084, 1002 cm^{-1}.

m.p. = 59 - 62 °C.

α_D ($CHCl_3$, c = 0.68): +122.0.

Preparation of carbocycle (46):

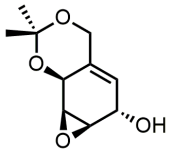

To a degassed solution of diene **47** (300 mg, 1.33 mmol) in CH_2Cl_2 (40 mL) was added Stewart-Grubbs' Catalyst (30 mg, 0.053 mmol). The mixture was refluxed for 72 hours under an argon atmosphere, cooled to room temperature, and concentrated. Purification of the crude material by column chromatography (80 to 100% EtOAc in pentane) afforded carbocycle **46** (232 mg, 1.18 mmol, 88%) as a white solid.

^{1}H NMR (400 MHz, $CDCl_3$) δ: 5.46 (m, 1H), 4.83 (m, 1H), 4.53 (m, 1H), 4.37 (d, *J* = 14.4 Hz, 1H), 4.17 (d, *J* = 14.4 Hz, 1H), 3.44 (m, 1H), 3.38 (m, 1H), 2.28 (br. d, *J* = 5.0 Hz, 1H), 1.51 (s, 3H), 1.43 (s, 3H).

^{13}C NMR (151 MHz, $CDCl_3$) δ: 134.1, 118.0, 100.4, 65.4, 63.5, 62.5, 53.6, 51.9, 27.0, 21.3.

HRMS: m/z calcd. for $C_{10}H_{15}O_4^+$: 199.0965 (M+H); found: 199.0973 (M+H).

IR: 3424, 2989, 1382, 1223, 1198, 1072, 1013 cm^{-1}.

m.p. = 80 - 83 °C.

α_D ($CHCl_3$, c = 0.78): -22.4.

Preparation of oxazolidinone (61):

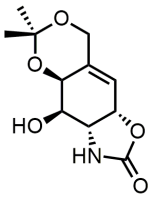

To a solution of carbocycle **46** (224 mg, 1.14 mmol) in CH_2Cl_2 (10 mL) was added dropwise acetyl isocyanate (ca. 1M in $ClCH_2CH_2Cl$, 2.4 mL, 2.4 mmol). The mixture was stirred for 15 minutes at room temperature, diluted with CH_2Cl_2 (50 mL), washed with $NaHCO_3$ (25 mL), washed with brine (25 mL), dried ($MgSO_4$), filtered, and concentrated. The crude residue was dissolved in MeOH (10 mL) and treated with Cs_2CO_3 (740 mg, 2.27 mmol). The resulting mixture was stirred for 1 hour at room temperature and then adsorbed onto ca. 2 g silica. Purification of the crude material by column chromatography (0 to 2% MeOH in EtOAc) afforded oxazolidinone **61** (93.8 mg, 0.39 mmol, 34%) as a white solid.

^{1}H NMR (400 MHz, $CDCl_3$) δ: 5.58 (m 1H), 5.45 (m, 1H), 5.16 (dd, *J* = 7.4, 3.5 Hz, 1H), 4.69 (m, 1H), 4.50 (d, *J* = 14.6 Hz, 1H), 4.39 (dd, *J* = 7.4, 2.9 Hz, 1H), 4.20 (d, *J* = 14.6 Hz, 1H), 4.17 (m, 1H), 2.67 (s, 3H), 1.55 (s, 3H), 1.43 (s, 3H).

^{13}C NMR (151 MHz, $CDCl_3$) δ: 159.3, 134.8, 116.5, 99.9, 72.0, 67.5, 65.3, 62.6, 53.5, 27.8, 20.9.

HRMS: m/z calcd. for $C_{11}H_{16}NO_5^+$: 242.1023 (M+H); found: 242.1038 (M+H).

IR: 3260, 2924, 1731, 1384, 1222, 1086 cm^{-1}.

m.p. = 179 - 182 ^oC.

α_D ($CHCl_3$, c = 0.74): -13.1.

Preparation of target (42):

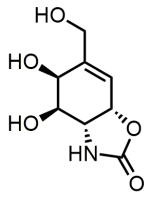

To a solution of oxazolidinone **61** (93.0 mg, 0.39 mmol) in 5:1 / MeOH:H_2O (8 mL) was added Amberlite® IR-120 H^+ form (ca. 100 beads). The resulting mixture was stirred for

16 hours at room temperature, filtered (MeOH rinse), and adsorbed onto ca. 0.5 g Celite®. Purification of the crude material by reversed phase column chromatography (H_2O) afforded target **42** (72.7 mg, 0.36 mmol, 92%) as a white solid.

^{1}H NMR (400 MHz, CD_3OD) δ: 5.89 (m, 1H), 5.16 (m, 1H), 4.22 (dt, *J* = 14.9, 1.6 Hz, 1H), 4.15 (dt, 14.9, 1.6 Hz, 1H), 4.11 (d, *J* = 3.2 Hz, 1H), 3.96 (apparent t, *J* = 8.3 Hz, 1H), 3.61 (dd, *J* = 8.9, 3.2 Hz, 1H).

^{13}C NMR (151 MHz, CD_3OD) δ: 161.8, 146.3, 118.9, 76.0, 73.4, 67.2, 63.7, 54.8.

HRMS: m/z calcd. for $C_{18}H_{12}NO_5^+$: 202.0710 (M+H); found: 202.0729 (M+H).

IR: 3307, 2920, 1732, 1393, 1232, 1145, 1094, 1053 cm^{-1}.

m.p. = 142 - 144 °C.

α_D (MeOH, c = 0.80): +90.5.

Preparation of aminodiol (62):

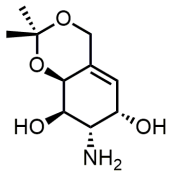

To a solution of carbocycle **46** (162 mg, 0.82 mmol) in CH_2Cl_2 (10 mL) was added dropwise acetyl isocyanate (ca. 1M in $ClCH_2CH_2Cl$, 1.6 mL, 1.6 mmol). The mixture was stirred for 15 minutes at room temperature diluted with CH_2Cl_2 (30 mL), washed with $NaHCO_3$ (15 mL), washed with brine (15 mL), dried ($MgSO_4$), filtered, and concentrated. The crude residue was dissolved in MeOH (10 mL), treated with Cs_2CO_3 (534 mg, 1.64 mmol), and stirred for 1 hour at room temperature. The mixture was then treated with H_2O (5 mL) and KOH (460 mg, 8.2 mmol) and stirred at 60 °C for 16 hours, cooled to room temperature, and adsorbed onto ca. 5 g silica. Purification of the crude material by column chromatography (70:30:1 / $CHCl_3$:MeOH:NH_4OH) afforded aminodiol **62** (85.0 mg, 0.39 mmol, 48%) as a white gum.

^{1}H NMR (400 MHz, CD_3CN) δ: 5.42 (s, 1H), 4.60 (s, 1H), 4.49 (d, *J* = 13.3 Hz, 1H), 4.33 (br. s, 1H), 4.00 (d, *J* = 13.3 Hz, 1H), 3.96 (apparent t, *J* = 3.9 Hz, 1H), 3.27 (br. s, 1H), 1.52 (s, 3H), 1.34 (s, 3H).

^{13}C NMR (151 MHz, CD_3CN) δ: 131.6, 123.9, 100.2, 71.0 (br.), 66.7, 65.5 (br.), 64.2, 54.5 (br.), 29.1, 20.4.

HRMS: m/z calcd. for $C_{10}H_{18}NO_4^+$: 216.1230 (M+H); found: 216.1246 (M+H).

IR: 3354, 2992, 1603, 1384, 1231, 1195, 1158, 1073 cm^{-1}.

α_D (CH_3CN, c = 2.50): +117.

Preparation of acetate (63):

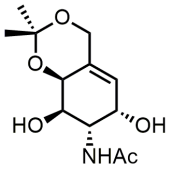

To a suspension of aminodiol **62** (150 mg, 0.69 mmol) in CH_2Cl_2 (7 mL) was added 2,6-lutidine (0.16 mL, 1.4 mmol) and Ac_2O (0.065 mL, 0.69 mmol). The resulting heterogeneous mixture was stirred for 5 minutes (during which time un-dissolved starting material disappeared) and adsorbed onto ca. 1 g silica. Purification of the crude material by column chromatography (12% MeOH in EtOAc) afforded acetate **63** (158 mg, 0.61 mmol, 89%) as a white solid.

^{1}H NMR (400 MHz, CD_3OD) δ: 5.51 (s, 1H), 4.55 (m, 3H), 4.38 (apparent t, *J* = 5.3 Hz, 1H), 4.10 (m, 2H), 1.99 (s, 3H), 1.54 (s, 3H), 1.39 (s, 3H).

^{13}C NMR (151 MHz, CD_3OD) δ: 174.2, 133.8, 123.4, 100.9, 69.0, 67.5, 64.8, 64.5, 54.2, 28.5, 22.6, 20.7.

HRMS: m/z calcd. for $C_{12}H_{19}NO_5Na^+$: 280.1155 (M+Na); found: 280.1177 (M+Na).

IR: 3333, 2989, 2448, 1639, 1384, 1197, 1087 cm^{-1}.

m.p. = 194 - 198 ^oC (dec.).

α_D (MeOH, c = 0.55): +103.

Preparation of target (43):

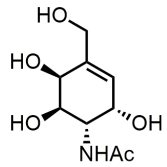

To a solution of acetate **63** (40.0 mg, 0.16 mmol) in 5:1 / MeOH:H_2O (1.5 mL) was added Amberlite® IR-120 H^+ form (ca. 50 beads). The resulting mixture was stirred for 16 hours at room temperature, filtered (MeOH rinse), and adsorbed onto ca. 0.25 g Celite®. Purification the crude by reversed phase column chromatography (H_2O) afforded target **43** (32.2 mg, 0.15 mmol, 96%) as a white solid.

^{1}H NMR (400 MHz, CD_3OD) δ: 5.84 (s, 1H), 4.25 (m, 2H), 4.14 (m, 3H), 3.84 (d, *J* = 9.9 Hz, 1H), 2.03 (s, 3H).

^{13}C NMR (151 MHz, CD_3OD) δ: 174.1, 142.4, 125.4, 68.8, 68.0, 66.4, 63.8, 51.8, 22.8.

HRMS: m/z calcd. for $C_9H_{15}NO_5Na^+$: 240.0842 (M+Na); found: 240.0843 (M+Na).

IR: 3322, 2911, 1622, 1548, 1420, 1098 cm^{-1}.

α_D (MeOH, c = 0.15): +126.

Preparation of target (44):

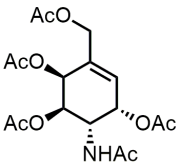

A microwave vial was charged with aminodiol **62** (25.0 mg, 0.17 mmol), MeOH (1 mL), and *p*-TsOH (1.1 mg, 0.006 mmol). The reaction vessel was sealed and the mixture was stirred for 8 hours at 100 °C, cooled to room temperature, quenched with Amberlyst® IRA 400 OH^- form (ca. 100 beads), filtered (MeOH rinse), and concentrated. The crude residue was concentrated twice from PhMe, dissolved in pyridine (1 mL), and treated with 4-dimethylaminopyridine (1 grain) and Ac_2O (0.22 mL, 2.33 mmol). The resulting mixture was stirred for 24 hours at room temperature, diluted with CH_2Cl_2 (10 mL), washed with NH_4Cl (5 mL), washed with $NaHCO_3$ (5 mL), washed with brine (5 mL), dried ($MgSO_4$), filtered, and concentrated. Purification of the crude material by preparative TLC (500 micron silica, 3% MeOH in CH_2Cl_2) afforded target **44** (19.8 mg, 0.051 mmol, 44%) as a white foam.

^{1}H NMR (600 MHz, $CDCl_3$) δ: 6.12 (d, *J* = 5.2 Hz, 1H), 5.69 (d, *J* = 4.1 Hz, 1H), 5.66 (d, *J* = 9.3 Hz, 1H), 5.38 (apparent t, *J* = 4.7 Hz, 1H), 5.30 (m, 1H), 4.78 (ddd, *J* = 11.8, 9.3, 4.3, 1H), 4.56 (d, *J* = 13.9 Hz, 1H), 4.45 (d, *J* = 13.9 Hz, 1H), 2.11 (s, 3H), 2.10 (s, 3H), 2.06 (s, 3H), 2.02 (s, 3H), 1.96 (s, 3H).

^{13}C NMR (151 MHz, $CDCl_3$) δ: 171.3, 170.5, 170.4, 170.1, 170.0, 135.6, 126.3, 68.2, 67.4, 65.3, 63.5, 46.2, 23.4, 21.0, 20.9, 20.8, 20.8.

HRMS: m/z calcd. for $C_{17}H_{24}NO_9^+$: 386.1446 (M+H); found: 386.1460 (M+H).

IR: 3287, 2942, 1741, 1658, 1540, 1436, 1370, 1219, 1017 cm^{-1}.

α_D ($CHCl_3$, c = 2.92): +197.

References

(1) Nakano, M.; Kakehi, K.; Tsai, M. H.; Lee, Y. C. *Glycobiology* **2004**, *14*, 431.

(2) Yoshida-Moriguchi, T.; Yu, L.; Stalnaker, S. H.; Davis, S.; Kunz, S.; Madson, M.; Oldstone, M. B. A.; Schachter, H.; Wells, L.; Campbell, K. P. *Science* **2010**, *327*, 88.

(3) Ohtsubo, K.; Marth, J. D. *Cell* **2006**, *126*, 855.

(4) Lowe, J. B. *Curr. Opin. Cell Biol.* **2003**, *15*, 531.

(5) Day, C. J.; Tran, E. N.; Semchenko, E. A.; Tram, G.; Hartley-Tassell, L. E.; Ng, P. S. K.; King, R. M.; Ulanovsky, R.; McAtamney, S.; Apicella, M. A.; Tiralongo, J.; Morona, R.; Korolik, V.; Jennings, M. P. *Proc. Natl. Acad. Sci. U. S. A.* **2015**, *112*, E7266.

(6) Zhu, X.; McBride, R.; Nycholat, C. M.; Yu, W.; Paulson, J. C.; Wilson, I. a. *J. Virol.* **2012**, *86*, 13371.

(7) Hart, G. W.; Akimoto, Y. In *Essentials of Glycobiology*; Varki, A., Cummings, R., Esko, J., Freeze, H., Stanley, P., Bertozzi, C., Hart, G., Etzler, M., Eds.; Cold Spring Harbor Laboratory Press: Cold Spring Harbor (NY), 2009.

(8) Rempel, B. P.; Withers, S. G. *Glycobiology* **2008**, *18*, 570.

(9) Sim, L.; Jayakanthan, K.; Mohan, S.; Nasi, R.; Johnston, B. D.; Pinto, B. M.; Rose, D. R. *Biochemistry* **2010**, *49*, 443.

(10) Coniff, R.; Krol, A. *Clin. Ther.* **1997**, *19*, 13.

(11) Kiso, M.; Mitamura, K.; Sakai-Tagawa, Y.; Shiraishi, K.; Kawakami, C.; Kimura, K.; Hayden, F. G.; Sugaya, N.; Kawaoka, Y. *Lancet (London)* **2004**, *364*, 759.

(12) Yuzwa, S. A.; Macauley, M. S.; Heinonen, J. E.; Shan, X.; Dennis, R. J.; He, Y.; Whitworth, G. E.; Stubbs, K. A.; McEachern, E. J.; Davies, G. J.; Vocadlo, D. J. *Nat. Chem. Biol.* **2008**, *4*, 483.

(13) Bergeron-Brlek, M.; Goodwin-Tindall, J.; Cekic, N.; Roth, C.; Zandberg, W. F.; Shan, X.; Varghese, V.; Chan, S.; Davies, G. J.; Vocadlo, D. J.; Britton, R. *Angew. Chemie - Int. Ed.* **2015**, 15649.

(14) Lombard, V.; Golaconda Ramulu, H.; Drula, E.; Coutinho, P. M.; Henrissat, B. *Nucleic Acids Res.* **2014**, *42*, 490.

(15) Koshland, D. E. *Biol. Rev.* **1953**, *28*, 416.

(16) Vocadlo, D. J.; Davies, G. J.; Laine, R.; Withers, S. G. *Nature* **2001**, *412*, 835.

(17) Nagae, M.; Tsuchiya, A.; Katayama, T.; Yamamoto, K.; Wakatsuki, S.; Kato, R. *J. Biol. Chem.* **2007**, *282*, 18497.

(18) Lairson, L. L.; Henrissat, B.; Davies, G. J.; Withers, S. G. *Annu. Rev. Biochem.* **2008**, *77*, 521.

(19) Yip, V. L. Y.; Varrot, A.; Davies, G. J.; Rajan, S. S.; Yang, X.; Thompson, J.; Anderson, W. F.; Withers, S. G. *J. Am. Chem. Soc.* **2004**, *126*, 8354.

(20) Rajan, S. S.; Yang, X.; Collart, F.; Yip, V. L. Y.; Withers, S. G.; Varrot, A.; Thompson, J.; Davies, G. J.; Anderson, W. F. *Structure* **2004**, *12*, 1619.

(21) Liu, Q. P.; Sulzenbacher, G.; Yuan, H.; Bennett, E. P.; Pietz, G.; Saunders, K.; Spence, J.; Nudelman, E.; Levery, S. B.; White, T.; Neveu, J. M.; Lane, W. S.; Bourne, Y.; Olsson, M. L.; Henrissat, B.; Clausen, H. *Nat. Biotechnol.* **2007**, *25*, 454.

(22) Zhang, J.; Shao, J.; Kowal, P.; Wang, P. G. In *Carbohydrate-Based Drug Discovery*; Wong, C.-H., Ed.; 2003; p 138.

(23) van Kooyk, Y.; Kalay, H.; Garcia-Vallejo, J. J. *Front. Immunol.* **2013**, *4*.

(24) Mesleh, M. F.; Rajaratnam, P.; Conrad, M.; Chandrasekaran, V.; Liu, C. M.; Pandya, B. A.; Hwang, Y. S.; Rye, P. T.; Muldoon, C.; Becker, B.; Zuegg, J.; Meutermans, W.; Moy, T. I. *Chem. Biol. Drug Des.* **2015**, *87*, 190.

(25) Platt, F. M.; Neises, G. R.; Dwek, R. A.; Butters, T. D. *J. Biol. Chem.* **1994**, *269*, 8362.

(26) Cox, T.; Lachmann, R.; Hollak, C.; Aerts, J.; van Weely, S.; Hrebícek, M.; Platt, F.; Butters, T.; Dwek, R.; Moyses, C.; Gow, I.; Elstein, D.; Zimran, A. *Lancet (London)* **2000**, *355*, 1481.

(27) Sawkar, A. R.; Cheng, W.-C.; Beutler, E.; Wong, C.-H.; Balch, W. E.; Kelly, J. W. *Proc. Natl. Acad. Sci. U. S. A.* **2002**, *99*, 15428.

(28) Errey, J. C.; Lee, S. S.; Gibson, R. R.; Fleites, C. M.; Barry, C. S.; Jung, P. M. J.; O'Sullivan, A. C.; Davis, B. G.; Davies, G. J. *Angew. Chemie - Int. Ed.* **2010**, *49*, 1234.

(29) Lee, S. S.; Hong, S. Y.; Errey, J. C.; Izumi, A.; Davies, G. J.; Davis, B. G. *Nat. Chem. Biol.* **2011**, *7*, 631.

(30) Wolfenden, R.; Lu, X.; Young, G. *J. Am. Chem. Soc.* **1998**, *120*, 6814.

(31) Gloster, T. M.; Davies, G. J. *Org. Biomol. Chem.* **2010**, *8*, 305.

(32) Asano, N. In *Iminosugars: From Synthesis to Therapeutic Applications*; Compain, P., Martin, O., Eds.; Wiley, 2008; p 7.

(33) Scott, L. I.; Spencer, C. M. *Drugs* **2000**, *59*, 521.

(34) Giugliani, R.; Waldek, S.; Germain, D. P.; Nicholls, K.; Bichet, D. G.; Simosky, J. K.; Bragat, A. C.; Castelli, J. P.; Benjamin, E. R.; Boudes, P. F. *Mol. Genet. Metab.* **2013**, *109*, 86.

(35) Fan, J. Q.; Ishii, S.; Asano, N.; Suzuki, Y. *Nat. Med.* **1999**, *5*, 112.

(36) Ermert, P.; Vasella, A. *Helv. Chim. Acta.* **1991**, *74*, 2043.

(37) Panday, N.; Canac, Y.; Vasella, A. *Helv. Chim. Acta.* **2000**, *83*, 58.

(38) Vocadlo, D. J.; Davies, G. J. *Curr. Opin. Chem. Biol.* **2008**, *12*, 539.

(39) Premkumar, L.; Sawkar, A. R.; Boldin-Adamsky, S.; Toker, L.; Silman, I.; Kelly, J. W.; Futerman, A. H.; Sussman, J. L. *J. Biol. Chem.* **2005**, *280*, 23815.

(40) Schueler, U. H.; Kolter, T.; Kaneski, C. R.; Zirzow, G. C.; Sandhoff, K.; Brady, R. O. *J. Inherit. Metab. Dis.* **2004**, *27*, 649.

(41) Witte, M. D.; Kallemeijn, W. W.; Aten, J.; Li, K.-Y.; Strijland, A.; Donker-Koopman, W. E.; van den Nieuwendijk, A. M. C. H.; Bleijlevens, B.; Kramer, G.; Florea, B. I.; Hooibrink, B.; Hollak, C. E. M.; Ottenhoff, R.; Boot, R. G.; van der Marel, G. a; Overkleeft, H. S.; Aerts, J. M. F. G. *Nat. Chem. Biol.* **2010**, *6*, 907.

(42) Kallemeijn, W. W.; Li, K.-Y.; Witte, M. D.; Marques, A. R. A.; Aten, J.; Scheij, S.; Jiang, J.; Willems, L. I.; Voorn-Brouwer, T. M.; van Roomen, C. P. A. A.; Ottenhoff, R.; Boot, R. G.; van den Elst, H.; Walvoort, M. T. C.; Florea, B. I.; Codée, J. D. C.; van der Marel, G. A.; Aerts, J. M. F. G.; Overkleeft, H. S. *Angew. Chemie* **2012**, *124*, 12697.

(43) Withers, S. G.; Street, I. P.; Bird, P.; Dolphin, D. H. *J. Am. Chem. Soc.* **1987**, *109*, 7530.

(44) Withers, S. G.; Rupitz, K.; Street, I. P. *J. Biol. Chem.* **1988**, *263*, 7929.

(45) McCarter, J. D.; Adam, M. J.; Withers, S. G. *Biochem. J.* **1992**, *286*, 721.

(46) Blanchard, J. E.; Gal, L.; He, S.; Foisy, J.; Warren, R. A. J.; Withers, S. G.

Carbohydr. Res. **2001**, *333*, 7.

(47) Vocadlo, D. J.; Bertozzi, C. R. *Angew. Chemie - Int. Ed.* **2004**, *43*, 5338.

(48) Saxon, E.; Bertozzi, C. R. *Science* **2000**, *287*, 2007.

(49) Stubbs, K. A.; Scaffidi, A.; Debowski, A. W.; Mark, B. L.; Stick, R. V.; Vocadlo, D. J. *J. Am. Chem. Soc.* **2008**, *130*, 327.

(50) Gloster, T. M.; Vocadlo, D. J. *Nat. Chem. Biol.* **2012**, *8*, 683.

(51) Gloster, T. M.; Zandberg, W. F.; Heinonen, J. E.; Shen, D. L.; Deng, L.; Vocadlo, D. J. *Nat. Chem. Biol.* **2011**, *7*, 174.

(52) Rillahan, C. D.; Antonopoulos, A.; Lefort, C. T.; Sonon, R.; Azadi, P.; Ley, K.; Dell, A.; Haslam, S. M.; Paulson, J. C. *Nat. Chem. Biol.* **2012**, *8*, 661.

(53) Nishimura, S. I.; Hato, M.; Hyugaji, S.; Feng, F.; Amano, M. *Angew. Chemie - Int. Ed.* **2012**, *51*, 3386.

(54) *Carbohydrates in Chemistry and Biology*; Ernst, B., Hart, G. W., Sinay, P., Eds.; Wiley-VCH, 2000.

(55) Mlynarski, J.; Gut, B. *Chem. Soc. Rev.* **2012**, *41*, 587.

(56) Li, Y.; Paddon-Row, M. N.; Houk, K. N. *J. Org. Chem* **1990**, *55*, 481.

(57) Evans, D. a; Nelson, J. V; Taber, T. R. *J. Am. Chem. Soc.* **1981**, *103*, 3099.

(58) Schetter, B.; Mahrwald, R. *Angew. Chemie - Int. Ed.* **2006**, *45*, 7506.

(59) Eder, B. U.; Sauer, G.; Wiechert, R. *Angew. Chemie - Int. Ed.* **1971**, *10*, 496.

(60) Hajos, Z. G.; Parrish, D. R. *J. Org. Chem.* **1974**, *39*, 1615.

(61) List, B.; Lerner, R. A.; Barbas III, C. F. *J. Am. Chem. Soc.* **2000**, *122*, 2395.

(62) Northrup, A. B.; MacMillan, D. W. C. *J. Am. Chem. Soc.* **2002**, *124*, 6798.

(63) Martinez, A.; Zumbansen, K.; Dohring, A.; Van Gemmeren, M.; List, B. *Synlett* **2014**, *25*, 932.

(64) Notz, W.; List, B. *J. Am. Chem. Soc.* **2000**, *122*, 7386.

(65) Córdova, A.; Notz, W.; Iii, C. F. B. *Chem. Commun.* **2002**, 3024.

(66) Enders, D.; Grondal, C. *Angew. Chemie - Int. Ed.* **2005**, *44*, 1210.

(67) Northrup, A. B.; MacMillan, D. W. C. *Science (80-.).* **2004**, *305*, 1752.

(68) Brown, K. L.; Damm, L.; Dunitz, J. D.; Eschenmoser, A.; Hobi, R.; Kratky, C. *Helv. Chim. Acta* **1978**, *61*, 3108.

(69) Zimmerman, H. E.; Traxler, M. D. *J. Am. Chem. Soc.* **1957**, *79*, 1920.

(70) Bahmanyar, S.; Houk, K. N.; Martin, H. J.; List, B. *J. Am. Chem. Soc.* **2003**, *125*, 2475.

(71) Schmid, M. B.; Zeitler, K.; Gschwind, R. M. *Angew. Chemie - Int. Ed.* **2010**, *49*, 4997.

(72) Hein, J. E.; Burés, J.; Lam, Y. H.; Hughes, M.; Houk, K. N.; Armstrong, A.; Blackmond, D. G. *Org. Lett.* **2011**, *13*, 5644.

(73) Zotova, N.; Franzke, A.; Armstrong, A.; Blackmond, D. G. *J. Am. Chem. Soc.* **2007**, *129*, 15100.

(74) Seebach, D.; Beck, A. K.; Badine, D. M.; Limbach, M.; Eschenmoser, A.; Treasurywala, A. M.; Hobi, R.; Prikoszovich, W.; Linder, B. *Helv. Chim. Acta* **2007**, *90*, 425.

(75) Blackmond, D. G.; Moran, A.; Hughes, M.; Armstrong, A. *J. Am. Chem. Soc.* **2010**, *132*, 7598.

(76) Kanzian, T.; Lakhdar, S.; Mayr, H. *Angew. Chemie - Int. Ed.* **2010**, *49*, 9526.

(77) Haindl, M. H.; Hioe, J.; Gschwind, R. M. *J. Am. Chem. Soc.* **2015**, *137*, 12835.

(78) Sharma, A. K.; Sunoj, R. B. *Angew. Chemie - Int. Ed.* **2010**, *49*, 6373.

(79) Bergeron-Brlek, M.; Teoh, T.; Britton, R. *Org. Lett.* **2013**, *15*, 3554.

(80) Díaz-Oltra, S.; Carda, M.; Murga, J.; Falomir, E.; Marco, J. A. *Chem. - A Eur. J.* **2008**, *14*, 9240.

(81) Britton, R.; Kang, B. *Nat. Prod. Rep.* **2013**, *30*, 227.

(82) Stambasky, J.; Hocek, M.; Kocovsky, P. *Chem. Rev.* **2009**, *109*, 6729.

(83) Bergeron-Brlek, M.; Meanwell, M.; Britton, R. *Nat. Commun.* **2015**, *6*, 6903.

(84) Chakladar, S.; Wang, Y.; Clark, T.; Cheng, L.; Ko, S.; Vocadlo, D. J.; Bennet, A. J.

Nat. Commun. **2014**, *5*, 5590.

(85) Roberts, J. D.; Mazur, R. H. *J. Am. Chem. Soc.* **1951**, *73*, 2509.

(86) Pengelly, R.; Chakladar, S.; Gloster, T. M.; Bennet, A. J. *Unpubl. Work*.

(87) Olah, George, A.; Reddy, V. P.; Prakash, G. K. S. *Chem. Rev.* **1992**, *92*, 69.

(88) Kallemeijn, W. W.; Witte, M. D.; Wennekes, T.; Aerts, J. M. F. G. *Adv. Carbohydr. Chem. Biochem.* **2014**, *71*, 297.

(89) Roeser, K. R.; Legler, G. *Biochim. Biophys. Acta* **1981**, *657*, 321.

(90) Doyle, M. P.; Forbes, D. C. *Chem. Rev.* **1998**, *98*, 911.

(91) Taron, M. W. Studies Toward the Total Synthesis of Biselide A, Simon Fraser University, 2015.

(92) Hoye, T. R.; Jeffrey, C. S.; Shao, F. *Nat. Protoc.* **2007**, *2*, 2451.

(93) Blakemore, P. R.; Cole, W. J.; Kocieński, P. J.; Morley, A. *Synlett* **1998**, No. c, 26.

(94) Williamson, K. L.; Lanford, C. A.; Nicholson, C. R. *J. Am. Chem. Soc.* **1964**, *86*, 762.

(95) Liang, Y.; Zhou, H.; Yu, Z.-X. *J. Am. Chem. Soc.* **2009**, *131*, 17783.

(96) Doyle, M. P.; Duffy, R.; Ratnikov, M.; Zhou, L. *Chem. Rev.* **2010**, 704.

(97) Merritt, R. F.; Johnson, F. A. *J. Org. Chem.* **1966**, *31*, 1859.

(98) Williamson, K. L.; Hsu, Y.-F. L.; Hall, F. H.; Swager, S.; Coulter, M. S. *J. Am. Chem. Soc.* **1968**, *90*, 6717.

(99) Koeners, H. J.; Kok, A. J.; Romers, C.; van Boom, J. H. *Recuil J. R. Netherlands Chem. Soc.* **1980**, *99*, 355.

(100) Hayek, S. S.; Abd, T. T.; Cribbs, S. K.; Anderson, A. M.; Melendez, A.; Kobayashi, M.; Polito, C.; Wang, Y. F. *Emerg. Microbes Infect.* **2013**, *2*, e17.

(101) Brockhausen, I.; Schachter, H.; Stanley, P. In *Essentials of Glycobiology*; Varki, A., Cummings, R., Esko, J., Freeze, H., Stanley, P., Bertozzi, C., Hart, G., Etzler, M., Eds.; Cold Spring Harbor Laboratory Press: Cold Spring Harbor (NY), 2015.

(102) Schubert, J.; Schwesinger, R.; Prinzbach, H. *Angew. Chemie Int. Ed.* **1984**, *23*, 167.

(103) Synthesis, A.; Kapferer, P.; Sarabia, F.; Vasella, A. **1999**, *82*.

(104) Ackermann, L.; El Tom, D.; Fürstner, A. *Tetrahedron* **2000**, *56*, 2195.

(105) Nicolaou, K. C.; Rodríguez, R. M.; Mitchell, H. J.; van Delft, F. L. *Angew. Chemie - Int. Ed.* **1998**, *37*, 1874.

(106) Evans, P. A.; Huang, M.-H.; Lawler, M. J.; Maroto, S. *Nat. Chem.* **2012**, *4*, 680.

(107) Skaanderup, P. R.; Poulsen, C. S.; Hyldtoft, L.; Jørgensen, M. R.; Madsen, R. *Synthesis (Stuttg).* **2002**, *2002*, 1721.

(108) Bernet, B.; Vasella, A. *Helv. Chim. Acta* **1979**, *62*, 1990.

(109) Draper, J.; Britton, R. A. *Unpubl. Work*.